SPHINGOSINE KINASE INHIBITION AMELIORATES CHRONIC HYPOPERFUSION-INDUCED WHITE MATTER LESIONS

YANG YING

(B.Sc. (Hons.), Zhejiang University)

DECLARATION

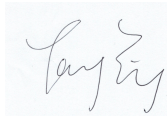I hereby declare that the thesis is my original work and it has been written by me in its entirety. I have duly acknowledged all the sources of information which have been used in the thesis.

This thesis has also not been submitted for any degree in any university previously.

Yang Ying

20 January 2016

ACKNOWLEDGEMENTS

First of all, I would like to express my deepest gratitude to my supervisor Prof. Peter Wong Tsun Hon for their continuous support during the past five years of my PhD study. Without his guidance and help, it is impossible for me to fulfil my research work and complete this thesis. The scientific advice and insightful discussions he provided about my research benefit me greatly. His patience, motivation and immense knowledge always inspire me greatly. Prof Wong has been so supportive and has given me much freedom to pursue various research ideas without objection. Besides, he provided me many opportunities to attend workshops, International conferences, which has been very helpful in broadening my vision.

I'm also extremely grateful to my Co-supervisor Dr. Lai Kim Peng Mitchell for his enlightening ideas, invaluable scientific advice and continuous support. His enthusiasm, extraordinary kindness and patience impressed me a lot. I'm also very grateful for introducing me collaborators and always encourage me when I met with difficulties. This thesis could not have been written without his valuable suggestions.

I would like to extend my heartfelt gratitude to all the lab members, past and present, for their help along these years. My sincere appreciation first goes to Mrs. Ting Wee Lee for her great work and patient assistance on administrative stuffs, such as reagents ordering, paper work filing and keeping the lab tidy and organized. Also I would like to express my gratitude to Ms Wu Qi, Mr Zhao Heng and Ms Chan Sujing for their guidance and technical support in the early years of my PhD as well as their warm

friendship. Genuine appreciation to Ms Zhao Huiand Ms Nur-Ezan Mohamed for their warm friendship.

Special thanks to Dr. Federico Tesio Torta, and Dr. Pradeep Narayanaswamy for their technical support and scientific suggestions on the collaborations in lipidomics analysis.

Many thanks to my friends for their constant encouragement thoughout these years.

Finally, I owe my gratitude to my family members. Their love and encouragement always support me to overcome difficulties.

TABLE OF CONTENTS

SUMMARY

White matter lesions (WML) are the white matter abnormalities characterized by myelin rarefaction, axonal loss, glia activation in the white matter of the cerebral hemisphere. WML are one of most common vascular pathologies of vascular cognitive impairment (VCI). Sphingolipids, as one of three major classes of lipids found in cerebral myelin membrane, are important structure components of white matter and some of the bioactive sphingolipids are also involved in various physiological and pathological processes as signaling mediators. Sphingosine-1-phosphate (S1P) is a well-known bioactive sphingolipid molecule. It is derived from phosphorylation of sphingosine by sphingosine kinase (SphK). Previous studies have demonstrated that SphK and S1P altered in hypoxia and the S1P signaling pathway is involved in regulating oligodendroglial lineage cell survival, proliferation, membrane dynamics and differentiation. Growing evidence suggests that the failure to form new myelin sheaths due to disruption of OPC differentiation is one factor underlying chronic white matter damage. However, the sphingolipid changes of hypoperfusion induced-WML are not known. In addition, it has not been revealed whether SphK and S1P signaling pathway is involved in the ischemic WML.

In this study, we demonstrated a lipidome of cerebral WML by LC-MS/MS analysis in a mouse bilateral carotid artery stenosis (BCAS) model of chronic cerebral hypoperfusion, showing a profile of individual lipid molecules belonging to ceramide, sphingomyelin, glycoceramide, sphingosine and S1P. Amounts of phospholipids including

phosphatidylcholine (PC), phosphatidylethanolamine (PE), phosphatidylserine (PS), phosphatidylglycerol (PG), and phosphatidylinositol (PI), lysoPC (LPC), lysoPE (LPE) and cholesterol were measured. Overall content reduction in glycosphingolipids and sphingosine and overall increase of S1P, PS and PG were found in white matters of BCAS mice compared with sham-operated ones. Besides, BCAS induced composition alteration of sphingolipid in white matters, in which very long acyl chain-sphingolipids reduced whereas long acyl chain-sphingolipid elevated. Cholesterol levels in white matters remained unchanged in BCAS mice. When SphK, S1P as well as markers of WML, hypoxia and oligodendrocyte progenitor cells (NG2$^+$) were measured in WML, it was found that in BCAS mice, hypoxia inducible factor (HIF)-1α, Sphk2, S1P, and NG2 were up-regulated in association with the accumulation of WML. Significantly, a SphK inhibitor SKI-II showed partial reversal of SphK2, S1P and NG2 elevation and amelioration of WML. In an in vitro model of hypoxia, SKI-II reversed the suppression of OPC differentiation induced by hypoxia indicating that the hypoxia inhibits OPC differentiation via S1P.

In conclusion, this study suggests a mechanism for hypoperfusion-associated WML involving various structural and bioactive lipid aberrations which may cause demyelination and HIF-1α-SphK2-S1P-mediated disruption of OPC differentiation, and proposes the SphK signaling pathway as a potential therapeutic target for white matter disease.

LIST OF TABLES

LIST OF FIGURES

ABBREVIATIONS

ACP	Acyl carrier protein
AD	Alzheimer disease
AP-2	Activator protein-2
BBB	Blood-brain barrier
BCAS	Bilateral common carotid artery stenosis
bFGF	Basic fibroblast growth factor
CADASIL	Dominant arteriopathy with subcortical infarct and leukoencephalopathy
CBF	Cerebral blood flow
CC	Corpus callosum
CCA	Common carotid arterie
Cer	Ceramide
CerS	Ceramide synthases
CNS	Central nervous system
CoCl$_2$	Cobalt chloride
DAPI	4',6-diamidino-2-phenylindole
DHC	Dihexosylceramides
DMEM	Dulbecco's Modified Eagle's Medium
DMS	N, N-Dimethylsphingosine
DMSO	Dimethyl sulfoxide
DNA	Deoxyribonucleic acid
ECA	External carotid artery
EDGE	Endothelial differentiation gene
EGF	Epithelial growth factor
ER	Endoplasmic reticulum
ERK	Extracellular-signal regulated kinase
ET-1	Vasoconstrictor endothelin-1
FADD	Fas-associated death domain protein
FGF	Fibroblast growth factor
FTY720	2-amino-2-[2-(4-octylphenyl)ethyl]propane-1,3-diol
GluCer	Galactosylceramide
HIF	Hypoxia inducible factor
HREs	Gypoxia response elements

i.p.	Intraperitoneally
ICA	Internal carotid artery
INF-γ	Interferon γ
JNK	c-Jun amino terminal kinase
JTE-013	1-(1,3-Dimethyl-4-isopropyl)-1H-pyrazolo[3,4-b]pyridin-6-yl)-4-(3,5-dichloro-4-pyridinyl)-semicarbazide
KB	Klüver-Barrera
LC	Liquid chromatography
LPS	Lipopolysaccharide
MBP	Myeline basic protein
MCAO	Middle common carotid artery occlusion
MHC	Monohexosylceramides
MMP	Matrix metalloproteinase
mRNA	Messenger ribonucleic acid
MS	Mass spectrometry
MS	Multiple sclerosis
MTT	3-(4,5-Dimethylthiazol-2-yl)-2,5-Diphenyltetrazolium Bromide
NADH	Nicotinamide adenine dinucleotide Hydrogen
NADPH	Nicotinamide adenine dinucleotide phosphate hydrogen
NF-κB	Nuclear factor κB
NG2	Neural/glial antigen 2
NGF	Nerve growth factor
OGD	Oxygen glucose deprivation
OLG	Oligodendrocyte
OPC	Oligodendrocyte progenitor cell
PAF	Platelet-activating factor
pBCCAL	Permanent bilateral common carotid artery ligation
pBCCAO	Permanent bilateral common carotid artery occlusion
PBS	Phosphate buffered saline
PC	Phosphatidylcholine
PDGF	Platelet-derived growth factor
PE	Phosphatidylethanolamine
PECAM-1	Platelet endothelial cell adhesion molecule
PG	Phosphatidylglycerol
PI	Phosphatidylinositol

PKC	Protein kinase C
PKD	Protein kinase D
PLP	Proteolipid protein
Pre-OLG	Premyelinating oligodendrocyte
PS	Phosphatidylserine
QQQ	Triple quadrupole
Q-TOF	Quadrupole-time-of-flight
RIPA	Radioimmunoprecipitation assay
ROS	Reactive oxygen species
S1P	Sphingosine-1-phosphate
S1PR	Sphingosine-1-phosphate receptor
SIVD	Subcortical ischemic vascular dementia
SKI-II	4-[[4-(4-chlorophenyl)-2-thiazolyl]amino] Phenol
SM	Sphingomyelin
SMS	Sphingomyelin synthase
Sph	Sphingosine
SphK	Sphingosine kinase
Spl	Sphingosine-1-phosphate lyase
SPT	Palmitoyl transferase
tMCAO	Transient middle cerebral artery occlusion
TMS	*N,N,N*-Trimethylsphingosine
TNF-α	Tumor necrosis factor α
VaD	Vascular dementia
VCD	Vascular cognitive disorders
VCI	Vascular cognitive impairment
VEGF	Vascular endothelial growth factor
VLC	Very long chain
WHO	World Health Organization
WML	White matter lesions
WMT	White matter tissues

PUBLICATIONS

Publication:

Ying Yang, Federico Torta, Ken Arai, Markus R. Wenk, Deron R. Herr, Peter T.-H. Wong, Mitchell .P. Lai. Sphingosine kinase inhibition ameliorates chronic hypoperfusion-induced white matter lesions. *Neurochem Int.* 2016 Mar;94:90-7. Epub 2016 Feb 24

International conference:

Yang Ying, Mitchell. P. Lai and Peter T.-H. Wong. To investigate the role of Sphingolipids in white matter lesions associated vascular cognitive impairment in a chronic hypoperfusion mouse model. 12th Biennial Meeting of Asian Pacific Society for Neurochemistry, August 24-26 2014, Kaohsiung, Taiwan (Poster presentation).

CHAPTER 1   INTRODUCTION
1.1   Vascular cognitive impairment

1.1.1   Definition of VCI

Cognitive impairment is a prominent health issue among older people. The prevalence of dementia is reported to be around ~5-7% in people older than 65 years (O'Brien et al. 2003) (Kalaria et al. 2008). As the second most common cause, cerebrovascular diseases including stroke, subcortical ischemic injury, and small-vessel disease, account for ~30% of the cases (Kalaria et al. 2008). Recently, the term "Vascular cognitive impairment" (VCI) has been designated as a syndrome with evidence of clinical stroke or subclinical vascular brain injury and cognitive impairment affecting at least one cognitive domain to describe the entire range of cognitive disorders from mild cognitive impairment to fully developed vascular dementia (VaD) (Gorelick et al. 2011).

1.1.2   Vascular neuropathological substrates

VCI includes a combination of variegated brain lesions in association with multiple neuropathological manifestations. The lesions may vary in size, number and location. Besides they also frequently observed in older people without cognitive impairments or in Alzheimer disease as well. These complexities add to difficulties in understanding the pathology underlying VCI.

1.1.2.1 Cerebral infarcts

Cerebral infarcts are tissue loss observed by naked eye or under the microscope in discrete brain regions (Gorelick et al. 2011). Historically, multiple infarcts in subcortical areas mainly white matter and basal ganglia

are thought to be the most common neuropathology in VCI (Ferrer 2010). Characteristics of multiple infarcts could be variable. Cerebral infarcts are common in older people with and without dementia. For example, White et all reported more than half of the autopsied decedents had brain infarcts in a study involved 363 aged Japanese-American men from the Honolulu-Asia Aging Study (White et al. 2005). Another study by MRC-CFAS in a large unselected, community-based elderly (70-103 years) UK population reported that infarcts were observed in 31% of the total 209 autopsy brain samples (Neuropathology Group. Medical Research Council Cognitive and Aging 2001). Sonnen et al evaluated 221 autopsies from an ongoing longitudinal, population-based study of brain aging and dementia (3400 people >65 years) and reported 33% of the 221 autopsies have microinfarcts in the brain. It is difficult to determine the threshold of necessary volume or number for VCI or VaD, since reported values varied significantly (Vinters et al. 2000) (Tomlinson, Blessed, and Roth 1970; Zekry et al. 2002). Increased volume and larger number of infarcts are generally thought to be associated with a greater likelihood of dementia (Neuropathology Group. Medical Research Council Cognitive and Aging 2001; Sonnen et al. 2007; Schneider et al. 2003). In addition, the location of infarcts also contributes to the inconsistent correlations (Ferrer 2010).

1.1.2.2 Lacunes

Lacunes are small cavities filled with cerebrospinal fluid in basal ganglia or white matter (Wardlaw 2008). They possibly arise from obstruction of the trunk of a perforating artery or small ramifications perforating artery followed by progressive hypoxia/ischemia (Wardlaw 2008). Haemorrhages

2

and dilatation of the perivascular space may also contribute to some lacunes (Ferrer 2010).

Lacunes are frequently seen in VCI (Neuropathology Group. Medical Research Council Cognitive and Aging 2001; Park et al. 2014). Gold et al. has also reported that thalamic and basal ganglia lacunes were associated with cognitive decline in subcortical ischemic vascular dementia (Gold et al. 2005). In addition, Lacunar stroke that characterized by periventricular white matter and basal ganglia lacunes has been reported to cause cognitive decline in 83% of the patients (Aharon-Peretz, Daskovski, and Mashiach 2002).

1.1.2.3 White matter lesions

White matter lesions (WML), also called leukoaraiosis, is the white matter abnormalities characterized by myelin rarefaction, axonal loss, glia activation in the white matter of the cerebral hemisphere, and dilatation of periventricular space (Pantoni and Garcia 1995). WML is frequently observed in 50% to 98% of community elderly (Xiong and Mok 2011) and in 64% to 100% of patients with vascular dementia (Pantoni and Garcia 1995). Contribution of WML to cognitive impairment has been well-documented (Gold et al. 2005) (de Groot et al. 2002) (de Groot et al. 2001) in clinical-pathological studies. Besides, animal models of white matter lesions induced by hypoperfusion also demonstrated cognitive deficits (Shibata et al. 2004; Shibata et al. 2007).

Subcortical ischemic vascular dementia (SIVD) is a subtype of VCI. Cerebral small-vessel disease is the main cause of SIVD (Roman et al. 2002). WML is one of the primary types of brain lesion in SIVD. Small vessel disease including arteriolosclerosis, arteriolar hyalinosis and fibrinoid

deposit induces microvascular changes in the white matter, resulting in hypoperfusion.

Clinical-pathological studies have found that these three types of cerebral lesions didn't occur alone in VCI. According to MRC CFAS study (Neuropathology Group. Medical Research Council Cognitive and Aging 2001), small-vessel disease characterized by WML is the most common pathology in a community-based elderly UK population (70-103 years), observed in 69% of subjects. Ccombined ischemic pathologies in the same brain were present in 39% subjects, 94% of whom had WML as one of the components. Another study by Gold et al (Gold et al. 2005) has also reported demyelination often co-existed in 95% of the cases with lacunes.

1.1.2.4 Vascular pathologies in Alzheimer's disease

Alzheimer's disease (AD), the most common form of dementia, is characterized by neuropathological hallmarks of amyloid angiopathy and neurofibrillary tangles. It accounts for 50-60% of the dementia (Kalaria, Maestre, and Arizaga 2008). Increasing evidence has shown that vascular pathologies also occur in AD. A population-based autopsy study reported that vascular pathologies were observed in 20% of the AD patients (Knopman et al. 2003). Another autopsy study also reported that minor and moderate vascular pathology in ~40% of AD brains which is about twice as frequent as in controls (Jellinger and Attems 2005). It is evident that vascular pathologies may be a contributing cause of cognitive decline in AD (Schneider et al. 2004). Conversely, amyloid deposition in cerebral blood ssels of AD brain induce vascular lesions and subsequent VaD (Bugiani 2004).

4

1.1.3 Risk factors

1.1.3.1 Demographic factors

Age is a substantial risk factor for VCI. Prevalence increased steeply with increasing age. One population based-study in middle-aged people in the UK has reported that the prevalence of VaD were 6.6/100 000, 32.6/100 000 and 38.7/100 000 respectively for age range of 50-54, 55-59, and 60-64(Harvey, Skelton-Robinson, and Rossor 2003). The prevalence of VaD increases exponentially in people after 65 years old, with a range of 0.6-2.1% (Gorelick et al. 2011; Kalaria, Maestre, and Arizaga 2008). Gender difference is controversial. Some studies observed a higher incidence of VaD in men than in women (Rocca et al. 1991) (Ruitenberg et al. 2001). Whereas, some reported no difference (Andersen et al. 1999). Besides, lower educational level is thought to increase the risk of VaD (Gorelick 1997).

1.1.3.2 Genetic factors

The genetic factors include cerebral autosomal dominant arteriopathy with subcortical infarct and leukoencephalopathy (CADASIL) and apolipoprotein E (apoE) ε4. CADASIL is a cerebrovascular small-vessel disease caused by mutations of the Notch3 gene (Joutel et al. 1996). The pathologies are characterized with diffuse WML and deep lacunes (Chabriat et al. 2009), which can induce recurrent strokes, or VCI cognitive impairment in young people. Several genome-wide studies have indicated the association of apoE and VaD (Debette et al. 2010) (Ikram et al. 2009), while there are also studies reported no association (Kim et al. 2008).

1.1.3.3 Life style factors

Long-term regular physical activity has been reported to strongly associate with less cognitive decline and less VaD (Ravaglia et al. 2008). Smoking is a well-studied risk factor for cognitive decline and cardiovascular system (Anstey et al. 2007). The association between obesity and VCI seemed to be variable with age. It is reported that obesity increased the risk of VCI in people <50 years old while reduced the risk in people >65 years old (Fitzpatrick et al. 2009). A 32-year prospective study has indicated a dementia-associated weight loss (Stewart et al. 2005) which may explain the different effect of BMI on VCI. Other possible life style factors include diet, alcohol consuming, and social support, but they are controversial (Gorelick et al. 2011)

1.1.3.4 Atherogenic factors

Atherogenic factors including hypertension, diabetes, hypercholesterolemia and elevated hyperhomocysteinaemia have been considered to increase the risk of VCI. Midlife hypertension is considered a risk factor for cognitive impairment in later life (Launer et al. 1995). This, however, still remains to be clarified (Gorelick et al. 2011). Several studies have shown that chronic hyperglycemia and diabetes are associated with VCI (Saczynski et al. 2008) (Cukierman-Yaffe et al. 2009). Patients with subcortical vascular white matter lesions caused by small vessel disease exhibited surprisingly high concentrations of homocysteine compared with controls and even to patients with cerebral macroangiopathy (Fassbender et al. 1999). Hyperhomocysteinaemia is an independent risk factor for SIVD,

particularly ischemic WML which may be associated with endothelial dysfunction (Hassan et al. 2004).

High cholesterol level in midlife has been reported to strongly increase the risk for cognitive decline and VaD in later life (Solomon et al. 2009). Similar to hypertension, the risk of higher cholesterol level in older people is inconsistent (Mielke et al. 2005).

1.1.4   Diagnosis

1.1.4.1 Diagnostic criteria

Several diagnostic criteria have been proposed for VCI. NINDS-AIREN criteria were devised in the early 90's and have been used in research as diagnostic tools to operationalize symptoms of the VaD (Roman et al. 1993). Modification of NINDS-AIREN has also been proposed for clinical trials (Erkinjuntti et al. 2000). These criteria were subsequently criticized for being mainly based on features of AD and memory may not necessarily be impaired in VCI and VaD. More recently, criteria for VCI from the American Heart Association/American Stroke Association (Gorelick et al. 2011) and the criteria for vascular cognitive disorders (VCD) from the VasCog society have been proposed (Sachdev et al. 2014). These criteria share three core elements: (1) presence of cognitive impairment, (2) presence of cerebral vascular pathologies and (3) a causal link between the two.

1.1.4.2 Cognitive evaluation

Vascular risk factors should be identified, including history of hypertension, diabetes, physical activity and smoking status as discussed above (Biessels 2015). Besides, manifestations of ischemic heart disease,

congestive heart failure, peripheral vascular disease, and stroke should be recorded. Family history might also be of importance as well (Biessels 2015).

Since VCI may include deficits in all cognitive domains especially executive dysfunction such as slowed information processing, reduced ability to shift from one task to another, and deficits of working memory (Hachinski et al. 2006), cognitive testing covering at least 4 domains should be assessed: executive/attention, memory, language and visuospatial functions (Gorelick et al. 2011). In addition, Behavioral changes such as mood and character changes and other symptoms of neurological deficits, gait and balance problems should also be taken account (Biessels 2015).

Rapid advances in neuroimaging techniques have provided powerful tool for evaluating vascular pathologies such as WML, brain atrophy and macroscopic infarcts. WML characterized by myelin rarefaction, axonal loss, glia cell activation in the white matter of the cerebral hemisphere, and dilatation of periventricular space (Pantoni and Garcia 1995) appears as hyperintense (WMH) on MRI FLAIR and T2/proton density-weighted images (Pantoni et al. 1999). WMH is highly correlated with ischemic WML but not AD pathology (Wardlaw et al. 2013). In addition, WML detected by WMH could be the only neuroimaging observation in younger people, and thus is essential for the diagnosis of CADASIL (Chabriat et al. 2009).

1.1.5 Therapeutic implications

Although increasing numbers of studies have been conducted in VCI or VaD over the past decades, there are no known curative therapies for VCI. Symptomatic treatment and management of vascular risks and have been primary approaches.

1.1.6 Symptomatic treatment

Many trials to test drugs approved for AD have failed. Evidence indicates that cholinesterase inhibitors may be promising in VaD (Erkinjuntti et al. 2004). Donepezil has shown modest cognitive benefit in pure VaD of 24-week (Black et al. 2003) (Wilkinson et al. 2003) and an extra 30-week extension study (Wilkinson et al. 2010). Galatamine may be beneficial for mixed dementia (Erkinjuntti et al. 2002). Other agents including vasodilators and antioxidants are disappointing (O'Brien et al. 2003).

1.1.6.1 Prevention

Lowering blood pressure in middle-aged and young-elderly can be beneficial for the prevention of late-life dementia by reducing the risk of stroke (Forette 2003; O'Brien et al. 2003). Besides, physical activity might be useful for the prevention (Sofi et al. 2011). The efficacy of controlling other risk factors such as cholesterol and diabetes are not well established (Gorelick et al. 2011).

Recently, a randomized double-blind, parallel, placebo-controlled trial involving 359 patients on a homocysteine-lowering therapy by daily B-vitamin supplementation with vitamins B12 and B6 for 2 years has suggested that there is a significant reduction in white matter hyperintensities volume change in sub-analysis of patients with MRI evidence of severe cerebral small vessel disease at baseline (Cavalieri et al. 2012).

1.2   Mechanisms of white matter lesions

Populations all over the world especially in developed economies are rapidly ageing due to advances in medicine helping more people to live longer. According to WHO, there were ~ 8% of global population was >65 years old by 2010, and it will increase to ~15% with ~2 billion by 2050(WHO 2015). While celebrating the advances in medicine helping people to live longer, we should also notice that 15-35% of older people to some extent experience disabilities in daily living (WHO 2015). Cognitive impairment in older people significantly affects the quality of their late-life and increases the burdens of both the family and society. Unfortunately, there are currently no curative therapies for both AD and VCI, the two most common types of cognitive impairments due to lacking of clear understanding of the pathophysiological mechanisms. Since WML is one of most common vascular pathologies in VCI and it has an essential role in diagnosis of VCI, it is of great importance to investigate the pathophysiological mechanisms in vascular WML. It is characterized by myelin rarefaction, axonal loss, glia activation and oligodendrocytes apoptosis. It is widely occurred and closely correlated with cognitive impairment in elderly people. Although, growing evidence has shown that it has an ischemic origin, the mechanism of WML is not fully understood.
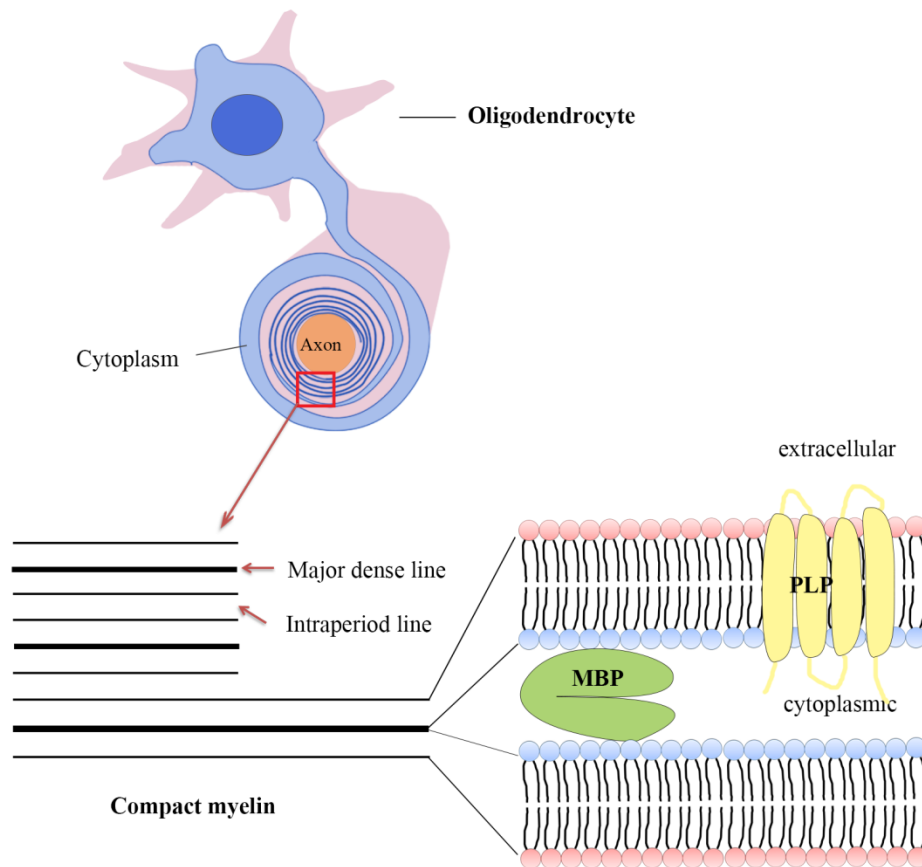
Figure 1.1 The structure of the myelin sheath and schematic representation of the major myelin components.
The myelin sheath forms from flattened cytoplasmic processes from the oligodendrocyte. Compacted cytoplasm forms the major dense line and close apposition of the membrane layers forms the intraperiod line. The myelin bilayer has an asymmetric lipid composition. Outer layer of the membrane contains glycosphingolipids such GalCer and sulfatides, while inner layer contains PI and PS. MBP is localized to cytoplasmic leaflets of the membrane. PLP is a transmembrane protein localized to the membrane bilayer. The figure is adapted from (Greer 2013) and(Aggarwal, Yurlova, and Simons 2011).

1.2.1 Composition of cerebral white matters

Cerebral white matters form the bulk of the deep parts of the brain, beneath the grey matter layer of the cortex. It consists mostly of glial cells and myelinated axons which give it the characteristic white colour. Oligodendrocytes send out sail-like extensions of their cytoplasmic membrane, wrapping up to multiple layers around the axon of an adjacent

neuron to form the myelin sheaths (Figure 1.1). Compacted cytoplasm forms the major dense line and close apposition of the membrane layers forms the intraperiod line (Greer 2013). Myelin is the essential component of white matter in the CNS, accounting for 40–50% on a dry weight basis (Baumann and Pham-Dinh 2001). Due to its characteristic electrical insulation, myelin facilitates impulse conduction while saving energy and space (Waxman 2004). The membrane composition of the myelin sheath is unique with a high proportion of lipid (~70% of dry mass) relative to protein (~30%), while the lipid to protein ratio is around 1:1 and 1:3 for most plasma and mitochondrial membranes, respectively (Petty 1993). An intimate understanding of myelin and its major components is required in order to study white matter pathologies.

1.2.1.1 Lipid composition in white matter and myelin

Nervous tissues are very rich in lipids among other tissues of the body. Lipids in adult cerebral white matter are about 1.6-fold of that in grey matters due to the presence of myelin (O'Brien and Sampson 1965). Cholesterol, phospholipids (glycerophospholipid), and sphingolipid are the three major lipid classes found in white matters and myelin.

1.2.1.1.1   Fatty acids

Fatty acids consist of a long hydrocarbon chain and a carboxylic acid group. Fatty acids in CNS appear primarily as esterified components of complex lipids as N-acyl groups of sphingolipids or O-acyl groups of glycerophospholipids. Variations in the structure of fatty acids, specifically the chain length and the number of double bonds, give rise to numerous distinct lipid molecules with distinct structural and functional roles. Fatty

acids with 14 to 24 carbon atoms and zero to six double bonds are the more abundant ones that could be observed in the brain. Figure 1.2 shows the chemical structures of two typical fatty acids with different hydrocarbon chains, stearic acid (C18:0) and nervonic (C24:1). These two are the most common acyl chain donors of sphingolipids in the brain. Most of these fatty acids contain an even number of carbon atoms while fatty acids with an odd number of carbon atoms can be observed in small amounts as well. The composition of fatty acids of lipids varies in different subclasses of lipids. Because of the accumulation of lipids during the periods of brain development and maturation, the overall content of fatty acids are increasing correspondingly, while the fatty acid composition remains relatively unchanged (Sastry 1985). Nevertheless, it has been reported that the fatty acid pattern of sphingomyelin shows significant alteration during the early brain development (Svennerholm and Vanier 1973).

Fatty acids can be taken up by the brain from the circulating blood or synthesized *de novo* in the brain. This process has been reviewed decades before (Olson 1966). Simply, the synthesis starts with the ATP-dependent carboxylation of acetyl-CoA into malonyl-CoA by carboxylase. Then the malonyl-CoA and an acetyl-CoA bind to a fatty acid synthase complex which contains an acyl carrier protein (ACP) domain and condensed to form acetoacetyl-ACP. Acetoacetyl-ACP was reduced to butryl-ACP by two NADPH$_2$. Butyl-ACP would then condense with another malonyl-CoA and repeat the reduction steps to produce growing fatty acid chain. Two carbons will be added to the acyl intermediates in each circle. When the fatty acid becomes C16 long, it will be released from the enzyme complex and produce

a palmitate. Since the fatty acids in CNS usually consist of long or very long acyl chain, most of palmitic acids will be subjected to chain elongation process in the mitochondria or microsomes in which C_2 units will be added from acetyl CoA involving either NADH or NADPH (Sastry 1985).
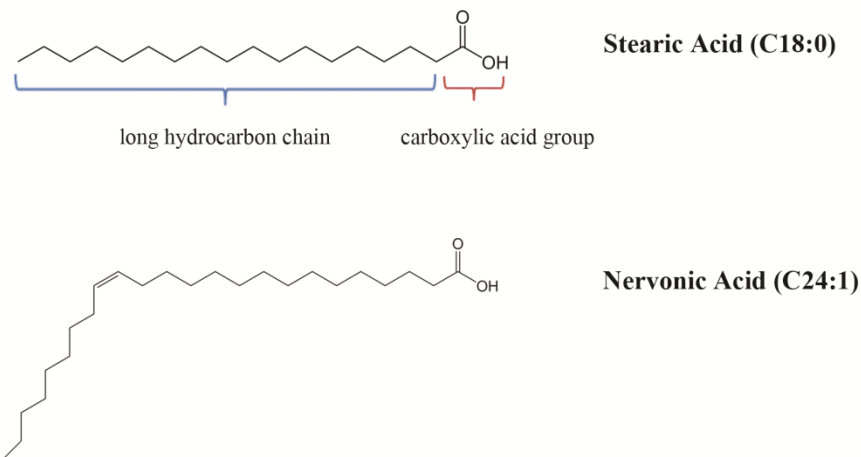
Figure 1.2 Chemical structure of Stearic acid and Nervonic acid.
Stearic acid (C18:0) and nervonic acid (C24:1) are common fatty acids in nerve tissues. Sphingolipids that contain C18 or C24 with no or one C=C double bond in the acyl chain are most commonly seen in white matters.

1.2.1.1.2   Cholesterol

Cholesterol is the major sterol and accounts for ~20% of total lipids in the adult white matters (O'Brien and Sampson 1965). As shown in Figure 1.3A, it has a steroid linked with a hydrocarbon tail at its end and a hydroxyl group attached at the other end. During brain developing, especially the myelinating period, cholesterol is largely synthesized in the brain (Sastry 1985). Cholesterol plays an important role in lipid raft assembly and in regulating the biophysical properties of cellular membrane (Simons and Ikonen 2000).

A, Cholesterol

Phosphatidylcholine (PC)

Phosphatidylethanolamine (PE)

Phosphatidylserine (PS)

Phosphatidylglycerol (PG)

Phosphatidylinositol (PI)

Ceramide

Glycosphingolipid

Sphingomyelin
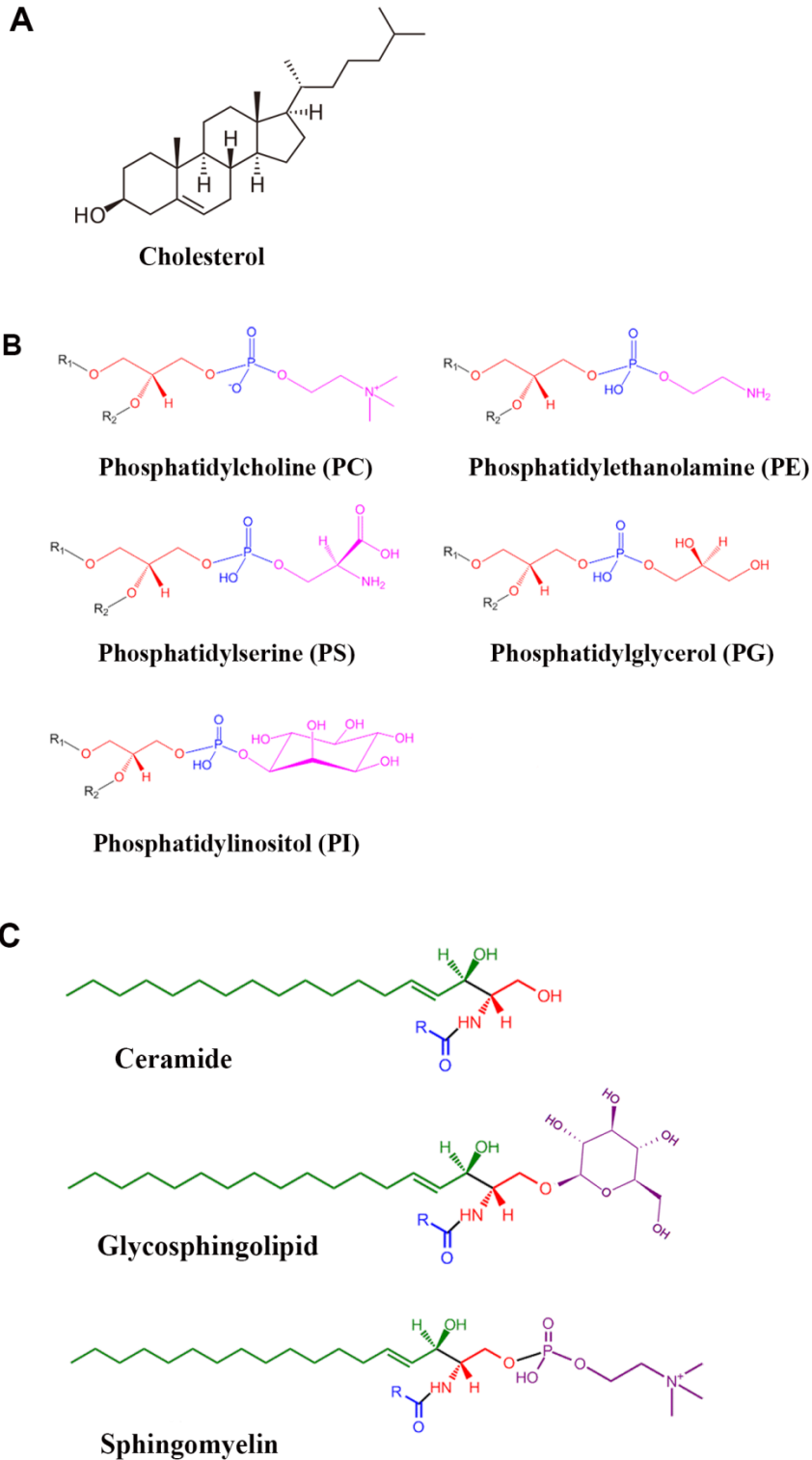
Figure 1.3 Representative chemical structures of three major myelin lipid classes

A, Cholesterol **B**, Phospholipid including phosphatidylcholine (PC), phosphatidylethanolamine (PE), phosphatidylserine (PS), phosphatidylglycerol (PG), and phosphatidylinositol (PI) **C**, Sphingolipid including ceramide (Cer), sphingomyelin (SM), glycosphingolipid.

1.2.1.1.3   Phospholipid

Phospholipids are derived from glycerol, in which the glycerol backbone is attached by fatty acids, a phosphate and a head group attached to the phosphate (Berg JM 2002). As shown in Figure 1.3.B, the head group, commonly include choline, ethanolamine, the amino acid serine, glycerol, and inositol, is linked to the phosphate via an ester bond to form several phospholipid subclasses, namely phosphatidylcholine (PC), phosphatidylethanolamine (PE), phosphatidylserine (PS), phosphatidylglycerol (PG), and phosphatidylinositol (PI), respectively. The two fatty acid chains are hydrophobic while the phosphoryl head group is hydrophilic and thus the phospholipid molecule is amphipathic. Total phospholipids account for about 30~40% of the total lipids in cerebral white matters and myelin (O'Brien and Sampson 1965) and PE, PC and PS are the three most abundant subclasses. Phospholipids are major structural components of membrane bilayers (van Meer, Voelker, and Feigenson 2008). Some of them are also bioactive lipids such as PS and PG (Kim, Huang, and Spector 2014) (Schenkel and Bakovic 2014). Lysophospholipids are derivatives of phospholipids where one acyl chain is missing and only one hydroxyl group of glycerol backbone is acylated (D'Arrigo and Servi 2010). Lysophospholipids are found only in small amounts in cellular membranes, acting as bioactive lipids in regulating various signalling processes (D'Arrigo and Servi 2010).

1.2.1.1.4   Sphingolipids

Sphingolipids are a class of complex lipids that contain a sphingoid base as its backbone (Figure 1.3C). Modification of this basic structure gives rise

to a vast family of sphingolipids including sphingosine, ceramides (Cer), sphingomyelin (SM), and glycosphingolipids as the major subclasses of sphingolipids. These subclasses of sphingolipids are interconvertible in sphingolipids metabolism (Hannun and Obeid 2008). Sphingolipids are components of all membranes but they are particularly abundant accounting for ~30% of the total lipids in white matters.

1.2.1.1.4.1   Ceramide

As shown in Figure 1.4, ceramides are synthesized do novo firstly from serine and palmitate to form the 3-keto-dihydrosphingosine through the action of palmitoyl transferase (SPT) (Sastry 1985). Then 3-ketohydrosphingosine is reduced to dihydrosphingosine. Ceramide synthases (CerS) then introduce a fatty acyl chain that may vary in the number of carbons (mainly 16-26C in the brain) to the C-2 amino group using acyl-CoA as substrate, producing the dihydroceramides. Ceramide is formed by desaturation via desaturase. Six members of CerS have been identified, namely CerS1-6 (Imgrund et al. 2009). Each of them has its special preference for fatty acid residue. It has been shown that CerS2 and CerS4 prefer very long chain (VLC) acyl-CoAs (C22-24 and C20 respectively), while CerS5 and CerS6 show a preference for shorter acyl-CoAs (C14-16). CerS1 uses long chain (LC) acyl-CoA (18C) mainly in neurons. CerS3 may be related with ultralong-chain (>C26) in the skin (Zigdon et al. 2013) (Jennemann et al. 2012). Ceramide is the central hub of sphingolipid metabolism. Glycosphingolipids, sphingomyelin and sphingosine are the derivatives of ceramide in the biosynthetic pathways of sphingolipids.
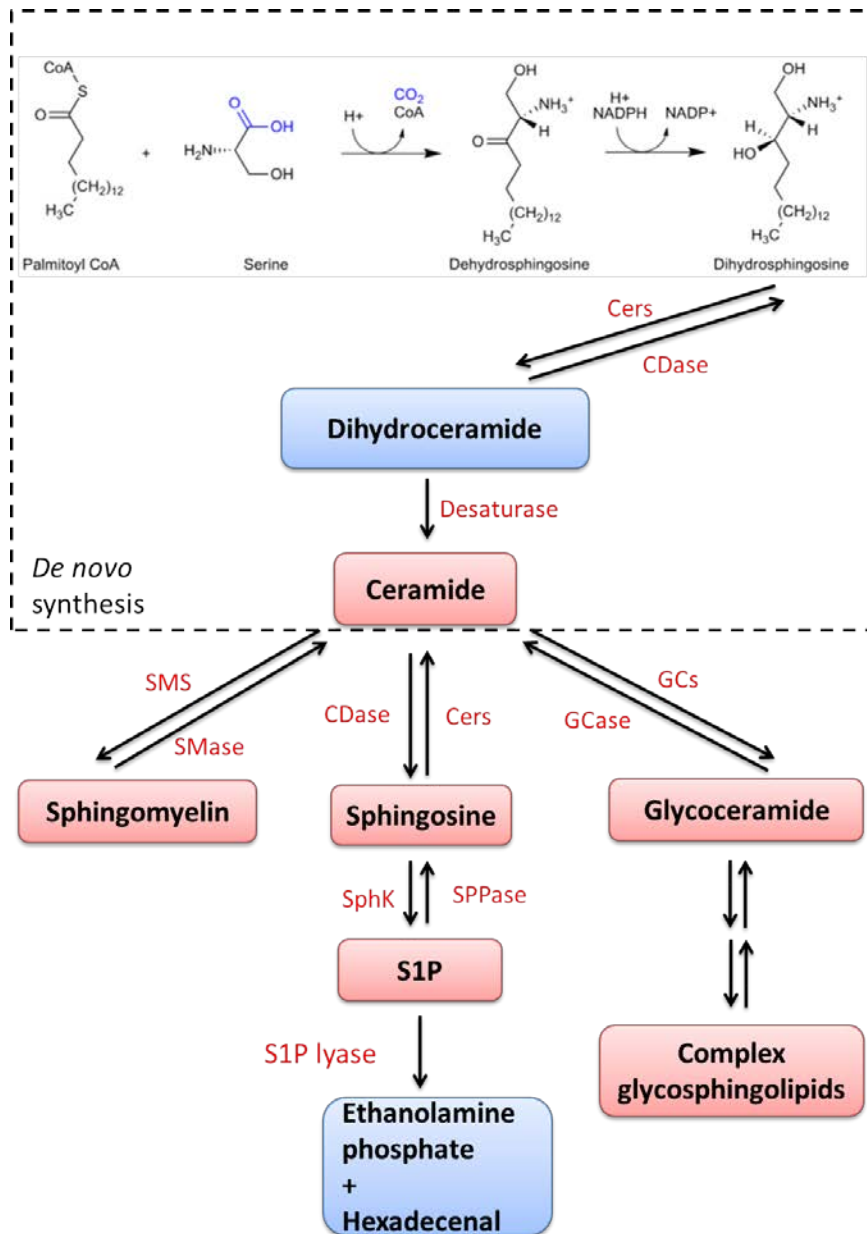
Figure 1.4 *De novo* synthesis of ceramide and sphingolipids metabolism
The *de novo* synthesis of ceramide is shown in the dotted box: Palmiate-CoA and serine condensation to form the dehydrosphingosine, followed by reduction to dihydrosphingosine. Then CerS adds an acyl chain to form dihydroceramide which is desaturated to become ceramide. Ceramide is considered to be the hub of sphingolipid metabolism, in which it can be converted to sphingomyelin and glycoceramide or more complex glycosphingolipids by SMS and GCs respectively. CDase uses ceramide as substrate to synthesize sphingosine that can be phosphorylated to S1P further. S1P lyase degrades S1P to ethanolamine phosphate and hexadecenal, which is the only exit point of sphingolipid metabolism. Abbreviations: CerS, ceramide synthase; CDase, ceramidase; SMS, sphingomyelin synthase; SMase, sphingomyelinase; GCs, glycosyl ceramide synthases; GCase, glycosyl ceramidase; S1P, sphingosine-1-phosphate; Sphk, sphingosine kinase; SPPase, sphingosine phosphate phosphatase.

18

1.2.1.1.4.2   Glycosphingolipid

Glucosylation and galactosylation of ceramide by glucosyl or galactosyl ceramide synthases (GCs) lead to the formation of glucosylceramide (GluCer) and galactosylceramide (GalCer), which are the two most abundant subclasses of glycosphingolipids. Glycosphingolipids are major component of myelin, accounting for 15-20% of the total lipids in the brain (Sastry 1985). It has been shown that the concentrations of glycosphingolipids in white matters and in myelin are, respectively, about 5-fold and 10-fold higher than those in grey matters (O'Brien and Sampson 1965). One or more monosaccharides can be added to hexolceramides (GluCer or CalCer) forming dihexolceramide (Lactoceramide) or more complex glycosphingolipids.

Sulfatides, produced by cerebroside sulfotransferase, are sulfate esters of galactocerebrosides at C-3 of the galactopyranoside moiety (Winzeler et al. 2011). They are primarily found within myelin, accounting for 4-6% of the total lipids in brain (Norton and Poduslo 1973). It is reported to be important for the maintenance of CNS myelin (Marcus et al. 2006).

Gangliosides are a group of complex sialic acid-containing glycosphingolipids which is substantially concentrated in grey matters. Several studies have shown that it might be involved in AD and angiogenesis in tumour growth (Yu et al. 2011).

1.2.1.1.4.3   Sphingomyelin

Upon synthesis on the cytosolic surface of the endoplasmic reticulum (ER), ceramide is transferred to Golgi apparatus where the bulk of ceramide receives a phosphocholine headgroup from PC to form sphingomyelin. This

process is catalyzed by a SM synthase (SMS) (Tafesse, Ternes, and Holthuis 2006). SM is a major lipid of the myelin membrane. It has been reported that during the myelinating period in brain development, the proportion of SM in myelin remained unchanged (O'Brien and Sampson 1965) while the fatty acid pattern of SM shows significant alteration (Svennerholm and Vanier 1973). The long acyl chain SM d18:1/18:0 decreased significantly from 82% to 33% and the very long acyl chain SM d18:1/24:1 increased significantly from 4% to 33% in white matters, suggesting the fatty acid pattern of SM plays an essential role in myelination.

1.2.1.2 Major protein in myelin

The protein composition of CNS myelin is unique when compared to other brain membranes, where the proteolipid protein and basic protein(s) making up 60 to 80% of the total protein.

1.2.1.2.1   Proteolipid protein (PLP)

PLP is the most abundant protein which accounts for more than half the total protein in CNS myelin (Quarles 2005). The full length PLP gene encodes a 276 amino acid with a molecular mass of 30 kDa. PLP is a tetraspan protein, with four transmembrane α-helices spanning the myelin membrane (Quarles 1999). DM20 is a minor isoform of PLP that arose from an alternative splicing of the gene, sharing complete sequence except for a 35 amino acid segment (Greer and Lees 2002). PLP/DM20 is extremely hydrophobic with net basic charge. Its hydrophobic character is further increased by the presence of 3 fatty acids, primarily palmitate, oleate or stearate in ester linkage to hydroxy amino acids (Quarles 1999).

In the CNS, PLP/DM20 is expressed by OLG on polysomes as mature protein directly and then transferred to the cell surface where they are incorporated into compact myelin (Greer and Lees 2002). Therefore, PLP/DM20 is thought to be involved in membrane adhesion and compaction of myelin by forming the double-spaced intraperiod line (Greer and Lees 2002).. It has been reported that mutation of PLP leading to the absence of PLP/DM20 in mice could induce hypomyelination due to premature deaths of OLG (Quarles 2005). However, PLP/DM20 -null mice can still form compact myelin sheaths but subsequently develop axonal swellings and degeneration, suggesting dysfunctions in maintenance and survival of axons (Griffiths et al. 1998).

1.2.1.2.2   Myelin basic protein (MBP)

MBP is a water soluble, positively charged extrinsic membrane protein, account for 30% of the total protein in CNS myelin (Quarles 2005). MBP has several isoforms ranging from 14 kD to 21.5 kD, arising from different transcription start site and also differential splicing of the oligodendrocyte lineage gene (golli) (Harauz, Ladizhansky, and Boggs 2009). The isoform of 18.5 kD is the predominant isoform in human mature myelin and therefore is classically considered to be of importance for myelin development and stability. It is located on the cytoplasmic leaflets of the OLG corresponding to the major dense line in myelin (Quarles 1999). However, increasing evidence has demonstrated that MBP is involved in not only membrane adhesion, but also in regulating OLG maturation and their myelin forming behavior (Hartman et al. 1982; Harauz, Ladizhansky, and Boggs 2009; Harauz and Boggs 2013). The absence of, or greatly reduced MBP in mice

would cause severe hypomeylination in CNS (Quarles 2005). Although the sequence of the MBP gene is highly conserved among mammalians, rodents appear to have a more complex system due to the existence of more MBP isoforms (Fannon and Moscarello 1991), with 14 kD-MBP being the predominant isoform in mature mice and rats. According to Fannon et al., the ability to produce the smaller and more cationic 14 kD-MBP may explain the rapid and shorter myelination period in rodents (Fannon and Moscarello 1991). Nevertheless, the variability of MBP in rodents is yet to be elucidated.

1.2.1.3 Synthesis of myelin components and initiation of myelin biogenesis

Figure 1.5 shows a scheme of the development of OPC to mature OLG (Nishiyama et al. 2009). First of all, oligodendrocyte progenitor cells (OPCs), characterized by the expression of neuron-glial antigen 2 (NG2) and platelet-derived growth factor alpha (PDGFRα) (but not MBP), begins their terminal differentiation and stop expressing NG2 and PDGFRα and thus transformed into premyelinating oligodendrocytes (pre-OLGs), characterized by the expression of O4 and GalCer (but still not MBP) (Nishiyama et al. 2009). This process has been thought to be regulated by inhibitory neuronal signals and complex regulators that can switch on myelin gene expression (Aggarwal, Yurlova, and Simons 2011).

The biogenesis of myelin requires major remodelling of the OLG plasma in which OLG delivers different components to the growing myelin sheath and undergoes cell-surface polarization (Maier, Hoekstra, and Baron 2008). In this stage, OLG generates large myelin-membrane sheets which are highly asymmetric and similar to compact myelin. It has been reported that MBP

contains a high density of positive-charges and can readily interact with the negatively charged cellular membrane. MBP's ability to compact cellular membrane is essential for myelin sheath formation while it is problematic for the integrity of intracellular membrane such as ER and Golgi apparatus (Muller et al. 2013). Therefore, OLG transform mRNA of MBP instead of the protein to cytoplasmic membrane. MBP is only expressed by myelinating OLG.

OPC(NG2+,PDGFα+
GalCer-,MBP-)

Proliferation

Premyelinating
OLG (NG2-, PDGFα-
O4+, GalCer+,MBP-)

Myelinating
OLG
(NG2-, PDGFα-,
GalCer+, MBP+)

Differentiation
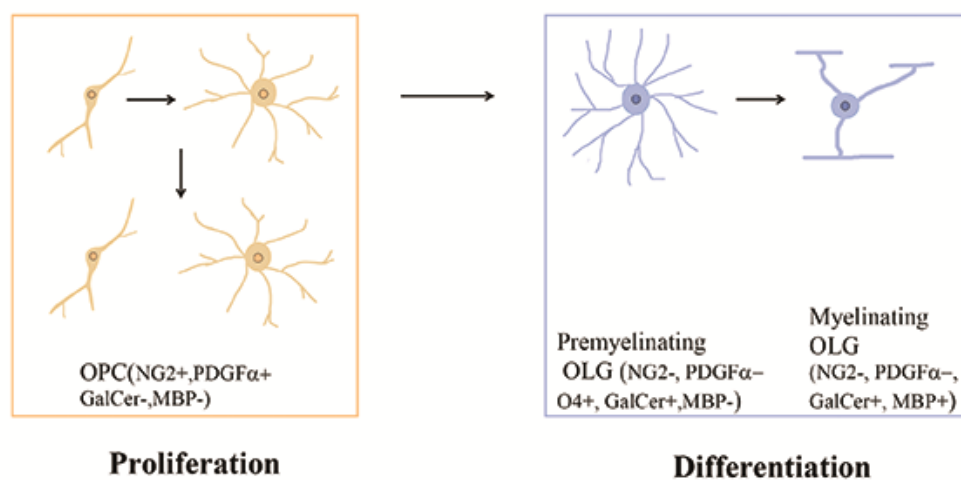
Figure 1.5 A scheme showing development of OPC to mature OLG
The two markers for polydendrocytes, NG2 and platelet-derived growth factor receptor-alpha (PDGFRα), are expressed by proliferating progenitor cells of the oligodendrocyte lineage. As OPCs undergo terminal differentiation into mature oligodendrocytes, they lose the expression of NG2 and PDGFRα and begin to express the immature oligodendrocyte antigen O4, followed by galactoceramide and subsequently myelin basic protein (MBP). Only myelinating OLG expresses MBP. Adapted from (Nishiyama et al. 2009).

1.2.1.4 Membrane structure of myelin

Myelin is a remarkably stable multilayered membrane structure assembled by the cytoplasmic membrane of mature OLG. As mentioned above, the basic membrane structure is composed of hydrophobic lipids such as glycosphingolipids and phospholipids and highly hydrophobic PLP

(Aggarwal, Yurlova, and Simons 2011) (Figure 1.1). Myelin components including lipids and proteins are not evenly distributed in the membrane. It has been widely accepted that different domains of different composition and physical properties can coexist within the bilayer (Gielen et al. 2006). Like from every cell type, there are the liquid-ordered membrane microdomains known as 'lipid raft' and fluid-liquid domains in the plasma membrane of OLG. Lipid raft is a cluster of sphingolipids and cholesterol in which sphingolipids associate laterally with one another and cholesterol filled the voids between the sphingolipids (Simons and Ikonen 1997). The closely-packed sphingolipid–cholesterol lipid rafts predominantly localized within the exoplasmic leaflet. Whereas fluid-liquid domains are consisted of phospholipid molecules (Simons and Ikonen 1997). Lipid rafts in myelin are reported to mediate sorting, trafficking and maintaining of the major myelin proteins (Maier, Hoekstra, and Baron 2008). It has been suggested that OLG produces GalCer and sulfatide prior to synthesizing PLP and MBP when they begin terminal differentiation (Aggarwal, Yurlova, and Simons 2011). Moreover, rafts provide signaling platforms important for regulation of myelin-related processes (Maier, Hoekstra, and Baron 2008). The gel- to liquid-crystalline phase transition temperature (T_m) of glycosphingolipids is usually very high compared to corresponding PC or SM, and it contributes to stabilizing lipid raft domains due to irreversible transitions into stable gel phases (Westerlund and Slotte 2009). Interdigitation describes the phenomenon whereby membrane may insert the methyl ends of long fatty acids from one side across the bilayer mid-plane to protrude amongst the acyl chains of the opposite side of the bilayer (Mehlhorn et al. 1988). It

24

normally occurs when the membrane lipids contains two acyl chains with significantly different length. Sphingolipids are the most common family of lipids with asymmetric acyl chains and therefore, interdigitation is supposed to occur in domains rich in sphingolipids (Boggs and Koshy 1994). Interdigitation of glycosphingolipids is thought to be one of the possible mechanisms of its membrane domains stabilizing function (Westerlund and Slotte 2009).

In compact myelin membrane, the hydrophobic molecules exert a repulsive force towards the aqueous cytosol and extracellular fluid. In addition to the repulsive forces, hydrogen bonds and Van de Waals dispersion forces provide intermolecular attractive forces. Hydrogen bonds are formed by the amide and free hydroxyl groups of glycosphingolipid located preferentially on the extracellular membrane in the vicinity of the lipid–water interface. Van der Waals forces are formed by interactions between the methylene groups in acyl chains of adjacent lipids molecules. Besides, the highly positively-charged extrinsic MBP interacts with the negatively charged lipids and thus brings the two bilayers closer together at the cytoplasmic membrane surfaces, forming the major dense line. It is believed that the stability of tightly packed myelin membrane is the result of a delicate balance between the repulsive forces and the attractive forces (Ohler et al. 2004) (Westerlund and Slotte 2009). Disturbance of the balance could disrupt normal myelin structure (Bradl 1999). The energy of the repulsive and attractive forces is associated with the biophysical properties and the composition of myelin lipids and proteins. For example, changes in the headgroup area of glycolipids can lead to changes in the curvature and

consequently contribute to change of adhesion between the bilayer (Ohler et al. 2004). Another example is that long acyl chain (LC) - sphingolipids have lower melting temperature than very long acyl chain (VLC) -sphingolipids, contributing to high membrane fluidity (Niemela, Hyvonen, and Vattulainen 2006). Therefore, an appropriate proportion of myelin components might be of particular importance in maintaining the myelin structure.

1.2.1.5 Lipid alteration in SIVD patients

Recently, the brain lipidomes of non-demented, SIVD and mix dementia patients have been analysed by liquid chromatography coupled to tandem mass spectrometry, providing relatively comprehensive knowledge of the lipid composition and changes of white and grey matters in these brains (Lam et al. 2014). The lipidome of SIVD appeared to be characterized by changes mainly in sphingolipids in the white matters including sphingolipid fatty acyl chain heterogeneity. There were decreases in Cer, GalCer and increases in PS and PG in the overall content.

1.2.2   Pathophysiology of WML

1.2.2.1 Non-vascular origins of WML

1.2.2.1.1   Age-related white matter changes

Age is almost no doubt a strong risk factor of white matter lesions. WMC are regularly found in community elderly with prevalence ranging from 50% to 98% (Xiong and Mok 2011). A population-based MRI Rotterdam Study including 1077 subjects aged between 60-90 years reported that only 5% of all subjects had no WML in periventricular or subcortical regions and the proportion with white matter lesions increased with age(de Leeuw et al. 2001). In the LADIS Study that enrolled 639 patients aged between 65 and

84 years, who, while being investigated for complaints minor neurological problems such as mild memory minor cerebrovascular events, age has also been reported to be significantly associated with WML(Inzitari et al. 2007). A very recent population-based study conducted in Japanese elderly people also s revealed that older age are significant predictors of severe WML(Yamawaki et al. 2015).

1.2.2.1.2   Autoimmune inflammation disease

Multiple sclerosis (MS) is an autoimmune inflammatory disease characterized by scattered lesions and demyelination in the white matter (Bruck 2005). MS is the most common human demyelinating disease. A series of immunopathological events are initiated, amplified and finally invaded of CNS parenchyma resulting in damaging of oligodendrocytes, myelin sheath and axons(Podbielska et al. 2013). Activated lymphocytes, macrophages, microglia can be observed in the white matter from multiple sclerosis brains (Bruck 2005). OLG death induced by inflammatory attack and recurrent immune attacks is one of the important pathophysiology of demyelination in MS (Patel and Balabanov 2012). Besides, inadequate remyelination process significantly contribute to lesions that remain largely or entirely demyelinated as well(Franklin 2002).

1.2.2.2 Vascular origins of WML

Pathologically, WML are characterized by partial loss of myelin, axons, and oligodendroglial cell; astrocytic gliosis and microglia activation. WML are also seen in small vessel diseases associated with stenosis resulting from hyaline fibrosis (Ferrer 2010).   The etiology of WML is yet to be fully

understood. But most evidence has suggested that WML is a result of incomplete ischemic injury.

1.2.2.2.1   Vascular risk factors of white matter lesions

Hypertension is an established risk factor for WML(Xiong and Mok 2011). Liao et al has shown that hypertension is associated with increased odds of WML in the ARIC study which contained a random sample of 1920 participants aged 55 to 72 years (Liao et al. 1996). In a prospective cohort study, duration of hypertension has been found to associate with WML and subjects with successfully treated hypertension had only moderately increased rates (de Leeuw et al. 2002).

Other vascular risk factors of white matter lesions include homocycteine level (Vermeer et al. 2002; Shimomura et al. 2008; Pavlovic et al. 2011), diabetes mellitus (van Harten et al. 2007), atherosclerosis(Manolio et al. 1999; Pico et al. 2002). However, these risk factors are less consistent since several studies reported negative associations (Longstreth et al. 2004; Suwa et al. 2015; Falvey et al. 2013). Besides, low vitamin B6 levels are reported to be associated with WML in dementia patients(Mulder et al. 2005) since adequate vitamin B6 levels are important for the conversion of homocysteine into cysteine(Selhub 1999). The inconsistency of these studies may be due to that these studies were mostly conducted in patients with all kinds of cerebral diseases, diabetes and etc. Therefore it's difficult to control confounding factors.

1.2.2.2.2   White matters lesions and ischemia

Historically, white matters are considered less vulnerable than grey matters to ischemic injury induced by a large-artery occlusion (Marcoux et al.

1982). However, several research have indicated that ischemia may primarily involve white matters capsular infarcts in subcortical areas (Bogousslavsky and Regli 1992) and extensive symmetrical necrotic lesions of the central white matters with minimal damage to grey matters (Ginsberg, Hedleywhyte, and Richardson 1976). Anoxic-ischemic effects due to carbon monoxide exposure induced characteristic white matter lesions in both humans and animals in the absence of grey matter damage (Pantoni, Garcia, and Gutierrez 1996). In addition bilateral common carotid artery (BCCA) occlusion in rats have been widely reported to cause mainly white matter lesions with little damage to grey matters (Wakita et al. 2002) (Kawaguchi et al. 2002) (Ohta et al. 1997). Recently, a mouse model of BCCA stenosis has been developed which induces only selective WML without grey matter injury (Shibata et al. 2004; Shibata et al. 2007).

1.2.2.2.3   Oligodendrocyte and ischemia

OLG and myelinated axons are components of white matters that are highly vulnerable to ischemia. Pantoni et al. reported that OLG swelling occurred as early as 30 minutes after middle common carotid artery occlusion (MCAO) (Pantoni, Garcia, and Gutierrez 1996). Besides, OLG showed greater vulnerability than neurons in the cerebral cortex and thalamus after transient global ischemia in rat (Petito et al. 1998). OLG is rich in microtubules as microtubules are important for transporting myelin proteins to their processes. Ischemia can induce a rapid increase of the immunoreactivity of the microtubule-associated protein, tau (Dewar and Dawson 1995) (Irving et al. 1997) in 40 minutes after the onset of ischemia.

In vitro, primary OLGs are less vulnerable than neurons but are more quickly injured than other glia cells including astrocytes, microglia, or endothelial cells under similar hypoxic conditions such as oxygen glucose deprivation (OGD) (Dewar, Underhill, and Goldberg 2003). Additionally, immature oligodendrocytes which express O4 have been reported to be more vulnerable than mature oligodendrocytes under OGD (Fern and Moller 2000).

1.2.2.2.4   Blood supply to white matters

In small vessel disease, stenosis of blood vessels due to thickening of the vessel wall and/or accumulation of type IV collagen leads to blood vessel occlusion, resulting in a chronic state of hypoperfusion in the region served by the occluded vessels. WM receive most of its blood supply through long penetrating arteries from the brain surface and anastomoses between the penetrating arteries are scarce or absent. As a result, WM is highly vulnerable to ischemia when these penetrating vessels are occluded for lack of collateral supply (Pantoni 2002) (Ferrer 2010) (Pantoni and Garcia 1997a).

1.2.2.3 Mechanism of oligodendrocyte injury in ischemic WML

Development of therapeutic approaches to ischemic WML requires improved understanding of the mechanisms for ischemic injury to OLG. Several mechanisms including oxidative stress, excitotoxicity, inflammation and apoptosis have been shown to initiate oligodendrocyte injury under hypoxic–ischemic conditions.

1.2.2.3.1   Oxidative stress

In ischemia or hypoxia, oxidative stress occurs when the balance between oxidants and antioxidants is disturbed, leading to oxidative cellular damage (Valko, Leibfritz et al. 2007). White matters seem to be especially

sensitive to oxidative stress due to the high content of lipids, high iron content, and decreased antioxidant enzymes in OLGs (Dewar, Underhill, and Goldberg 2003). Free radicals can remove a hydrogen atom from a methylene group of a fatty acid, leaving the fatty acid carbon with an unpaired electron. In aerobic conditions, the carbon radical can react with oxygen to produce a peroxyl radical, which is reactive enough to remove hydrogen from fatty acid side chains to form a lipid hydroperoxide and carbon radical. This process known as lipid peroxidation, once initiated, can lead to the formation of many lipid hydroperoxides (Benzie 1996). The serum levels of lipid peroxidation markers such as 4-hydroxynonenal (4- and malondialdehyde are associated with cognitive deficits in AD and VCI patients (Casado, Encarnacion Lopez-Fernandez et al. 2008, Torres, Quaglio et al. 2011). Therefore, lipid peroxidation may play a role in the pathogenesis of dementia of the Alzheimer's type (AD) and vascular dementia. Miyamoto et al. (Miyamoto, Maki, et al. 2013) has shown an increase of reactive oxygen species (ROS) in cerebral WML induced by chronic hypoperfusion in mice. In addition, early oligodendrocyte lineage cells have been shown to be even more vulnerable to oxidative stress than mature OLG *in vitro* (Dewar, Underhill, and Goldberg 2003). In addition, elevated oxidative stress interfered with OPC differentiation and thus could attenuate white matter renewal *in vivo* (Miyamoto, Maki, et al. 2013).

1.2.2.3.2   Inflammation

Inflammatory response in the regions of myelin loss in VCI patients has been demonstrated (Rosenberg 2009). Microglia activation and matrix metalloproteinase (MMP) elevation have been observed in patients with VaD

31

(Akiguchi et al. 1997) (Rosenberg, Sullivan, and Esiri 2001) and in experimental WML of animals (Farkas et al. 2004; Watanabe et al. 2006). Small vessel disease could lead to blood-brain barrier (BBB) damage and chronic leakage of fluid and macromolecules in the white matters (Pantoni 2002). BBB permeability has been found in patients with WML (Xiong and Mok 2011) and experimental ischemic WML (Ueno et al. 2002) (Jalal et al. 2012). Disruption of BBB can cause the production of several inflammatory substances, leading to further white matter injury (Rosenberg 2009).

Cytokines including interleukins 1–10, tumor necrosis factor α (TNF-α), and interferon γ (INF-γ) can be produced by macrophages and lymphocytes in inflammatory tissues (Feghali and Wright 1997). Activation of cytokine receptors has been reported to induce oligodendroglial death in adult demyelinating disorders (Casaccia-Bonnefil 2000).

In addition OPC is sensitive to inflammatory injury such as cytokine (Baerwald and Popko 1998), which impairs their proliferation or differentiation abilities of myelin repair.

Other inflammatory mediators are also reported to be involved in hypoperfusion-induced WML. Liu et al. (Liu et al. 2013) found that C5 complement protein, a potent inflammatory mediator, deposited in white matter of mouse subjected to chronic hypoperfusion and worsen the WML.

1.2.2.3.3   Apoptosis

Apoptosis is programmed cell death which is highly regulated (Kerr, Wyllie, and Currie 1972). It can be beneficial for helping body to eliminated dysfunctional cells or destructive for inducing undesired cell death and tissue damage (Thompson 1995). Bcl-2 protein family are well-established key

regulators of apoptosis (Czabotar et al. 2014). They can be divided into subfamilies of proapoptotic molecules such as Bax and BaK or prosurvival molecules such as bcl-2 and Bcl-Xl (Martin and Elkon 2004). Apoptosis is well-known to depend on the cell death execution of cysteine-requiring aspartate-directed proteases (caspases) (Kumar 2007). During cerebral ischemic injury, apoptosis can occur through two pathways: the intrinsic and extrinsic (Unal-Cevik et al. 2004). In intrinsic pathway, cerebral ischemia increases cytosolic calcium levels that could induce truncated Bid (tBid). tBid interacts with Bak and Bax located to the outer membrane of mitochondria, causing mitochondrial membrane rupture and cytochrome c releasing (Eskes et al. 2000). Then caspases-9 and subsequently caspases-3 are activated, which leaves nDNA repair enzyme leading to DNA damage and apoptosis (Kumar 2007). In extrinsic pathway, cerebral ischemia induces forkhead family of transcription factors and its target genes such as Fas ligand (FasL) that triggers recruitment of the Fas-associated death domain protein (FADD). FaDD activates cascade of caspases resulting in apoptosis (Martin-Villalba et al. 1999).

A number of studies have reported an increase of apoptotic cells, predominantly OLGs, in autopsy brain slices from patients with WMLs (Brown et al. 2000; Brown et al. 2002). It has been reported that chronic cerebral hypoperfusion induced WMLs in association with up-regulation of apoptotic signaling such as TNF-alpha and Bax and DNA fragmentation in OLG (Tomimoto et al. 2003). Shibata et el. has reported that inhibition of caspases in OLG of a transgenic mouse line that selectively expresses p35, a broad-spectrum caspase inhibitor significantly reduced ischemia-induced cell

injury in vivo (Shibata et al. 2000). Besides, glutamate toxicity can contribute to the oligodendroglia apoptosis via caspase-3 activation (Ness and Wood 2002).

1.2.2.3.4   Failure in OPC differentiation

Advances in understanding the mechanism of brain injury and neurodegeneration such as excitotoxicity, oxidative stress, and apoptosis have provided a number of targets and drugs for neuronal disorders. However, almost all clinical trials of neuroprotectants for the treatment of acute stroke have failed (Lo 2010). There is an emerging concept that CNS pathophysiology is significantly influenced by a balance between initial injury and endogenous repair (Lo 2010). For example, ischemic brain injury can cause a wide spectrum of neurovascular deleterious responses. At the same time many endogenous neuroprotective responses such as compensatory neurogenesis, angiogenesis, neuroplasticity and vascular remodelling can occur (Miyamoto, Maki, et al. 2013). A central principle of regenerative biology is that processes controlling tissue generation during development often control its regeneration (Gallo and Deneen 2014). Although the most rapid and dramatic myelination in human brain occurs between midgestation and the end of the second postnatal year, it continues into the third decade in the brain (Kinney et al. 1994). Several researches have indicated that OPC can still generate myelin-forming mature oligodendrocytes in the adult cerebral white matters, sustaining the white matter homeostasis by endogenous repair and renewal process (Nishiyama 2007; Levine, Reynolds, and Fawcett 2001). OPCs react rapidly in response to various demyelinating injuries. They can proliferate and migrate to the

lesion sites (Polito and Reynolds 2005). OPC number decreases upon onset and progression of remyelination concomitant with appearance of BrdU+ mature oligodendrocytes have been reported (Watanabe, Toyama, and Nishiyama 2002; Reynolds et al. 2002), suggesting at least a part of OPCs differentiation into mature OLG. However, the extent and quality of endogenous remyelination is usually suboptimal because multiple factors could restrict the multiple remyelination steps including lacking of necessary factors that promote oligodendrogenesis, cell death among newly generated OLG, inhibitory factors from the post –injury environment that impede remyelination and deficient expression of the key growth factors for proper re-construction of myelin sheaths (Alizadeh, Dyck, and Karimi-Abdolrezaee 2015). Miyamoto et al. (Miyamoto et al. 2010) have shown that chronic hypoperfusion causes WML and significant OPC generation. However the differentiation of the newly produced OPC has been disrupted in vivo and in vitro where chemical hypoxic reagent $CoCl_2$ which act as HIF-1α stabilizer can attenuate primary OPC differentiation (Miyamoto et al. 2010). Edaravone, a radical scavenger, can rescue OPC differentiation, ameliorate myelin loss, and restore working memory function (Miyamoto et al. 2010). However, clinical trials of antioxidants in treating VCI are disappointing (O'Brien et al. 2003). Therefore, investigations into alternative mechanisms and signalling pathways that involved in this hypoxia-induced differentiation disruption may be of great importance in understanding and repairing WML for therapeutic purposes.

1.2.3 Animal models of WML

In order to further understand the pathogenesis, pathology, molecular mechanism of WMLs, a number of animal models for white matter damage have been developed. In terms of similarity to human WMLs, models using those gyrencephalic species such as rabbits, dog, cats and sheep may appear to have some advantages over the rodent models (Hagberg, Peebles, and Mallard 2002). However, rodents are more widely available, less expensive and more used by researchers than any other species. Here, we focus on the rodent models. These models are generally divided into three categories: ischemia/hypoperfusion, infection/inflammation and excitotoxicity models.

1.2.3.1 Ischemia/hypoperfusion models

In ischemic models, hypoperfusion of focal or global can be induced by occlusion or stenosis of the common carotid arteries (Choi et al. 2011) (Jiwa, Garrard, and Hainsworth 2010).

Rat permanent bilateral common carotid artery occlusion or ligation (pBCCAO or pBCCAL) (Ni et al. 1994), and mouse bilateral carotid stenosis (BCAS) (Shibata et al. 2004) belong to the global hypoperfusion models. They can be further divided into chronic or transient models according to whether there is reperfusion. Middle cerebral artery occlusion (MCAO) (Roof et al. 2001) is a popular focal ischemia model which is widely used in stroke studies. It can induce cortical, caudate and subcortical white matter lesions.

In the vessel occlusion models above, white matter lesions are consistently reported. Histological examinations show demyelination (Pantoni, Garcia, and Gutierrez 1996; Wakita et al. 2002), loss of myelin

basic protein (Walker and Rosenberg 2010) and microglial and astrocyte activation (Farkas et al. 2004). Cognitive impairment has also been observed in these models (Ni et al. 1994) (Ohta et al. 1997) (Shibata et al. 2007). Besides the white matter lesions, grey matter lesions and neuronal loss are sometimes observed in relatively more severe ischemia models such as pBCCAo in rats, tMCAO (Ohtaki et al. 2006) (Pappas et al. 1996). Besides, transient MCAO is more suitable to be used as a stroke model since it mainly induces large infarcts in cortex instead of diffused WML in subcortical region. pBCCAo or pBCCAL in rats can produce a chronic reduction in CBF by 50% to 70% (Hainsworth and Markus 2008), which could be too severe for mice resulting in low survival rate during the surgery.

BCAS was first introduced by Shibata et al. (Shibata et al. 2004). A ~30% of CBF reduction was induced by two external microcoils with an inner diameter of 0.18mm. WM lesions in the corpus callosum, the anterior commissure and optic tract occurred after 14 days without any grey matter involvement. Therefore BCAS is a suitable vascular WML model in mice with its selective injury in white matters (Shibata et al. 2004) and is now widely used.

Except for these vessels occlusion models, stereotaxic vasoconstrictor endothelin-1 (ET-1) injection also induces transient focal lesions. Hughes et al. (Hughes et al. 2003) reported an acute reduction in local MRI perfusion in the injected hemisphere after 1 hour, oligodendrocytes showed enhanced Tau-1 staining throughout the lesioned cortical white matters from 6 hours, a loss of neurons observed after 24h in grey matters. However, no disruption of the BBB was observed. Frost et al. (Frost et al. 2006) have shown after

careful control of the amount and time course of ET-1, white matter lesion could be confined to a small area, where demyelinated and tissue necrosis were observed.

Cerebral autosomal dominant arteriopathy with subcortical infarct and leukoencephalopathy (CADASIL) is a cerebrovascular small-vessel disease caused by mutations of the Notch3 gene in chromosome 19 (Joutel et al. 1996). It is characterized by frequent migraine attacks, recurrent strokes, progressive white matter degeneration resulting in early-onset of VCI and progressing into VaD later in life (Ayata 2010) . Notch3 gene is a member of a transmembrane receptor family (Drosophila notch homologues 1 to 4) and is predominantly expressed by vascular smooth muscle cells (Joutel et al. 2010). Notch signaling plays a fundamental role in regulating cell fate including differentiation, proliferation, and apoptotic programs (Artavanis-Tsakonas, Rand, and Lake 1999).To date Notch3 knockout mouse models and 4 Notch3 mutant mouse models expressing common CADASIL mutations have been developed (Ayata 2010). CADASIL Notch3 knockout or transgenic mice show progressive white matter damages (Joutel et al.), providing insight into the nature of Notch 3 in CADASIL pathologies and in smooth muscle degeneration for vascular dysfunction, and the relevance of vascular dysfunction for WML (Ayata 2010) non-ischemic WML models.

1.2.3.2 Infectious/inflammatory models

Lipopolysaccharide (LPS) is the infectious agent most often used to produce white matter damage in developing brains (Juskewitch et al. 2012) partly through activation of toll-like receptor 4 on immune cells with

initiation of a generalized inflammatory response (Aderem and Ulevitch 2000).

1.2.3.3 Excitotoxicity models

Brain lesion in the white matters can also be induced by excitatory amino acid receptor agonist supporting the excitotoxicity hypothesis of WMLs. Marret et al. reported that subcortical injection of ibotenate, a glutamatergic agonist, could induce injury in white matter (Marret et al. 1995). However, excitotoxicity models show little specificity towards inducing white matter damages (Nishio et al. 2010).

Disrupter energy metabolism is one of the major events leading to nerve cell damage in neurological abnormalities. Several mitotoxin injection models are developed in which white matter lesions had been observed. McCracken et al. (McCracken, Dewar, and Hunter 2001) showed systemic injection of the mitochondrial inhibitor 3-nitropropionic acid could induce white matter lesions including axonal bulbs and swellings within the striatal white matter tracts. It is questionable if this type of models shows any particular specificity towards WML.

1.3   Sphingosine-1-phosphate: A Bioactive Sphingolipid

Sphingolipids are named after Sphinx, a Greek mythological creature due to its mysterious nature. Over more than 100 years later we have obtained increasing understanding of other sphingolipids such as ceramides, glycosphingolipids and sphingomyelin, while we are now starting to learn more about sphingosine-1-phosphate (S1P). It is derived from sphingosine, and was originally thought to be only an intermediate in the metabolism of sphingolipids, it is now becoming as a prominent lipid regulator mediating several important physiological and pathophysiological processes in higher organisms such as cell growth and programmed cell death (Spiegel and Milstien 2003).

1.3.1   S1P synthesis and degradation

Similar to other signaling molecules, the amount of S1P in tissues is low in the region of several magnitudes smaller than other sphingolipids. Trace signaling molecules interact with high-affinity receptors that are capable of sensing their low levels (Hannun and Obeid 2008). Thus S1P levels in cells have to be precisely regulated. Sphingosine kinase (SphK) is the enzyme that catalyzes the sphingosine phosphorylation to form S1P (Spiegel and Milstien 2003). S1P can be dephosphorylation reversibly back to sphingosine by specific S1P phosphatase SPP. Another degradation pathway is irreversible in which a pyridoxal phosphate-dependent S1P lyase (Spl) degrades S1P to hexadecenal and phosphoethanolamine (Spiegel and Milstien 2003). This Spl degradation breaks down S1P into non-sphingolipid molecules and is the unique exit point of the whole sphingolipid metabolism (Hannun and Obeid 2008).

1.3.1.1 Sphingosine Kinases

1.3.1.1.1   Two isoforms of Sphingosine Kinase: SphK1 and SphK2

Two isoforms of SphK have been identified. In humans, although the SphK1 and SphK2 genes are located on different chromosomes, chromosome 17 (17q25.2) and 19 (19q13.2) respectively, the two isoforms are highly homologous with five conserved domains (C1-C5) (Bryan et al. 2008). C1-C3 contains the conserved catalytic domain similar to diacylglycerol kinase and ceramide kinase. C2 contains the ATP binding domain at SGDGX(17-21)K(R) sequence (Pyne et al. 2009). The unique sphingosine recognition site lies with C4 domain, which is important for the specificity of this kinase.

Murine SphK1 is a 49kD protein and was cloned earlier (Kohama et al. 1998) SphK2 was cloned and characterized later from mouse and human (Liu, Sugiura, et al. 2000). On the basis of homology to SphK1, SphK2 shares around 80% sequence similarity with SphK1 but have an added 200 amino acids at its N-terminus region, which makes it a predicted 68 kD protein. Besides, transmembrane domains are found at the N-terminus region of SphK2.

It has been reported that SphK2 has lower substrate specificity than SphK1. The preferred substrates of SphK1 are D-erythro-sphingosine and D-erythro-dihydrosphingosine whereas SphK2 also phosphorylate phytosphingosine, DL-threo-dihydrosphingosine and FTY720, a S1P analogue also named as Fingolimod (Liu, Sugiura, et al. 2000). It is a novel immunosuppressant in Phase III clinical trials for the treatment of MS and for organ transplantation. While, other research has found that SphK2 is the

main isoform that phosphorylates FTY720, the efficiency is only at 15% of the rate of phosphorylation of its natural substrate sphingosine (Paugh et al. 2003). Thus, FTY720 is actually a competing SphK2 inhibitor. In addition, FTY720 has been reported to inhibit both gene expression and protein level of SphK2 in neuroblastoma cell lines (Li, Hla, and Ferrer 2013). Substrates specificity difference may suggest that significant differences exist in their substrate binding pockets. However, the physiological significance of this difference in substrate specificity remains unknown.

1.3.1.1.2   Localization of SphKs

Lacking of transmembrane domains or identifiable nuclei localization sequences, SphK1 is mainly cytosolic (Kohama et al. 1998). It is ubiquitously expressed in adult brain, heart, spleen, lung, kidney, and testis but mRNA levels are highest in adult lung and spleen and there were barely detectable levels in skeletal muscle and liver (Kohama et al. 1998). SphK2 is highly expressed in the brain, kidney, and liver (Liu, Sugiura, et al. 2000). It seems that SphK2 is the predominant isoform in the brain, showing higher activity and mRNA expression levels in neuronal and glial cells (Blondeau et al. 2007). Because of the transmembrane domains and nuclear localization signal sequences ((RGRRGGRRR) with an arginine cluster in the N-terminal, SphK2 localization is variable and depends on the types of cells (Igarashi et al. 2003) (Bryan et al. 2008). For instance, SphK2 is present in the plasma membrane, mitochondria, ER, Golgi, and in the cytosol of HEK 293 cells (Hait et al. 2006) and it is predominantly localized in the nucleus in COS7, MCF7, HeLa, and NIH 3T3 cells (Okada et al. 2005; Sankala et al. 2007).

1.3.1.1.3   Activation and regulation

SphK activity is upregulated by both posttranslational and transcriptional processes. In addition, both enzymes also possess intrinsic catalytic activity in the absence of agonist stimulation (Pitman, Pham, and Pitson 2012). This basal SphK activity has been proposed to have a housekeeping role in maintaining cellular sphingosine and ceramide levels (Neubauer and Pitson 2013).

1.3.1.1.3.1   Post-translational activation of SphK1 and SphK2

A wide range of agonists including various cytokines such as tumor necrosis factor-α (TNF-α), interleukins and hormones and growth factors such as platelet-derived growth factor (PDGF), epithelial growth factor (EGF), vascular endothelial growth factor (VEGF), platelet-activating factor (PAF), nerve growth factor (NGF), basic fibroblast growth factor (bFGF), and lysophosphatidic acid has been demonstrated to active SphK1 through post-translational modifications (Bryan et al. 2008 ; Wattenberg, Pitson, and Raben 2006). SphK1 activation results from phosphorylation of serine 225. SphK1 has a binding site for extracellular-signal regulated kinase (ERK) 1/2 and both ERK1 and ERK2 phosphorylate SphK1 at Ser225 (Pitson et al. 2003). However, Wattenberg et al. pointed out that the enzymatic increase by 1.5 to 3-fold on the catalysis is relatively moderate. Instead the phosphorylation-induced translocation of SphK1 is the key to SphK signalling function. It seems that both SphK synthesize S1P within membrane compartments and thus localization of SphK to membrane is needed. Agonist mentioned above induce translocation of SphK1 binding to anionic lipids in the plasma membrane, resulting in the activation of SphK1

43

(Wattenberg, Pitson, and Raben 2006) (Hannun and Obeid 2008). Besides, several adaptor proteins such as PRK118 (Hayashi et al. 2002), aminoacylase 1 (Maceyka et al. 2004) and PECAM-1 (Fukuda et al. 2004) have been indicated to influence the translocation of SphK1.

Similar to SphK1, the catalytic activity of SK2 can be rapidly stimulated by a number of agonists, including EGF (Hait et al. 2005), TNF-α (Mastrandrea, Sessanna, and Laychock 2005), IL-1b (Mastrandrea, Sessanna, and Laychock 2005). Like SphK1, SphK2 activation is also regulated by phosphorylation via ERK1/2 at Ser351 and Thr578 (Hait et al. 2007). Little is known about the translocation of SphK2. It has a nuclear localization signal sequence within its N-terminal region. It has been observed that SphK2 can enter the nucleus and cause inhibition of DNA synthesis, resulting in cell cycle arrest at G1/S phase (Igarashi et al. 2003). Another study has reported that protein kinase D (PKD) could phosphorylate SphK2 at a putative nuclear export sequence, inducing SphK2 to translocate from the nucleus to cytoplasm.

1.3.1.1.3.2   Transcriptional regulation of SphK1

Little has been known about how SphK expression is regulated. A 55-bp fragment containing a activator protein-2 (AP-2) and two specificity protein1 (SP1) localized ahead of exon 1d has been reported to mediate NGF induced rat SphK1 gene transcription (Sobue et al. 2005). Histamine is also found to upregulate SphK1 expression via PKC and ERK pathway and AP-2 and SP1 binding motifs in endothelial cell line EA.hy 926 (Huwiler et al. 2006). In addition, hypoxia increases both the activity and expression of SphK1 in glioma cells (Anelli et al. 2008). Hypoxia can stabilize hypoxia-inducible

factors (HIFs). HIFs bind to hypoxia response elements (HREs) and consequently regulate a number of down-stream genes transcriptions. SphK1 possesses multiple putative HRE sites (Anelli et al. 2008). Schwalm et al. (Schwalm et al. 2008) have reported that both HIF-1α and HIF-2α were upregulated by hypoxia in endothelial cell line EA.hy 926, inducing SphK1 gene transcription via binding to the HREs in the promoter region of SphK1. There is also some evidence showing that SphK1 may regulate HIF-1α levels (Cho et al. 2014) via a S1P/Akt/GSK3β pathway (Ader, Malavaud, and Cuvillier 2009; Ader et al. 2015). Thus, it seems possible for a bi-directional regulatory mechanism between HIFs and SphK1. It is unclear whether SphK2 contains HREs, but hypoxia and HIF-1α have been shown to activate the activity and the expression of SphK2 both *in vivo* and *in vitro* (Wacker, Park, and Gidday 2009; Wacker, Perfater, and Gidday 2012; Yung et al. 2012; Schnitzer et al. 2009).

1.3.1.1.4   Inhibitors of SphK

A number of SK inhibitors have been generated which show potential for development as therapeutics for cancer and some other diseases (Pitman and Pitson 2010).

1.3.1.1.4.1   Non-specific inhibitors

N, N-Dimethylsphingosine (DMS) is a naturally occurring N-methylated analogue of D-erythro-sphingosine. It is a direct competitive inhibitor for purified SphK1 and recombinant SphK1 with a K_i of 8 μM (Pitson et al. 2000). DMS also inhibits human recombinant SphK2 with a K_i of 12 μM non-competitively (Liu, Sugiura, et al. 2000). Nevertheless a study pointed

out that purified SphK2 from rat was not inhibited by DMS because of the poor affinity of DMS to SphK2 (Vessey et al. 2007).

N,N,N-Trimethylsphingosine (TMS) is also an analogue of D-*erythro*-sphingosine and competitively inhibits purified recombinant human SphK1 with a Ki of 3.8 μM (Kohama et al. 1998). Inhibition on SphK2 of TMS has not been reported.

A number of earlier studies have reported SphK up-regulations in cancer cells and the anti-cancer effects of DMS and TMS by reducing chemotherapeutic resistance (Xia et al. 1999) (Jendiroba et al. 2002) (Endo et al. 1991). However, DMS and TMS are in fact non-specific inhibitors for SphK. Both of these two also inhibits PKC (French et al. 2003). DMS has also been reported to inhibit ceramide kinase (Sugiura et al. 2002). Besides, DMS enhances the activity of EGF receptor tyrosine kinase (Igarashi et al. 1989) (Igarashi et al. 1990) and protein kinase A (Ma et al. 2005). Thus conclusions on the association of SphK inhibition and anti-cancer effect might be compromised due to possible actions on other enzymes.

1.3.1.1.4.2   SKI-II

SKI-II [2-(p-hydroxyanilino)-4-(p-chlorophenyl) thiazole], has been shown to be a SphK1/Sphk2 dual inhibitor with a slightly higher potency towards SphK2 than towards SphK1 with a K_i values of 16.1 and 7.9 L μM for SphK1 and SphK2 respectively (Gao et al. 2012). It inhibits SphK specifically without inhibiting ERK2, PI3k, and PKC-α up to 60 μM (French et al. 2003). X-ray co-crystal structure analyses revealed that SKI-II binds to the sphingosine binding site (Gustin et al. 2013), which may explain its higher specificity for SphK over other kinases (French et al. 2003). SKI-II

inhibited S1P production in breast cancer cell line MDA-MB-231 which expresses high levels of SK activity (French et al. 2003) and in mouse mammary adenocarcinoma cells with an IC50 of <1 μM (French et al. 2006). Moreover, SKI-II was shown to be orally bioavailable and could be measured at therapeutically relevant levels in vivo with a half-life of >8 hours (French et al. 2006). SKI-II has been shown to inhibit hypoxia-induced SphK activation in mice by oral gavage at 100mg/kg (Yung et al. 2012) (Kim et al. 2007). Intraperitoneal injection with SKI-II at a dose of 50mg/kg could reduce endogenously generated S1P and ameliorate antigen-induced bronchial smooth muscle hyperresponsiveness (Chiba et al. 2010). Interestingly, a few studies reported that 10μM SKI-II not only inhibits SphK1 activity but also reduces the protein expression by enhancing the degradation of this enzyme via an ubiquitin-proteasomal pathway and/or activation of the proteasome in various cell lines (Loveridge, Tonelli et al. 2010, Ren, Xin et al. 2010, Cingolani, Casasampere et al. 2014). It is not clear whether SKI-II can degrade SphK2 in a similar manner. SKI-II is commercially available and is one of the most commonly used SphK inhibitors.

1.3.1.1.4.3   Selective SphK1 or SphK2 inhibitors

Growing evidence has shown that SphK1 and SphK2 have different, even opposite functions in many situations (Maceyka et al. 2005). Therefore, it is necessary to apply isoform-selective inhibitors to further elucidate their roles in regulating cell signalling pathways.

ABC294640 is a selective SphK2 competitive inhibitor with a K_i of 7.3μM (Gao et al. 2012). No effect was observed on SphK1, or the closely

related diacylglycerol kinase, at concentrations up to 100 µM (French et al. 2010). It has been reported to inhibit S1P production in human retinal endothelial cells (Maines et al. 2008), in rodent models of inflammatory disease (Maines et al. 2010) and ischemic injury (Yung et al. 2012) and also a variety of other diseases (Neubauer and Pitson 2013). ABC294640 exhibits anti-tumour activity in various cancer cells (French et al. 2010) (Beljanski, Knaak, and Smith 2010). It also has oral bioavailability in a rat model of diabetic retinopathy (Maines et al. 2006). ABC294640 is now in the early-phase clinical trial for treating solid tumor.

CB5468139 or SKI-I, is a potent selective SphK1 inhibitor with a K_i of 0.3 µM which decreased kidney adenocarcinoma A498 proliferation (Gao et al. 2012). However, it affect several other signalling proteins including FAK, p53, AKT as well (Gao et al. 2012).

1.3.2 S1P regulating cell fate: an Intracellular Mediator:

S1P may have dual functions. First, it might act as intracellular regulators to regulate survival and growth. Second, it couple S1P receptors in both an autocrine and paracrine manner and subsequently activate numerous downstream signaling pathways (Spiegel and Milstien 2003).

Ceramide and sphingosine have generally been associated with cell death via apoptosis or growth arrest (Hannun and Obeid 2002). By contrast, S1P has been widely reported to enhance growth and cell survival processes in diverse cell types (Spiegel and Milstien 2002). Elevated S1P levels promote proliferation, accelerate the G_1–S transition of the cell cycle, and induced DNA synthesis have been shown in in NIH 3T3 fibroblasts and HEK293 cells (Olivera et al. 1999). Increased intracellular S1P levels could suppress

apoptosis induced by serum-withdraw through blocking c-Jun amino terminal kinase (JNK) and activation of the caspases cascade (Edsall et al. 2001). In addition, S1P have its role in Ras and nuclear factor κB (NF-κB) signalling (Shu et al. 2002; Nava et al. 2002; Xia et al. 2002). Recent studies have suggested a pathway in which VEGF stimulated SphK1 via PKC to produce S1P, which acted as an intracellular second messenger to mediated VEGF-induced activation of Ras and consequently MAPK/ERK signalling and cell growth (Shu et al. 2002).

1.3.3   S1P receptors

S1P was first reported as the ligand for the orphan G-protein-couple receptor (GPCR) endothelial differentiation gene 1 (S1P1, EDG1) receptor. Since then, it has been known that another important role of S1P is to act as a ligand of the EDG family. By now, five members of the receptors which have high affinity for binding with S1P and dihydro-S1P have been identified. They are S1P1 (EDG1), S1P2 (EDG5), S1P3 (EDG3), S1P4 (EDG6), and S1P5 (EDG8). They are ubiquitously expressed and bind to a variety of G proteins, which enable S1P to initiate various downstream physiological processes such as cytoskeleton rearrangement (Singleton et al. 2005), cell motility (Rosenfeldt et al. 2001; Sugimoto et al. 2003), angiogenesis (Wang et al. 1999) and vascular maturation (Liu, Wada, et al. 2000). S1P receptors may differentially regulate the Rho family, particularly Rho and Rac (Lee et al. 1999).

1.3.4   S1P receptors in the brain

The brain has the highest concentration of S1P compared to the other tissues in rat (Edsall and Spiegel 1999). S1P receptors are also abundant in

both neurons and glia in CNS (Bryan et al. 2008). NGF-induced elevation of S1P regulates neurite outgrowth /extension in neurons via S1P1 with Rac (Toman et al. 2004). S1P1 activation has been reported to induce depolarization-induced glutamate release in hippocampus neurons (Kajimoto et al. 2007), promote neural stem cells and astrocyte motility to site of injury (Kimura et al. 2007; Mullershausen et al. 2007), mediate ERK activation in C6 glioma and astrocytes (Sato, Ui, and Okajima 2000) (Osinde, Mullershausen, and Dev 2007). Whereas, S1P2 is reported to inhibit neurite extension in neurons via Rho (Toman et al. 2004), inhibit glioblastoma motility (Malchnkhuu et al. 2008) and increase glioma invasion (Young and Van Brocklyn 2007). Besides, S1P2 null mice exhibit spontaneous seizures (MacLennan et al. 2001), and loss of vestibular function (MacLennan et al. 2006). S1P3 may inhibit neurite extension in PC12 cells (Toman et al. 2004). S1P4 has only been found in lymphatic and hematopoietic tissues (Schulze et al. 2011). S1P5 is selectively expressed in oligodendrocytes (Yu et al. 2004), suggesting an essential role of S1P5 in oligodendrocyte lineage cells.

1.3.5 SphK/S1P/S1PR signaling in regulation oligodendroglial lineage cells

S1P receptors are expressed in rat OLG with a relative mRNA abundance of S1P5>S1P1=S1P2>S1P3 and S1P1=S1P2=S1P5>S1P3 (Novgorodov et al. 2007; Yu et al. 2004). On the other hand, human OLGs express the receptor mRNA in a relative abundance of S1P5>S1P3>S1P1 (Miron et al. 2008). S1P receptors regulate OPC and OLG growth and survival differentially. Jung et al. (Jung et al. 2007) indicated that FTY720P, a potent agonist on S1P1, S1P3, S1P4 and S1P5 protect rat primary OLG but not OPC from

deaths during serum withdrawal through activation of ERK1/2 and Akt. Another study by Jaillard et al. (Jaillard et al. 2005) have also reported that S1P promoted the survival of mature OLG isolated from adult rat brain through activation of S1P5, but not pre-OLG. Although it seemed that S1P receptor activation did not protect the survival of pre-OLG or OPC in stress conditions, S1P1 has been shown to be involved in the PDGF-induced OPC proliferation (Jung et al. 2007). They found that PDGF downregulated S1P5 and upregulated S1P1 and promoted OPC proliferation, which could be abrogated by silencing S1P1. Cui et al. have demonstrated that FTY720P (50 nM) or S1P treatment without PDGF did not influence the proliferation of human OPC. In contrast, both S1P and FTY720P promote the proliferation of OPC under PDGF supplemented condition. Jung et al. (Jung et al. 2007) also indicated that treatment of low concentration of FTY720P (10nM) for 72 hours enhanced OPC differentiation while high concentration of FTY720P (0.1-1μM) inhibits OPC differentiation. S1P1 specific agonist SEW2871 alone had no effect on OPC differentiation (Jung et al. 2007). Whereas, Hu et al. (Hu et al. 2011) reported that 10nM FTY720P first inhibited OPC maturation as evidenced by the retraction of oligodendrocyte processes and then promoted the proliferation but continuously inhibited the differentiation during 98 h of treatment. Additionally, S1P5 receptor activation has been reported to impede OPC migration (Novgorodov et al. 2007) and regulate process retraction in pre-oligodendrocytes (Jaillard et al. 2005) (Miron et al. 2008), both of which may hinder remyelination after white matter injury (Keirstead and Blakemore 1999). Overall, the regulatory function of the SphK/S1P/S1PR pathway on OLG and OPC survival,

proliferation and differentiation appears complex. S1P and S1P receptors appear to function differentially in different stages, under different conditions and in different cell types and species. All these add to the difficulty in elucidating the mechanism of SphK/S1P/S1PR signalling in regulating oligodendrocyte lineage cells.

1.3.6 SphK/S1P/S1PR signaling in hypoxia/ischemia

As mentioned above, SphK/S1P appears to interact with HIF (Schwalm et al. 2008) (Cho et al. 2014), suggesting that SphK/S1P/S1PR pathway may have their roles in hypoxic/ischemic injuries. The mRNA transcript expression of SphK1 and SphK2 was increased by short-term hypoxia (2 days), while SphK1 transcript, but not SphK2, was increased under chronic hypoxia (14 days) in human pulmonary smooth muscle cells (Ahmad et al. 2006). Besides, the author also indicated that the increased ability of S1P to activate p38 MAPK while under chronic hypoxia improved the ability of S1P to stimulate the phosphorylation of ERK1/2(Ahmad et al. 2006). SphK2 promoter processes transcriptional sites for CREB that can be phosphorylated by hypoxia (Pyne et al. 2009). Schnitzer et al. (Schnitzer et al. 2009) have shown that hypoxia enhanced SphK2 activity and led to the S1P-mediated chemoresistance in A549 lung cancer cells. It is well known that solid tumor growth induces tissue hypoxia, which in turn leads to induction of VEGF through a HIF1α-dependent mechanism (Ferrara, Gerber, and LeCouter 2003). Thus the anti-cancer effect of several SphK inhibitors may be due to this mechanism. ABC294640 the selective SphK2 inhibitor is now in the early-phase clinical trial for treating solid tumor. Moreover, it has also been reported that S1P2 was strongly induced in endothelial cells of the

mouse retina during hypoxic stress, resulting in pathological angiogenesis. Thus, antagonism of the S1P2 receptors may be a novel therapeutic approach of pathologic ocular neovascularization (Skoura et al. 2007).

Recently, several studies have shown that hypoxic preconditioning induced stroke tolerance in mice via SphK2/S1P signaling pathway. It has been shown that both activity and expression of SphK2, while not SphK1, rapidly increased in the mouse brain during 4h-hypoxic preconditioning associated with the stabilization of HIF-1α (Wacker, Park, and Gidday 2009; Wacker, Perfater, and Gidday 2012) (Yung et al. 2012). Isoflurane-preconditioning has also been shown to protect mouse brain against ischemic stroke and activate SphK2 in mice (Yung et al. 2012). SphK2 inhibition by DMS, SKI-II and ABC294640 abrogated the preconditioning-induced tolerance (Wacker, Park, and Gidday 2009) (Wacker, Perfater, and Gidday 2012) (Yung et al. 2012). In addition, pre-conditioning exhibited no protective effect in SphK2$^{-/-}$ mice (Yung et al. 2012; Wacker, Perfater, and Gidday 2012).

1.4   Research rationale and objectives

WML is one of the most important vascular pathological aspects of VCI. However, there are currently no effective measures to ameliorate WML and VCI due to lacking of knowledge of the mechanism that how vascular diseases induce WML and cognitive impairment. Based on above review, WML is characterized with myelin loss and lipid components are essential for the stable structure and proper functions of myelin and the high lipid content makes white matter extremely vulnerable to ischemia. Although the brain lipidome of SIVD patients has been revealed, it is not known if lipid

changes can be found in WML induced by chronic hypoperfusion in mouse. In addition, WML is associated with loss of OLG and disruption of OPC differentiation caused by hypoxia. SphK/S1P/S1PR signaling pathway has been reported to interact with hypoxia and regulates OPC and OLG survival, proliferation and differentiation profoundly. Yet no evidence has indicated the role of SphK/S1P/S1PR pathway in vascular WML. Therefore, the objectives of the present study include:

- Hypothesis 1: Chronic hypoperfusion causes alterations in the lipidome of white matters. To investigate the alterations of three major myelin lipid classes including cholesterol, sphingolipid and phospholipid and the individual sphingolipid molecules in hypoperfusion-induced WML

- Hypothesis 2: Lipid changes are associated with myelin loss and white matter lesions. To explain the possible mechanism by which lipid changes induce the myelin loss

- Hypothesis 3: S1P plays an essential role in white matter lesions. To investigate S1P and sphingosine levels in WML and the activity and expression of SphK in WML induce by hypoperfusion in vivo

- Hypothesis 4: Treatment with a SphK inhibitor, SKI-II, can attenuate white matter lesions. To investigate the effect of SphK inhibition by SKI-II in WML, the expression of SphK in rat primary OLG under chemical-hypoxic condition, and if OPC differentiation disruption induced by hypoxia is related with SphK/S1P/S1PR pathway.

CHAPTER 2   METHOD AND MATERIAL

2.1   Animal

All of the animal experimental protocols in this study were approved by IACUC (Institutional Animal Care and Use committee) of the National University of Singapore. 9- week male C57BL/6 mice and advance pregnant Sprague Dawley Rat were obtained from the University Laboratory Animals Centre and maintained in the University Animal Holding Unit on a 12 h light/dark cycle and they were allowed free access to food and water until the mice reach the desirable age (10-12 week) and weight (25~29g) or the rats give birth. Careful considerations and efforts have been made to minimize the suffering and number of animals.

2.2   Bilateral common carotid artery stenosis model (BCAS)

10-week-old male C57BL/6 mice (25-29g) were anaesthetized with a ketamine/ medetomidine cocktail (100 mg/kg, 10 mg/kg, i.p.), purchased from the University Animal Holding Unit. Temperature of mice was maintained at 36.5 °C to 37.5 °C with a heating pad throughout the surgery. Chronic hypoperfusion was induced by bilateral common carotid artery stenosis (BCAS) as previously described (Shibata et al. 2004). After anaesthesia, a midline incision (~1.5 cm) was made at the neck of the mouse. Then the right common carotid artery (CCA) was carefully isolated from surrounding tissues under a surgical microscope (Olympus America). Two 7-0 silk sutures (B. Braun, Melsungen, Germany) were placed under the right CCA around the distal and proximal parts respectively. Then the artery was carefully and gently lifted a little by the sutures and placed between the loops

of the microcoils as shown in Figure 2.1A (inner diameter 0.18mm, Sawane

Spring Co, Japan). The microcoil was rotated around the CCA until CCA

was put in the loops as shown by Figure 2.1B. The distal end of the

microcoil should be just below the carotid bifurcation (Figure 2.1C). Then

the 7-0 silk suture was removed gently. Five minutes later, a second

microcoil was twined around the left CCA with the same procedures.
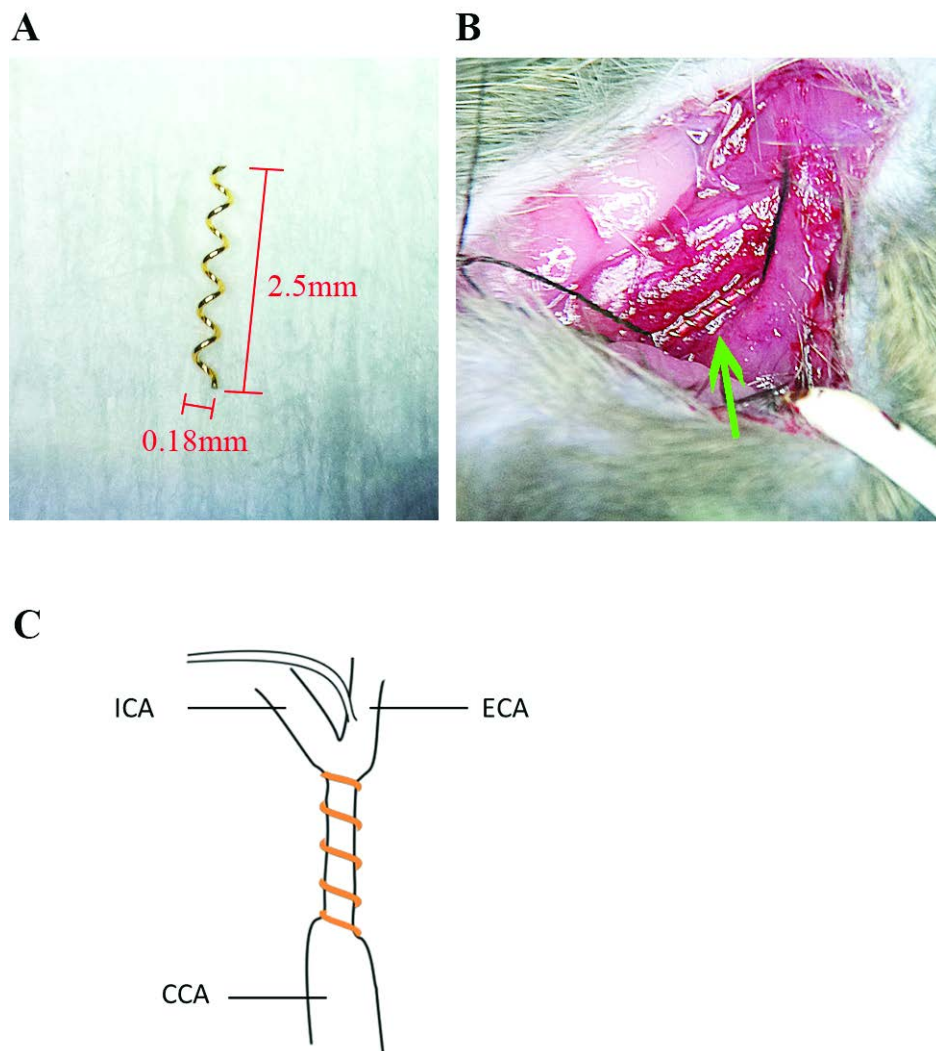
Figure 2.1 Scheme of BCAS surgery
A, Microcoil (length 2.5mm, inner diameter 0.18mm). **B,** CCA narrowed by
the microcoil, indicated by the green arrow. C, Microcoil was located just
below the bifurcation. Abbreviations: ICA, internal carotid artery; ECA,
external carotid artery; CCA, common carotid artery.
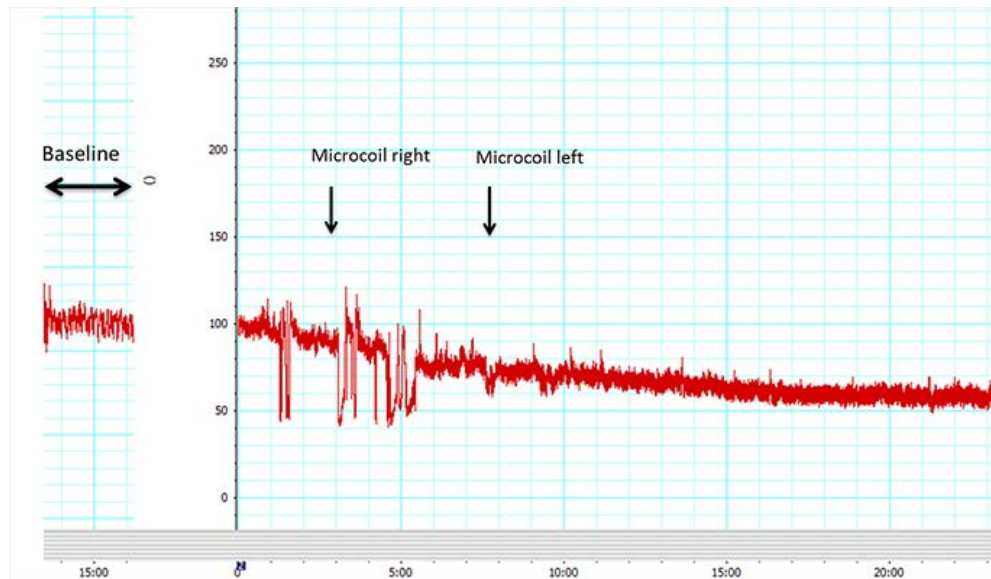
Figure 2.2 Relative CBF during the BCAS surgery
The diagram indicated a representative time course of the hypoperfusion.
CBF measurement was set at 100% before the microcoils were put in place.
It can be seen that CBF was reduced to ~60 % of baseline 15-30 min after
the placement of the two microcoils.

2.3 Cerebral blood flow measurement

After mice were deeply anesthetized, skin overlying the right skull was
reflected. A plastic guide cannula (inner diameter 1.5 mm, and length ~4 mm)
for a laser-Doppler flowmetry probe was temperately glued perpendicularly
to the skull at 1 mm posterior and 3 mm lateral to the bregma. The cerebral
blood flow (CBF) was record for 5~10 min for the pre-surgery baseline (set
as 100%). The CBF was monitored during the whole process of the BCAS
surgery and an extra 15 mins after the microcoils implantation. Then the
probe and guide cannula were removed followed by closing of the incision
on the head with 4-0 nylon sutures. Atipamezole was injected (i.p.) with the
dose of 1 mg/ kg (purchased from University Animal Holding Unit) to
reverse the sedative and analgesic effects of ketamine/medetomidine cocktail.
Sham-operated animals underwent the same procedures but without the

twined the microcoils. The CBF values were expressed as a percentage of the baseline value The CBF values were expressed as a percentage of the baseline value. A reduction of CBF to ~60% should be observed (Figure 2.2). The midline cervical incision was closed with 4-0 nylon sutures (B. Braun, Melsungen, Germany).

2.4   Barnes maze

Barnes Maze is a dry-land maze test for spatial learning and memory in which mice escaped from a brightly exposed circular open platform to a small dark chamber. The protocol used in this study is mainly adapted from a previous study by Sunyer et al. (Sunyer et al. 2007).

2.4.1   Equipment and field setup

2.4.1.1 Animals

Mice subjected with BCAS or sham-operated 15 days before. Before starting each experiment, mice were acclimated to the testing room for 1 h. There were 9 mice in each of the two groups in this study.

2.4.1.2 The maze

As shown in Figure 2.3A, the maze is in blue color to provide enough contrast for computer tracking software between C57BL/6 mice which are black and the open surface. The circular platform has a diameter of 68.5 cm with 16 equally distributed holes (6.2 cm diameter; 5 cm between holes) along the perimeter and is elevated 105 cm above the floor. In the Barnes maze, a small dark recesses chamber is located under one of the holes under the platform called a "goal box". Mice received stimulus would escape from the surface to the goal box. All the holes should look the same from the

center of the maze so that the mice could not discriminate visually the hole

with goal box under it from the other holes.
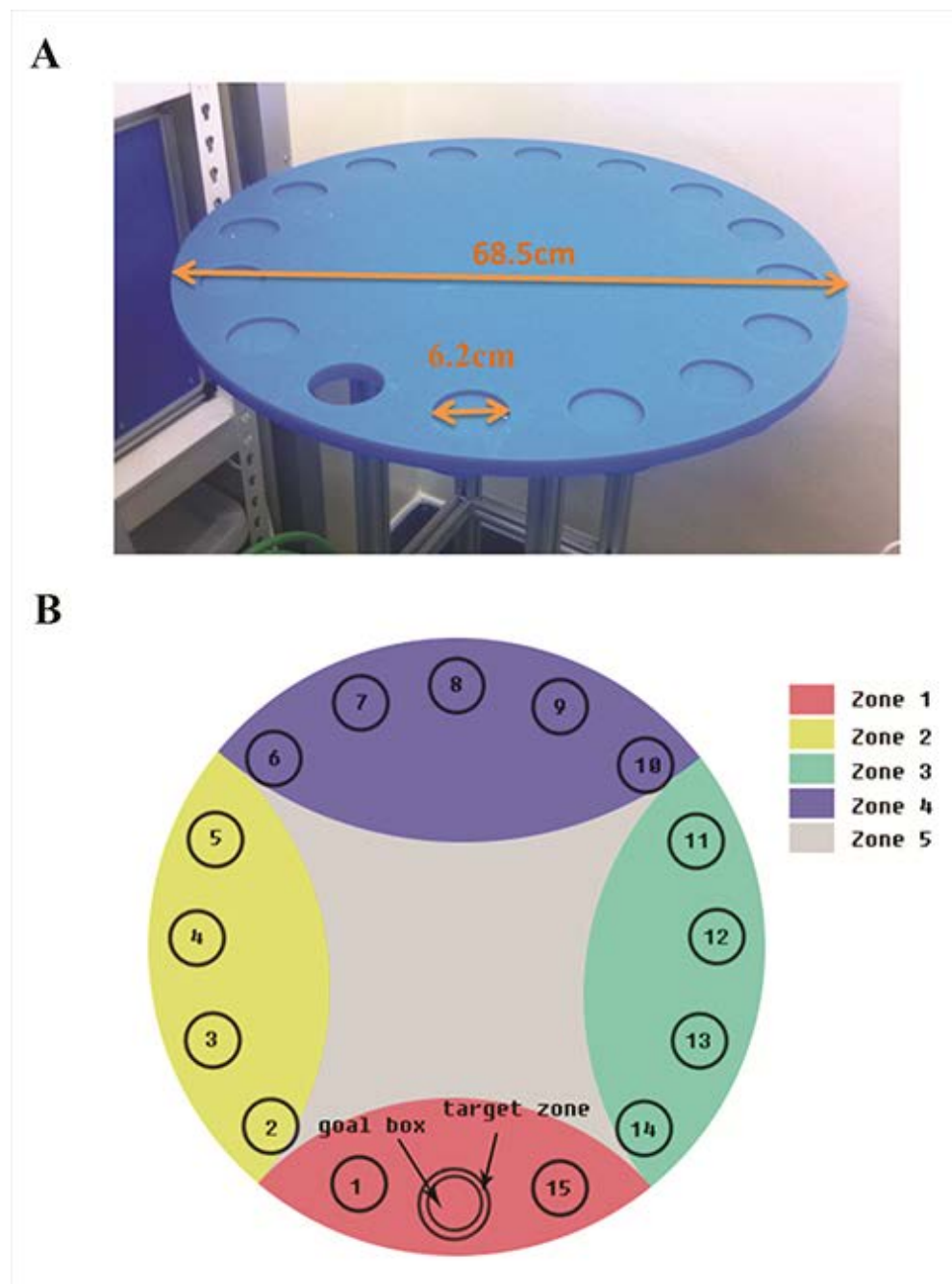
Figure 2.3 Settings for the Barnes Maze
A, A picture of the blue color platform with diameter of 68.5cm and holes with diameter of 6.2cm. **B**, Location of holes and goal box and the zone settings for the video tracking system. Target zone was set so that the software could detect the head deflections or mouse body into the goal box.

2.4.1.3 Stimulus/reinforcement

Bright light and noise were used as reinforcements in this study. The light was located right above the center of the platform. A 2000 Hertz pure tone of Sine wave generated by an online program on the website: http://onlinetonegenerator.com/ played at the maximum volume was used at the aversive noise. The same parameters were used during the whole experiments.

2.4.1.4 Room configuration

Four curtains with different shapes in different colors (triangle, rectangle, circle and/or a cross) were hanging surrounding the maze, which would be used as the visual cues of the mice. Besides, other furniture in the room such as a door, a desk, a shelf could also be the visual cues for the mice. Thus, these cues were kept exactly in the same location during the whole experiments. The video-tracking system was sensitive to light reflections from the platform surface and thus, the dome light of the room was kept to the same luminance location during the whole experiments.

2.4.1.5 Video-tracking system

A camera was located right above the platform was used record the videos. EthoVision XT Version 10.0 (Nolduls Techonology, Netherlands) was used to tracking the trace of mice on the platform. Settings were kept the same during the whole experiment. Latency, errors and path length can be measured and analyzed directly by the tracking system.

2.4.2   Adaptation period

The first day of the test is adaptation period. The mouse was placed in the middle of the maze covered by a black chamber. 10 s later the mouse was

released from the chamber and the noise was played at the same time. The mouse was allowed to explore the platform to find the escape box. If the mouse didn't not find or enter the escape box with 2 min, it would be guide to the escape box gently and the noise should be stopped immediately after the mouse went into the box. The mouse was allowed to stay in the escape box for 30 S. Then the mouse was sent back to its cage and the platform was swapped and cleaned with 75% alcohol to eliminate the odor before the next mouse was placed onto the maze. There was only one section for adaptation period.

2.4.3　Spatial acquisition phase

24 h after adaptation period, the acquisition phase began. The mouse was placed in the center of the maze covered by black chamber just the same as in adaptation period. As soon as the chamber was lifted, the noised and video tracking was swift on. The trial ended when the mouse entered the escape box or after 5 min it had elapsed. If the mouse didn't enter the escape box, it would be guided into it gently and let it stay inside for 30 S. The noise was shut down immediately the mouse entered the escape box. After that the mouse was sent back to its home cage until the next trial. The platform was cleaned with 75% alcohol to avoid olfactory cues. Each mouse received 3 trials per day with an inter-trial interval of 1 h and there were 3 consecutive training days in the acquisition phase.

2.4.4　Probe trial

The probe trial was conducted 24 h after the last training day to assess if the animal remembered the location of target goal. The escape box was removed and the target hole was closed. The mouse was put on the surface

and relapsed as it is done in acquisition phase but allowed to explore the maze for 2 min with the noise on.

2.4.5 Data analysis

2.4.5.1 Acquisition phase

Primary latency (s) primary path length (cm) and primary errors are designated as the time, moving distance and pokes in wrong holes before the mouse reached the target hole for the first time. These parameters were measured by the tracking software and were averaged in blocks of trials per day. Difference between sham and BCAS groups were analyzed by Student's t-test. Primary errors were checked manually because the software might not be accurate to detect the head deflections into wrong holes.

Searching strategy is an important parameter to indicate if the mouse had learnt to escape with spatial memory. The search strategies can be defined into three categories: direct, serial or mixed. In direct strategy, the mouse moved directly to the target hole or to the two holes adjacent to the target hole (Hole 1 and Hole 15 as shown in Figure 2.3.B). In serial strategy, the mouse first visited wrong holes and then searched at least two adjacent holes in serial manner in clockwise or counter-clockwise direction to find the target hole. In mixed strategy, the mouse searches holes separated and in unorganized manner other than direct or serial strategy. Only direct strategy is considered to be the spatial strategy. Searching strategies were determined manually with the video records of each trial and analyzed with Fisher's exact test to show the association of the strategy and the surgery types (BCAS or sham).

2.4.5.2 Probe trial

In addition to primary latency, primary path length, primary errors and searching strategy, total errors during the 2 min and accumulative time (Duration) of mouse spent in each of the four zones were measured by the tracking software to demonstrate the preference to the target holes. The maze platform was divided into five zones as shown in Fig 2.3.B. The differences of duration of each zone within the group were compared by paired t-test and by student's t-test between groups.

2.5   SKI-II Treatment

(4-[[4-(4-Chlorophenyl)-2-thiazolyl]amino]phenol) also named as SKI-II (Selleckchem) , was dissolved in Dimethyl sulfoxide (DMSO, Sigma) at the concentration of 25mg/ml. BCAS mice were divided into three groups: BCAS, BCAS-Vehicle and BCAS-SKI-II. BCAS-SKI-II mice received SKI-II (50mg/kg, i.p) immediately after the surgery and every other day thereafter up to day 15, while the another group received vehicle (DMSO, 50 µl) on the same regimen. The rest received nothing. N values of each experimental group are listed in the figure legends of the respective experiments.

2.6   Coronal brain slice Preparation

2.6.1   Reagent

Chemicals are purchased from Sigma-Aldrich if not stated otherwise.

2.6.2   Procedure

Fifteen days after surgery, the mice were anaesthetized with ketamine/medetomidine and underwent intra-cardiac perfusion with 0.01M

PBS at a rate of 2.5mL / min until the perfusate exiting the right atrium was clear, followed by 4% paraformaldehyde in 0.1 M PBS (25 ml). The brains were post-fixed in the same paraformaldehyde solution overnight at 4 °C. Then brains were dehydrated in 20% sucrose solution at 4 °C overnight before proceeding to dehydration with 30% sucrose solution for 1 day. Before fast freezed in liquid nitrogen, brains were coated with Tissue-Tek Optimal Cutting Temperature compound (Sakura Finetek, Torrance, CA, USA) and then placed in the cryostat (Leica Biosystems, Wetzlar, Germany) chamber. Coronal sections (12 μm) were cut with a cryostat at -20ºC and mounted onto glass slides (Matsunami Glass, Osaka, Japan) and stored at -80 °C for use.

2.7   White matter tissue isolation

Fifteen days after surgery, the mice were anaesthetized with ketamine/medetomidine and underwent intra-cardiac perfusion with 25 ml of 0.01M PBS to flush out the blood. Then the skulls were removed and brains were quickly taken out and placed ventral side down in a brain tissue matrix (on ice). Brains are subsequently sectioned to five 1mm coronal blocks. Corpus callosum (CC) and internal capsule (IC) were isolated using sharp forceps under a surgical microscope. Each sample then was divided into two equal parts and weighted quickly before collecting to microtubes (Eppendorf), and then put in lipid nitrogen immediately, and stored at -80 °C until use for further protein or lipid extraction respectively.

2.8   Kluver-Barrera staining

2.8.1   Reagent

0.1% Luxol Fast Blue solution   1g of Luxol Fast Blue MBS dissolved in 1000ml 95% ethanol, with 0.5ml glacial acetic acid

0.2% Cresyl Violet solution   2g Cresyl Echt Violet dissolved in 1000ml distilled water, 15 drops of 15% glacial acetic acid to every 100ml and filtered just before using

0.05% Lithium Carbonate solution   0.5g Lithium Carbonate(Li_2CO_3) in 1000ml distilled water

2.8.2   Procedure

Slide-mounted brain sections prepared as described above were immersed in 95% alcohol for 10 to 15 mins for hydration and then were transferred to 0.1% Luxol Fast Blue Solution in 56ºC oven overnight (no more than 18h). After the sections were cooled down to room temperature, excess stain was rinsed off with 95% alcohol followed by washing in distilled water. Then the sections were differentiated in 0.05% Li2CO3 solution for 30 seconds followed by differentiation in 70% alcohol for 30 seconds. The two differentiation steps should be repeated until the grey matter is clear and white matter is sharply defined under microscope. When differentiation is completed, the sections were placed in distilled water before counterstain in 0.2% Cresyl Violet Solution for 15 mins. Then sections were washed in distilled water and then differentiated in 2 changes of 95% alcohol for 5 min each followed by 2 changes of absolute ethanol for dehydration and 2 changes of histo-Clear for clearance for 5 mins each change. Finally, the sections were mounted with CV Ultra mounting media (Leica Biosystem) and dried before microscope checking.

2.9   Immunofluorescence staining

2.9.1   Reagent

PBS-Tx	0.01 M PBS with 0.1% Triton-X100
Blocking buffer	5% goat serum in PBS-Tx
Primary antibody	Anti- HIF-1α (GeneTex Inc. U.S) in PBS-Tx (1:1000)
Secondary antibody	Alexa Fluor® 488, 594 or 647 dye (Millipore) in 0.01M PBS (1:200)

2.9.2   Procedure

Slide-mounted brain sections were dried at room temperature followed by washing with PBS-Tx three times. After that, sections were blocked with blocking buffer for 1 h at room temperature to block the unspecific binding. Then the sections were incubated with primary antibody overnight at 4°C. On the next day, sections were washed with 0.01M PBS 3 times, each time for 10 mins and then incubated with secondary antibody at room temperature. One hour later, then slides were washed in 0.01M PBS three more times followed by nuclei counterstained with DAPI for 3 min. Sections were mounted with coverslips via ProLong® Gold Antifade Mountant (Life Technologies, USA), waiting for analysis under microscope.

2.10   Microscopy

The microscope used in this study is the Olympus IX71 microscope with QImaging Exi Aqua digital camera (objective lens used included UPLFLN 10X2PH, NA 0.3; LUCPLFN40X, NA 0.60; UPLFLN 100×OI2 NA 1.3). All images were acquired by Image-Pro Insight (version 8.0) at room temperature.

2.11 Western blot analysis

2.11.1 Reagent

Lysis buffer	RIPA buffer (Cell signaling Technology, USA) containing protease inhibitor cocktails (Roche, Germany) and phosStop (Roche, Germany)
1X Running buffer	3.0 g of Tris base, 14.4 g of glycine, and 1.0 g of SDS dissolved in 1000 ml distilled H_2O
1X Transfer buffer	3.0 g of Tris base, 14.4 g of glycine dissolved in 800 ml distilled H_2O and 200 ml absolute methanol
1X PBST	0.01M PBS with 0.1% Tween-20

2.11.2 Sample preparation

Isolated white matter tissues were homogenized in cold lysis buffer on ice quickly (20µl lysis buffer per 1 mg wet tissue). Homogenized lysates were centrifuged for 15 min at 14000 rpm in a precooled centrifuge (4°C). The supernatant containing the cytosolic fraction was collected carefully to a new microtube. Protein concentrations were determined by Pierce™ BCA Protein Assay Kit (ThermoFisher Scientific, USA) with bovine serum albumin as standard (Pierce Biotechnology, Rockford, IL, USA) for calibration. All samples were adjusted to 20 mg/µl with PBS buffer and then diluted with Laemmli buffer (Bio-Rad, Hercules, CA, USA) at a 1:1 ratio followed by boiling the mixture at 95-100°C for 5 min.

2.11.3 Western blot

Equal amounts of protein (50-150 mg/well according to different target protein) were separated by 5-15% sodium dodecyl sulfate-polyacrylamide (SDS/PAGE) gel. To be specific, 5% gel was used for NG2, 8% gel was used for HIF-1α 15% gel was used for MBP and 10% gel for other target protein. Then the protein was transferred onto polyvinylidene difluoride

(PVDF) membrane (Bio-Rad, USA) in transfer buffer. After that, the membrane was blocked with 10% nonfat dry milk (Bio-Rad, USA) in PBST buffer at room temperature for 1 h to prevent unspecific binding. Then the membrane was incubated with primary antibodies against MBP (1:2000, Cell signaling Technology, USA,), NeuN (1:5000, Cell Signaling Technology, Danvers, MA, USA), SphK1 (1:1000, Cell signaling Technology, USA), SphK2 (1:1000, Santa Cruz, USA), HIF-1α (1:1000, GeneTex Inc. USA), NG2 (1:500, Merck-Millipore, USA), CerS2 (1:5000, Sigma-Aldrich, USA), β-actin (1:1000, Cell Signaling Technology, USA) or GAPDH (1:5000, Merck-Millipore, USA) at 4 ℃ overnight. On the next day, the membranes were washed in PBST buffer three times for 10min each time and then subjected to incubation with corresponding horseradish peroxidase-conjugated (HRP) secondary antibodies (1:10000, Merck-Millipore, USA) at room temperature for 1 h. Protein bands were visualized by Luminate Forte/Crescendo Western HRP Substrates (Millipore Corporation, Billerica, MA, USA) and transilluminator (UVItec Limited, Cambridge, UK). The density of the bands was quantified by densitometry analysis using UVIband software (UVItec Limited, Cambridge, UK). Protein levels were normalized to β-actin or GAPDH.

2.12 Lipid extraction

2.12.1 Reagent

Extraction solvent	1:1 butanol : methanol with internal standards from Avanti polar lipids (Alabaster, AL, USA)

2.12.2 Procedure

Internal standards (IS) including PC 14:0/14:0, PE 14:0/14:0, PS 14:0/14:0, d6 CE (for PC, PE, PS, cholesterol respectively) at a final concentration of 100 ng/ml and IS including Lyso PC 17:0, PG 14:0/14:0, C17 Cer, C8 GluCer (for lysophospholipids, PG, Cer and SM, and glycoCer) at a final concentration of 50 ng/ml were added to ice-cold extraction solvent. Then the extraction solvent was added to each white matter tissue (WMT) sample isolated before at the ratio of 50 μL per 1 mg wet tissue and then WMT were dissected, minced and sonicated at 4°C for 1 h. Sample lysates were then centrifuged for 10 min at 14,000 rpm. The total lipid extract (supernatant) was collected and aliquot for following analysis.

2.13 Lipid analysis

2.13.1 Reagent

All solvents for LC-MS analysis were LC-MS grade and were purchased from Fisher Scientific and Merck Millipore if not stated otherwise.

2.13.2 Phospholipid and sphingolipid

The samples (1 μl) were injected to liquid chromatography-tandem mass spectrometry (LC-MS/MS) analysis with an Agilent system (1200 HILIC-chip system connected to Agilent 6540 / 6550 Q-TOF and Agilent 6490 QQQ mass spectrometers). Separation of lipids was carried out using an isocratic mobile phase Solvent A and B (tetrahydrofuran: methanol: water in the ratio 30:20:50 and 75:20:5 respectively, both containing 10 mM ammonium formate) as previously described (Weir et al. 2013). Lipids were eluted under gradient conditions (300μl/min) 0% solvent B to 100% solvent

B to 8.0 min, 2.5 min at 100% solvent B, then return to 0% solvent B over 0.5 min then 10.5 min at 0% solvent B before the next injection. Mass spectrometer was operated in positive mode for multiple-reaction monitoring (MRM). The MRM list of transitions was shown in Table 2.1(sphingolipid) and Table 2.2 (phospholipid).

2.13.3 S1P

Before injection, the sample was subjected to derivatization as previously described (Narayanaswamy, Shinde et al. 2014). Briefly, total lipid extract (50 µl) was mixed with internal standard (S1P d18:1 13C2D2, 50 µl, 20 ng/ml, Toronto Research Chemicals) and TMS-diazomethane (10 µl, 2M in hexane, Acros Organics, USA) and incubated for 20 min at room temperature under thorough mixing (750 rpm). The derivatization reaction was stopped by the addition of acetic acid followed by centrifugation for 10 min at 14,000 rpm. The supernatants were collected and samples (1 µl) were subjected to liquid chromatography-tandem mass spectrometry (LC-MS/MS) analysis with an Agilent system (1200 HILIC-chip system connected to Agilent 6540 / 6550 Q-TOF and Agilent 6490 QQQ mass spectrometers) as previously described (Narayanaswamy, Shinde et al. 2014). Mobile phase Solvent A and B consisted of 50% and 90% acetonitrile in water respectively, containing 25 mM ammonium formate pH 4.6. Analytes were separated with the following gradient: 100% B from 0 to 1.5 min, 40% B from 1.5 to 8.5 min, 30% B from 8.5 to 10.5 min, and 0% B from 11.5 to 13.0 min, 100% B from 13.1 to 19 min. Mass spectrometer was operated in positive mode for MRM. The MRM list of transitions was shown in Table 2.3.

2.13.4 Cholesterol

Cholesterol were analysed using an Agilent HPLC 1100 system with Zorbax Eclipse XDB-C18 column (Agilent) coupled with an Applied Biosystems 3200 QTrap mass spectrometer (Applied Biosystems, Foster City, CA) as previously described (Shui et al. 2011)Briefly, chloroform: methanol in ration of 1:1 as the mobile phase at a flow rate of 0.5 ml/min was used to elute the analytes. The monitored MRM transitions for internal standard were 375.4/161.0 and 369.4/161.0 for cholesterol.

2.13.5 Lipidomics data processing

Data were extracted with Analyst Software (Applied Biosystems, Foster City, CA, USA). The amounts of lipid classes and individual species were normalized by the incorporated internal standard concentration, and then normalized to total protein concentration of their correspondent half part of WML used for western blot analysis. Mass fraction or molar fraction was obtained by normalization of the total amounts of lipids for further analysis.

2.14 Primary oligodendroglia lineage cell culture

The procedures were adapted from previous studies (Chen et al. 2007; Miyamoto, Maki, et al. 2013).

2.14.1 Reagent

DMEM20S	DMEM/F12 (Gibco, USA) with 20% FBS (Biowest, USA), 1% penicillin / streptomycin (Gibco, USA) 1mM sodium pyrumate
OPC medium	Neurobasal (Gibco, USA) supplied with GlutaMAX (Gibco, USA) , 10 ng / mL PDGF, 10 ng/ml FGF (both from Peprotech, USA), 1% penicillin / streptomycin, and 2% B27 (Gibco, USA)
OLG medium	DMEM supplied with GlutaMAX, 1% penicillin / streptomycin, 10 ng / mL CNTF, 50 ng / mL T3 and 2% B27

2.14.2 Equipment setup

75 cm2 flasks were coated with filtered 0.01% poly-D-lysine (Sigma-Aldrich, USA) for 1-2 h in in 37 °C incubator or overnight at room temperature. Then the coating solution was removed and the flask was washed three times with sterile distilled H2O and dried completely in a tissue culture hood.

48-well plates, Petri dishes and round coverslips placed in 24-well plates were coated with filtered 0.005% poly-D-ornithine (Sigma-Aldrich, USA) for 1-2 h in in 37 °C incubator or overnight at room temperature. Then the coating solution was removed and the flask was washed three times with sterile distilled H2O and dried completely in a tissue culture hood.

Microdissecting scissors and forceps should be autoclaved in advance. And all the procedures should be done in a biosafety cabinet (BSC).

2.14.3 Dissection and plating and culture of neonatal rat cortices

Two P1–2 rat pups were anaesthetized by burying them in ice for 1-5 min and soaked in 70% alcohol for sterilization. The skin was cut open along the midline of the head from the base of the skull towards the mid-eye area using microdissecting scissors followed by cutting and removing the skull with a curved forceps. Then the cortices were separated and transferred to a 60 mm Petri dish placed on ice containing 5ml ice-cold HBSS using another forceps (Gibco, USA). It's important to use different scissors or forceps to remove skin, skull and the brain cortices respectively to avoid contamination. Remaining heads were subject to the same procedures. The meninges were gently peeled off from the cortices and then the cortices were transferred to a fresh 60 mm Petri dish placed on ice containing 5ml ice-cold HBSS added

with 0.5ml 10x trypsion (Biowest,USA) and 0.001% DNase I. After cutting the cortices into ~1 mm3 chunks with a microdissecting scissors, the tissue was incubated in the tissue culture incubator at 37 °C for 10-15 min. Then the digested contents were transferred into a 50 ml sterile centrifuge tube. 5ml DMEM 20S was added to the sterile centrifuge tube to stop the digestion and then cells were collected by centrifugation at 100g (~800 rpm) for 5 min. The supernatant was aspirated carefully and discarded. Then 10ml DMEM was added to the tube for trituration and dissociation with pipette until homogenous. Then the homogenous suspension was passed through a 40 μm cell strainer placed on a 50 ml conical tube and transferred into one coated T75 flask. The flask was incubated at 37°C and 5% CO_2 for 8-10 days. The DMEM20S medium was changed every three days.

2.14.4 OPC isolation and culture

When the mixed glial cells were confluent, the flasks were shaken on an orbital shaker (220 rpm) for 1 h to remove the microglia, and then changed to new medium followed by 18~20 h shaking. The medium was collected and plated on uncoated 10 mm petri-dish for 1 h at 37°C to allow contaminating astrocytes and microglia attach firmly to the surface. Non-adherent cells were then centrifuged and re-suspended in OPC medium and then plated onto poly-D-ornithine-coated plates or 60mm petri dish (Day 0). The OPC medium was half changed every two days. Cells would be ready for use on Days 4-5. To differentiate the OPCs from OLGs, the medium was changed to OLG medium.

2.14.5 Chemical induction of hypoxia in vitro

CoCl2 (up to 50 µM) was added to the media of cultured OPCs at Day 4-5 in order to chemically induce HIF-1α and mimic chronic hypoxia (Piret et al. 2002) with or without co-treatment with SKI-II (25 µM, dissolved in DMSO) or FTY720 (10nM or100nM, dissolved in DMSO). After treatment of 72 h, cell viability was assessed by MTT assays following standard protocols. Cells grown on round coverslips were subjected to immunofluorescence staining. Briefly, the coverslips with cells grown onto it were washed with ice-cold PBS, fixed with 4% paraformaldehyde for 15 min then washed three times with PBS-Triton X-100 (0.1%), followed by blocking in 3% bovine serum albumin in PBS for 1 h. Then the cells were then incubated with primary antibodies against MBP (1:200, GeneTex, USA), NG2 (1:200, Merck-Millipore, USA) or HIF-1α (1:100, GeneTex, USA) at 4°C overnight, washed with PBS three times, and incubated with fluorochrome (Alexa Fluor® 488 or Alexa Fluor® 594)-conjugated secondary antibodies. Before mounting the coverslips on to glass slides, nuclei were counterstained with DAPI, then viewed under an Olympus IX71 microscope with QImaging Exi Aqua digital camera (objective lens used included UPLFLN 10X2PH, NA 0.3; LUCPLFN40X, NA 0.60; UPLFLN 100×OI2 NA 1.3). All images were acquired by Image-Pro Insight (version 8.0) at room temperature.

Cells in petri dish were collected for western blot analysis. Having aspirated the medium, cells were washed with ice-cold PBS and harvested in 200µl RIPA buffer (as described above for white matter tissue) per 60mm petri dish. Cell lysates were briefly sonicated for 10 seconds followed with

centrifugation at 14000 rpm for 15 min at 4 °C. The supernatant was collected and further processes as described above for white matter tissues. Processed samples were subjected to western blot analysis with 10% SDS/PAGE gel and incubated with anti-SphK2 (Santa Cruz, USA) and β-actin (Cell signaling, USA) antibodies and secondary antibodies.

2.15 Quantification of immunofluorescence staining

Images of six randomly-chosen views under 40X objective lens were acquired for one biological sample. The intensity of HIF-1α of each cell in the six images was measured by Image J software and expressed as grey scale value in which black was 0 and pure white due to over expose was 255. The intensity of HIF-1α for this sample was the average value of all cells in the six images. Total three samples for each experimental group were measured.

Similar to HIF-1α, the data used for calculation of OLG (MBP-positive) to OPC (NG2 positive) ratio were collected from the same view-chosen method from five samples for each experimental group.

2.16 Statistical analysis

All statistical analyses of the data were performed by SPSS 19 (IBM, Armonk, NY). Differences between two groups were compared with Student's t-test. Differences among three or more groups were analyzed by one-way ANOVA with post-hoc comparisons of Bonferroni test. Two-way ANOVA with repeated measurements post-hoc comparisons of Bonferroni test was used as well in Barnes maze experiments. Besides, Fisher's exact

test was performed for analyzing the association between searching strategy

and groups in Barnes maze. Values are expresses as Mean ± SEM.

Table 2.1 MRM List of Sphingolipids

Name	Transition	Name	Transition
Cer d16:1/C22:0	594.7 -> 236.4	SM 30:1 (IS)	647.5 -> 184.1
Cer d18:0/C22:0	624.7 -> 266.4	SM 31:1	661.5 -> 184.1
Cer d18:0/C24:0	652.7 -> 266.4	SM 32:0	677.6 -> 184.1
Cer d18:0/C24:1	650.7 -> 266.4	SM 32:1	675.5 -> 184.1
Cer d18:1/C16:0	538.5 -> 264.3	SM 32:2	673.5 -> 184.1
Cer d18:1/C17:0 (IS)	552.5 -> 264.3	SM 33:1	689.6 -> 184.1
Cer d18:1/C18:0	566.6 -> 264.3	SM 34:0	705.6 -> 184.1
Cer d18:1/C20:0	594.6 -> 264.3	SM 34:1	703.6 -> 184.1
Cer d18:1/C22:0	622.6 -> 264.3	SM 34:2	701.6 -> 184.1
Cer d18:1/C24:0	650.6 -> 264.3	SM 34:3	699.5 -> 184.1
Cer d18:1/C24:1	648.6 -> 264.3	SM 35:1	717.6 -> 184.1
Cer d18:1/C26:1	678.7 -> 264.4	SM 35:2	715.6 -> 184.1
Cer d18:2/C16:0	536.7 -> 262.4	SM 36:1	731.6 -> 184.1
Cer d18:2/C22:0	620.7 -> 262.4	SM 36:2	729.6 -> 184.1
Cer d18:2/C24:1	646.7 -> 262.4	SM 36:3	727.6 -> 184.1
DHC 16:0	862.6 -> 264.3	SM 37:2	743.5 -> 184.1
DHC 18:0	890.7 -> 264.3	SM 38:1	759.6 -> 184.1
DHC 20:0	918.7 -> 264.3	SM 38:2	757.6 -> 184.1
DHC 22:0	946.7 -> 264.3	SM 39:1	773.7 -> 184.1
DHC 24:0	974.8 -> 264.3	SM 41:1	801.7 -> 184.1
DHC 24:1	972.7 -> 264.3	SM 41:2	799.7 -> 184.1
dhCer 18:0	568.6 -> 550.6	SM 42:1	816.7 -> 184.1
dhCer 22:0	624.6 -> 606.6	Sphd16:1	272.2 -> 254.2
dhCer 24:0	652.7 -> 284.3	Sphd18:0	302.3 -> 284.2
dhCer 24:1	650.6 -> 632.6	Sphd18:1	300.3 -> 282.2
MHC 16:0	700.6 -> 264.3	Sphd18:2	298.3 -> 280.2
MHC 18:0	728.6 -> 264.3	GluCer d18:1/8:0 STD	588.8 -> 264.3
MHC 20:0	756.6 -> 264.3		
MHC 22:0	784.7 -> 264.3		
MHC 24:0	812.7 -> 264.3		
MHC 24:1	810.7 -> 264.3		

Table 2.2 MRM List of Phospholipids

Name	Transition	Name	Transition
LPC 14:0	468.3 -> 184.1	oddPC 39:6	820.6 -> 184.1
LPC 15:0	482.3 -> 184.1	oddPC 39:7	818.6 -> 184.1
LPC 16:0	496.3 -> 184.1	PC 14:0 14:0 (IS)	678.5 -> 184.1
LPC 16:1	494.3 -> 184.1	PC 30:0	706.5 -> 184.1
LPC 17:0 (IS)	510.4 -> 184.1	PC 32:0	734.6 -> 184.1
LPC 17:1	508.4 -> 184.1	PC 32:1	732.6 -> 184.1
LPC 18:0	524.4 -> 184.1	PC 32:2	730.5 -> 184.1
LPC 18:1	522.4 -> 184.1	PC 32:3	728.5 -> 184.1
LPC 18:2	520.3 -> 184.1	PC 34:0	762.6 -> 184.1
LPC 18:3	518.3 -> 184.1	PC 34:1	760.6 -> 184.1
LPC 20:1	550.4 -> 184.1	PC 34:2	758.6 -> 184.1
LPC 20:2	548.4 -> 184.1	PC 34:2 + 2O	790.6 -> 184.1
LPC 20:3	546.4 -> 184.1	PC 34:2 + O	774.6 -> 184.1
LPC 20:4	544.3 -> 184.1	PC(O-34:3) +2O	774.6 -> 184.1
LPC 22:0	580.4 -> 184.1	PC(P-34:2) +2O	774.6 -> 184.1
LPC 22:1	578.4 -> 184.1	PC 34:3	756.6 -> 184.1
LPC 22:5	570.4 -> 184.1	PC 34:4	754.5 -> 184.1
LPC 22:6	568.3 -> 184.1	PC 36:0	790.6 -> 184.1
LPC 24:0	608.5 -> 184.1	PC 36:1	788.6 -> 184.1
LPC 26:0	636.5 -> 184.1	PC 36:2	786.6 -> 184.1
oddPC 29:0	692.5 -> 184.1	PC 36:3	784.6 -> 184.1
oddPC 31:0	720.6 -> 184.1	PC 36:4	782.6 -> 184.1
oddPC 31:1	718.5 -> 184.1	PC 36:5	780.6 -> 184.1
oddPC 33:0	748.6 -> 184.1	PC 36:6	778.5 -> 184.1
oddPC 33:1	746.6 -> 184.1	PC 38:2	814.6 -> 184.1
oddPC 35:0	776.6 -> 184.1	PC 38:3	812.6 -> 184.1
oddPC 35:1	774.6 -> 184.1	PC 38:4	810.6 -> 184.1
oddPC 35:2	772.6 -> 184.1	PC 38:5	808.6 -> 184.1
oddPC 35:3	770.6 -> 184.1	PC(P-34:2)	742.5 -> 184.1
oddPC 35:4	768.6 -> 184.1	PC(P-34:3)	740.6 -> 184.1
oddPC 35:5	766.5 -> 184.1	PC(P-36:4)	766.6 -> 184.1
oddPC 37:4	796.6 -> 184.1	PC(P-36:5)	764.6 -> 184.1
oddPC 37:5	794.6 -> 184.1	PC(P-38:4)	794.6 -> 184.1
oddPC 37:6	792.6 -> 184.1	PC(P-38:5)	792.6 -> 184.1
oddPC 39:5	822.6 -> 184.1	PC(P-38:6)	790.6 -> 184.1
oddPC 39:6	820.6 -> 184.1	PC(P-40:5)	822.6 -> 184.1
PC(P-40:6)	818.6 -> 184.1	PE 35:2	730.5 -> 589.5
PC 38:7	804.6 -> 184.1	PE 36:0	748.6 -> 607.6
PC 40:4	838.6 -> 184.1	PE 36:1	746.6 -> 605.6
PC 40:5	836.6 -> 184.1	PE 36:2	744.6 -> 603.5
PC 40:6	834.6 -> 184.1	PE 36:3	742.5 -> 601.5
PC 40:7	832.6 -> 184.1	PE 36:4	740.5 -> 599.5

PC 40:8	830.6 -> 184.1	PE 36:5	738.5 -> 597.5
PC(16:0/22:6)	806.6 -> 184.1	PE 38:3	770.6 -> 629.6
PC(18:2/20:4)	806.6 -> 184.1	PE 38:4	768.6 -> 627.5
PC(O-16:0/0:0)	482.4 -> 104.1	PE 38:5	766.5 -> 625.5
PC(O-18:0/0:0)	510.4 -> 104.1	PE 38:6	764.5 -> 623.5
PC(O-18:1/0:0)	508.4 -> 104.1	PE 40:4	796.6 -> 655.6
PC(O-20:0/0:0)	538.4 -> 104.1	PE 40:5	794.6 -> 653.6
PC(O-20:1/0:0)	536.4 -> 104.1	PE 40:6	792.6 -> 651.5
PC(O-22:0/0:0)	566.5 -> 104.1	PE 40:7	790.5 -> 649.5
PC(O-32:0)	720.6 -> 184.1	PE(14:0/0:0) (IS)	426.3 -> 285.2
PC(O-32:1)	718.5 -> 184.1	PE(16:0/0:0)	454.3 -> 313.3
PC(O-32:2)	716.6 -> 184.1	PE(18:0/0:0)	482.3 -> 341.3
PC(O-34:1)	746.6 -> 184.1	PE(18:1/0:0)	480.3 -> 339.3
PC(O-34:4)	740.6 -> 184.1	PE(18:2/0:0)	478.3 -> 337.3
PC(O-36:2)	772.6 -> 184.1	PE(20:4/0:0)	502.3 -> 361.3
PC(O-36:4)	768.6 -> 184.1	PE(22:6/0:0)	526.3 -> 385.3
PC(O-38:4)	796.6 -> 184.1	PE(O-18:0/22:5)	780.6 -> 639.6
PC(O-38:5)	794.6 -> 184.1	PE(P-20:0/20:4)	780.6 -> 639.6
PC(O-40:6)	820.6 -> 184.1	PC(O-22:1/0:0)	564.4 -> 104.1
PC(O-40:7)	818.6 -> 184.1	PC(O-24:0/0:0)	594.5 -> 104.1
PC(P-30:0)	690.4 -> 184.1	PC(O-24:2/0:0)	590.5 -> 104.1
PC(P-32:0)	718.5 -> 184.1	PE(O-18:1/18:2)	728.6 -> 587.5
PC(P-32:1)	716.6 -> 184.1	PE(P-18:0/18:2)	728.6 -> 587.5
PC(P-34:1)	744.6 -> 184.1	PE(O-18:1/20:3)	754.6 -> 613.6
PE 14:0/14:0 (IS)	636.5 -> 495.5	PE(O-18:2/18:2)	726.5 -> 585.5
PE 32:0	692.5 -> 551.5	PE(P-18:0/20:4)	752.6 -> 611.5
PE 32:1	690.5 -> 549.5	PE(O-18:2/20:3)	752.6 -> 611.5
PE 34:1	718.5 -> 577.5	PE(O-18:2/22:5)	776.6 -> 635.5
PE 34:2	716.5 -> 575.5	PE(P-18:0/22:6)	776.6 -> 635.5
PE 34:3	714.5 -> 573.5	PE(O-34:1)	704.6 -> 563.5
PE 35:1	732.6 -> 591.5	PE(O-34:2)	702.5 -> 561.5
PE(P-16:0/18:1)	702.5 -> 561.5	PI 38:3	906.6 -> 629.6
PE(O-36:2)	730.5 -> 589.5	PI 38:4	904.6 -> 627.6
PE(O-36:5)	724.5 -> 583.5	PI 38:5	902.6 -> 625.6
PE(P-16:0/20:4)	724.5 -> 583.5	PI 38:6	900.6 -> 623.6
PE(O-36:6)	722.5 -> 581.5	PI 40:4	932.6 -> 655.6
PE(P-18:0/22:5)	778.5 -> 637.5	PI 40:5	930.6 -> 653.6
PE(O-40:6)	778.5 -> 637.5	PI 40:6	928.6 -> 651.6
PE(P-16:0/18:1) FA	702.5 -> 339.3	PS 14:0 14:0 (IS)	680.5 -> 495.5
PE(P-16:0/18:2)	700.5 -> 559.5	PS 17:0 17:0 (IS)	764.5 -> 579.5
PE(P-16:0/18:2) FA	700.5 -> 337.3	PS 36:1	790.6 -> 605.6
PE(P-16:0/20:4) FA	724.5 -> 361.3	PS 36:2	788.5 -> 603.5
PE(P-16:0/22:5)	750.5 -> 609.6	PS 38:3	814.6 -> 629.6
PE(P-16:0/22:5) FA	750.5 -> 387.3	PS 38:4	812.5 -> 627.5

PE(P-16:0/22:6)	748.5 -> 607.5		PS 38:5	810.5 -> 625.5
PE(P-16:0/22:6) FA	748.5 -> 385.3		PS 40:5	838.6 -> 653.6
PE(P-18:0/18:1)	730.5 -> 589.5		PS 40:6	836.5 -> 651.5
PE(P-18:0/18:1) FA	730.5 -> 339.3			
PE(P-18:0/18:2) FA	728.6 -> 337.3			
PE(P-18:0/20:4) FA	752.6 -> 361.3			
PE(P-18:0/22:5) FA	778.5 -> 387.3			
PE(P-18:0/22:6) FA	776.6 -> 385.3			
PE(P-20:0/20:4) FA	780.6 -> 361.3			
PG 14:0 14:0 (IS)	684.6 -> 495.5			
PG 16:0 18:1	766.6 -> 577.5			
PG 17:0 17:0 (IS)	768.6 -> 579.5			
PG 18:0 18:1	794.6 -> 605.6			
PG 18:1 18:1	792.6 -> 603.5			
PI (20:4/0:0)	638.3 -> 361.3			
PI 32:0	828.6 -> 551.6			
PI 32:1	826.5 -> 549.5			
PI 34:0	856.6 -> 579.6			
PI 34:1	854.6 -> 577.6			
PI 36:1	882.6 -> 605.6			
PI 36:2	880.6 -> 603.6			
PI 36:3	878.6 -> 601.6			
PI 36:4	876.6 -> 599.6			
PI 38:2	908.6 -> 631.6			

Table 2.3 MRM List of S1P

Name	Transition
13C2D2_S1P(IS)	440.3 -> 60.1
S1P (d18:0)	438.3 -> 60.1
S1P (d18:1)	436.3 -> 60.1
S1P (d18:2)	434.3 -> 60.1
S1P (d20:1)	464.4 -> 60.1

CHAPTER 3   THE LIPIDOME OF WHITE MATTER LESIONS IN MOUSE BRAIN INDUCED BY GLOBAL CHRONIC HYPOPERFUSION

3.1   Introduction

Dementia and cognitive impairment have become increasingly prominent healthcare issues in the aged population. Cerebrovascular diseases are now recognized as a major contributor of cognitive impairment (Kalaria et al. 2008). In particular, white matter lesions (WML), characterized by loss of oligodendrocytes, myelin rarefaction and axonal damage are frequently observed in patients with vascular cognitive impairment (Ferrer 2010; Gorelick et al. 2011). White matter lesions are believed to contribute to the rapid decline of global function in elderly patients (Inzitari et al. 2007). Furthermore, research in animal models have shown that WML induced by hypoperfusion can cause working memory deficits (Shibata et al. 2007), and treatments which ameliorated WML also restored working memory function (Miyamoto, Maki, et al. 2013; Dong et al. 2011; Washida et al. 2010).

Oligodendrocytes (OLGs) form sail-like extensions of their cytoplasmic membrane, which wrap around the axon up to 150 layers thick to form the myelin sheaths. Myelin is the essential constituent of white matter in the CNS, making up 40–50% of the dry weight (Baumann and Pham-Dinh 2001) and gives white colour of WM in CNS. Due to the multiple membrane layers, myelin contains around 80% lipid content, consisting of mainly three classes including cholesterols, phospholipids and sphingolipids (O'Brien and Sampson 1965). These lipids act as structural lipids that form the matrix of

cellular membranes(van Meer, Voelker, and Feigenson 2008), providing barrier function, fluidity characteristics that are essential for cell division, reproduction, membrane vesicle trafficking, and raft supporting membrane proteins. Moreover, several lipids such as ceramides, S1P have been found to act as first of second messengers that regulate various cell signalling pathways (Spiegel and Milstien 2003). Myelin loss which is usually demonstrated with Kluver-Barrera staining(Kluver and Barrera 1953), a method in which luxol fast blue stains for myelin with Nissl counterstain, is one of the most prominent characteristics of WML. However, little is known about the alterations of lipids in the WML induced by hypoperfusion. Besides, thousands of chemically distinct lipid species derived from various combinations of backbone structures containing fatty acids markedly increase the degree of difficulty in studying these lipids. Lipidomics, as an emerging field of analysis of lipids at the systems-level, is based on LC-MS/MS and provides detailed analysis and global characterization of the structure and function of lipids in a living system (Harkewicz and Dennis 2011). In fact, lipidomics has uncovered lipid aberrations in a variety of diseases. For example, Lam et al. (Lam et al. 2014) reported aberrations of sphingolipids and phospholipids in the postmortem brain tissues from patients suffered subcortical ischemic vascular dementia.

Global hypoperfusion through vessel occlusion or stenosis is widely used for experimental vascular dementia models. Bilateral common carotid stenosis (BCAS) in C57BL/6 mice has been described to produce a prolonged global cerebral blood flow reduction by ~20-30% by narrowing the bilateral common carotid arteries (CCAs) with microcoils, causing

selective WML without apparently histological abnormalities in the grey matter (Shibata et al. 2004) in 2 weeks after the BCAS surgery.

In this section, the pathological characteristics of WML and cognitive deficits induced by chronic cerebral hypoperfusion in mice are described. More importantly, a total of 200 distinct lipid species covering the most abundant ones from 13 lipid subclasses, including neutral lipids such as free cholesterols; sphingolipids subclasses of ceramide (Cer), glycosphingolipid, sphingomyelin(SM); phospholipid including lysophosphatidylcholine (LPC), phosphatidylcholine (PC), lysophosphatidylethanolamine (LPE), phosphatidylethanolamine (PE), phosphatidylserine (PS), phosphatidyglycerol (PG), and phosphatidylinositol (PI) in cerebral WMT are profiled and analysed by lipidomics in sham-operated mice and BCAS mice.

3.2 Results

3.2.1 BCAS causes global CBF decrease and hypoxia in mouse brain

The CBF was recorded for 5-10 mins before the implantation of the microcoils and set to 100% as the pre-implantation baseline. At 15 min after bilateral implantation of the microcoils, CBF decreased to 62.8 ± 2.4% of pre-implantation baseline (Figure 3.1), indicating that coils successfully narrowed the carotid artery and reduced the global cerebral perfusion. As expected, CBF remained unchanged (97.7±6.7%) in sham-operated mice.
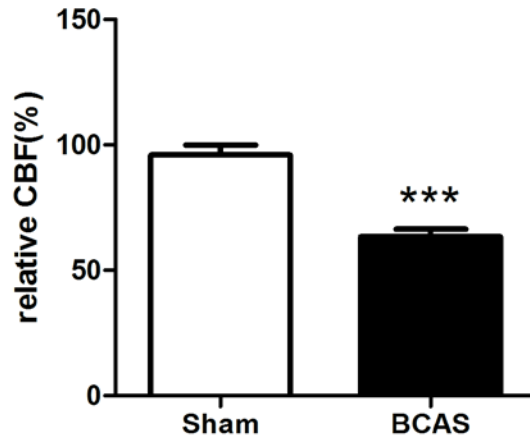
**Figure 3.1 rCBF in sham-operated and BCAS mice**
Reduction in relative cerebral blood flow (rCBF) at 15 min after bilateral implantation of microcoils to constrict the common carotid arteries. CBF was expressed as percentage of the baseline level obtained pre-implantation. Bars represent mean ± S.E.M., N =11 per group. ***$p < 0.005$ by Student's *t*-test, t = 7.6.

Figure 3.2 showed the immunofluorescent intensity of HIF1-α enhanced significantly both in cortex and CC at 15 days after the surgery. Besides, Western blot revealed that HIF1-α increased to nearly 2-fold in CC (Figure 3.3). HIF1-α expression shows strong evidence for a hypoxic response within the brain and BCAS created a long lasting hypoperfusion condition in the brain.
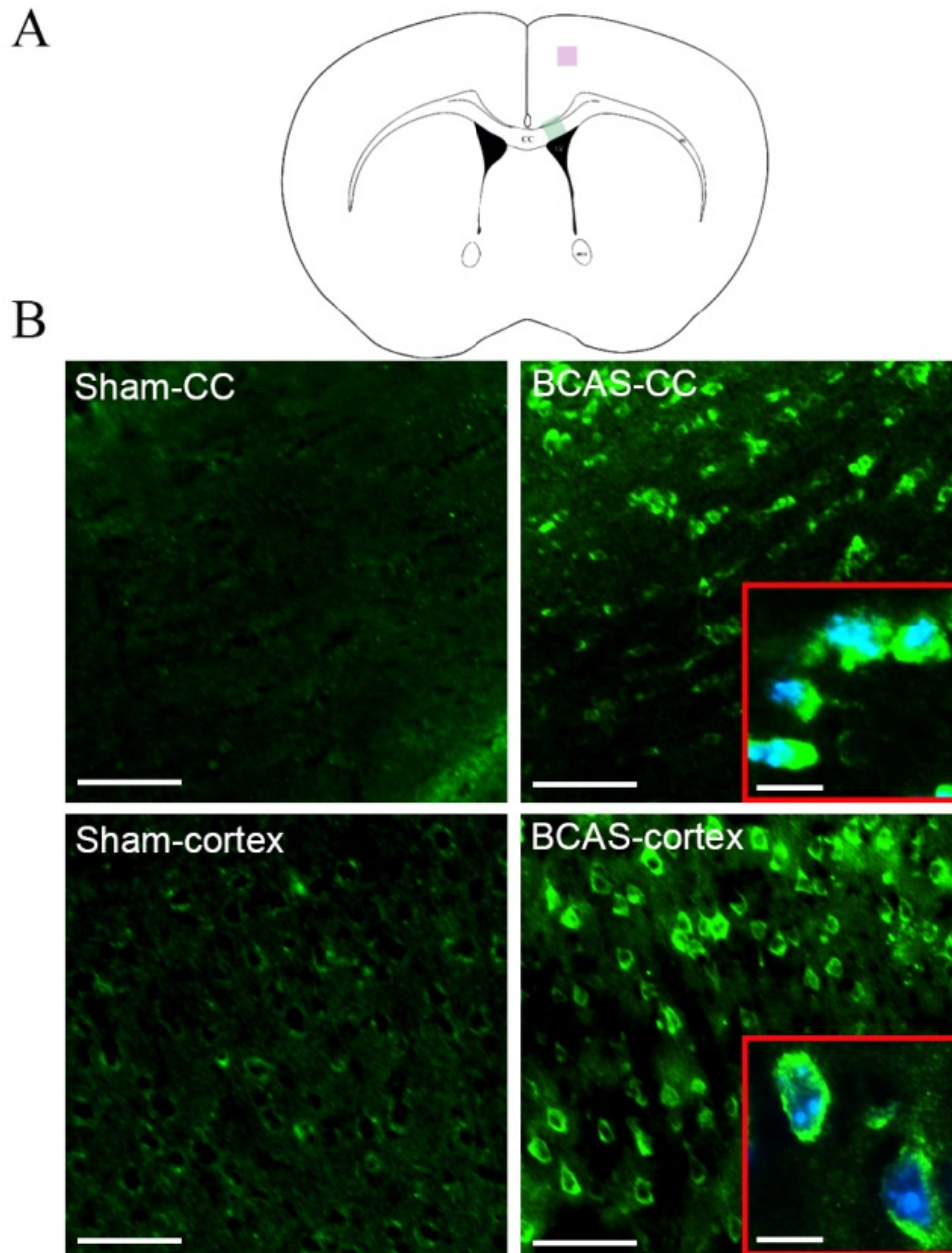
Figure 3.2 Representative image of HIF-1α immunofluorescence in the brain at 15 days after BCAS

A, Schematic diagram showing coronal section of the mouse brain at the level of 0.5-1 mm anterior to bregma. Green and red shaded rectangles indicate the representative images of CC region (upper panel) or cortex region (lower panel) shown in B. **B,** Left panel: Sham-operated, Right panel: BCAS. Scale bar = 60μm. Insets of right panel: images of higher magnification showing HIF-1α (green) staining co-localized with nuclei (stained with DAPI, blue). Scale bar =10 μm. Abbreviations: CC, corpus callosum; BCAS, bilateral common carotid artery stenosis.
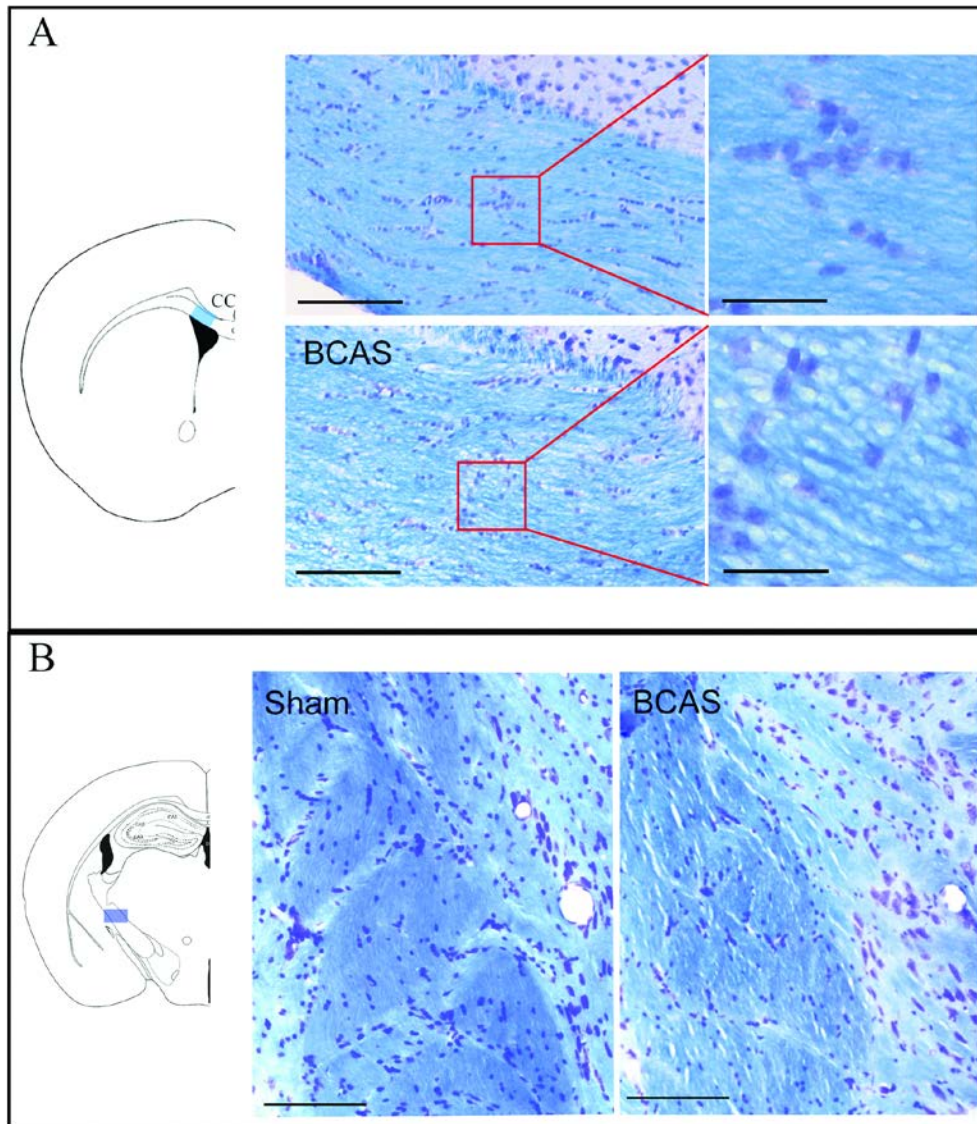
84
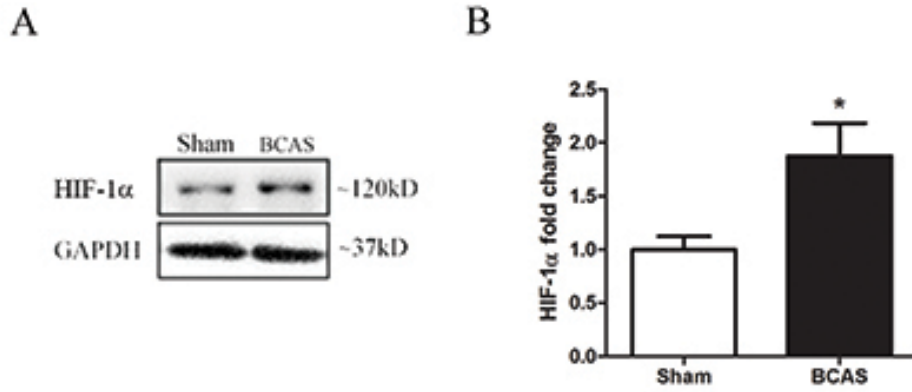
Figure 3.3 Up-regulation of HIF-1α expression in white matter tissues following BCAS.
A, representative immunoblot and **B**, bar graph of white matter tissue HIF-1α immunoreactivity (as mean ± S.E.M. fold-change relative to mean value of sham animals), normalized to GAPDH. N=6, *p < 0.05 by Student's t-test, t = 2.6.

3.2.2 Selective White matter lesions induced by hypoperfusion

Fifteen days after implantation, BCAS mice showed myelin loss characterized by the obviously reduced integrity of myelin sheaths and the intensity of myelinated fibres in BCAS mice in white matters such as the corpus callosum (Figure 3.4A) and internal capsule (Figure 3.4B), as revealed by Kluver-Barrera staining. The remaining fibres are apparently disordered with the appearance of vacuoles in the myelin sheaths. Furthermore, immunoreactivity of myelin basic protein (MBP) decreased by around 50% in WMT of BCAS mice (Figure 3.5). MBP is exclusively expressed in matured OLGs and thus is a marker for mature OLG. Both these observations are indicative of WML development following BCAS.

Figure 3.4 Kluver-Barrera staining in white matter regions
A, Representative images in CC of sham-operated mice (upper panel) and
BCAS mice (lower panel). Panel on the right shows high magnification
images of the areas defined by the red squares on the left panels. Schematic
diagram shows coronal section of the mouse brain at the level of 0.5-1 mm
anterior to bregma. **B**, Representative images in internal capsule. Scale bars
= 120 µm. Schematic diagram shows coronal section of the mouse brain at
the level of 1.3-1.8 mm posterior to bregma.

Figure 3.5 Down-regulation of MBP expression in white matter tissues following BCAS.
A, representative immunoblot and **B**, bar graph of white matter tissue myelin basic protein (MBP) immunoreactivity (as mean ± S.E.M. fold-change relative to mean value of sham animals), normalized to β-actin. N=6, ***p < 0.001 by Student's t-test, t = 5.6.
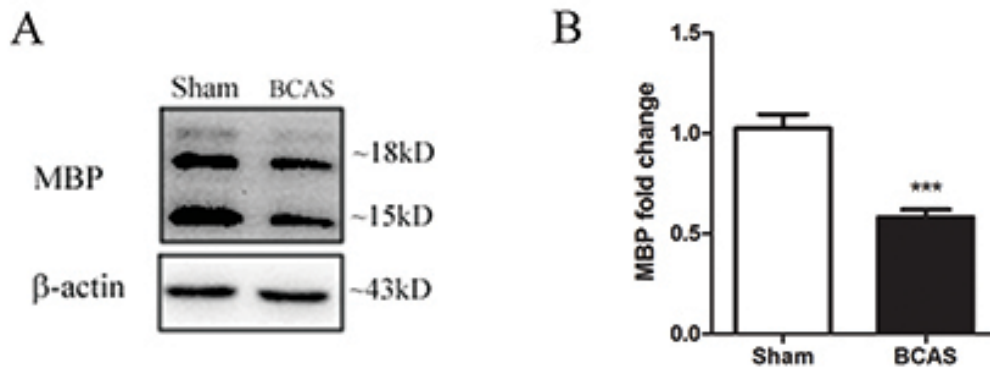
There were no apparent neuronal injuries in the cortex and hippocampus as shown by KB staining (Figure 3.6B and C respectively). Immunoreactivity of NeuN in cortex confirmed the observation of KB staining (Figure 3.7). From the above evidence, it is concluded that global chronic hypoperfusion caused selective WML without apparent cortical or hippocampus neuronal damage.
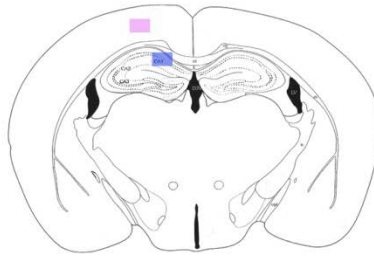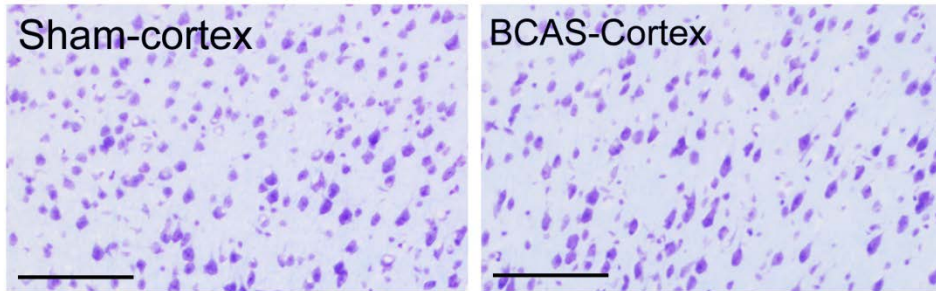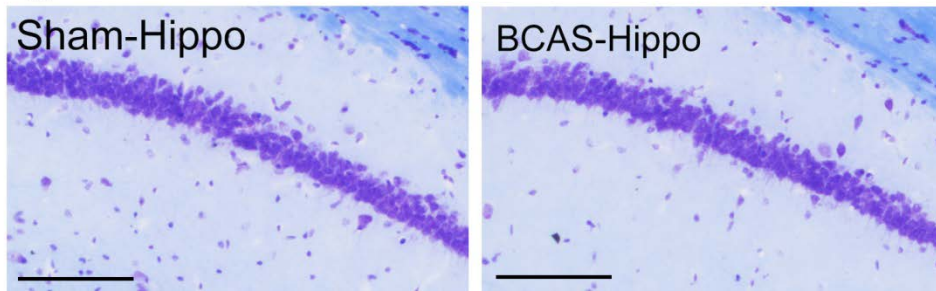
Figure 3.6 Kluver-Barrera staining in grey matter regions
A, Schematic diagram showing coronal section of the mouse brain at the level of 1.3-1.8 mm posterior to bregma. Red and blue shaded rectangles show the areas of images shown in **B** (cortex) and **C** (CA1 hippocampus), respectively. Scale bar = 120 μm. Abbreviation: Hippo, hippocampus.
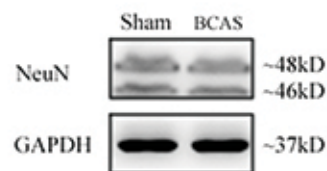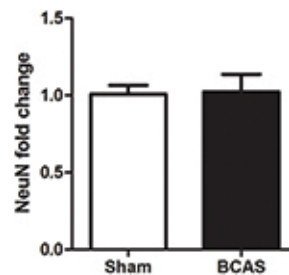
Figure 3.7 Levels of NeuN in cortex of sham and BCAS mice.
A, Representative immunoblots and **B**, bar graph of cortical NeuN immunoreactivity (as mean ± S.E.M. fold-change relative to mean value of sham animals), normalized to GAPDH. N=6.

3.2.3 Cognitive impairment in BCAS mice

Barnes Maze, similar to Morris Water Maze and to the radial-arm maze, is a test for spatial learning and memory, where the mouse is placed into the maze and was allowed to find the escape box. More details of the experimental settings and procedures have been described in Chapter 2, section 4). It has a 3-day acquisition phase and a probe trial 24 h after acquisition phase. Primary latency (s) primary path length (cm) and primary errors are designated as the time, moving distance and pokes in wrong holes before the mouse reached the target hole for the first time (Sunyer et al. 2007). They are commonly used to evaluate the whether the mouse have learnt the task during the acquisition phase, since it is assumed that mice that remember the location of the target hole will have a shorter latency and will search fewer holes by directly moving towards the target hole. Searching strategy is an important parameter to indicate if the mouse had learnt to solve the task with spatial memory. The search strategies can be defined into three categories: direct, serial or mixed (Definition of the three strategies has been described in Chapter 2, Section 4.5.1. Only direct strategy is considered that the mouse is using spatial memory (Sunyer et al. 2007). Therefore, searching strategy the mouse using to escape is an important indicator of its spatial memory as well. Barnes maze test was performed in mice at 15 days after surgery in this study.

Barnes maze test was performed in mice at 15 days after surgery in this study. During 3-day spatial acquisition phase, the primary path length (Figure 3.8A), primary errors (Figure 3.8B) and primary latency (Figure 3.8C) to the target hole decreased significantly (analysed by two-way

ANOVA with repeated measures) in both sham-operated and BCAS group, with $F_{(2,16)}=15.5$, $p<0.000$, $F_{(2,16)}=6.1$, $p<0.05$ and $F_{(2,16)}=14.7$, $p<0.000$ respectively, but there is no difference between the two groups of animals with $F_{(1,8)}=0.9$, $F_{(1,8)}=1.4$, $F_{(1,8)}=0.8$ respectively.
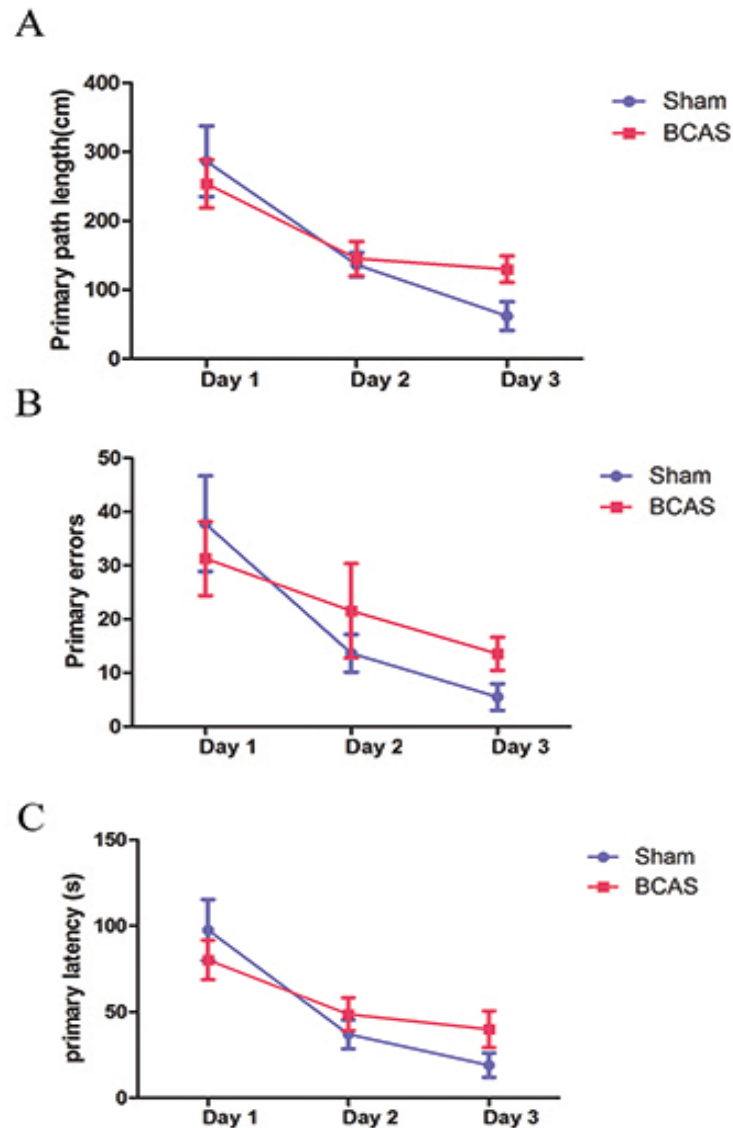
Figure 3.8 Barnes Maze performance of sham and BCAS mice during the acquisition phase
Two-way ANOVA with repeated measures shows that these three parameters decrease in both sham and BCAS mice during three days of the acquisition phase with $F_{(2,16)}=15.5$, $p<0.000$, $F_{(2,16)}=6.1$, $p<0.05$ and $F_{(2,16)}=14.7$, $p<0.000$ for **A**, primary path length **B**, primary errors and **C**, primary latency respectively. N=9. Although the data show some separation between the 2 groups on Day 3, they fail to reach statistical significance.

However, during the acquisition phase, the sham-operated mice showed increasing use of the direct searching strategy in favour of the serial mixed strategy (Figure 3.9A), suggesting that the sham-operated mice were relying more on their spatial memory to solve the task. On the other hand, the BCAS mice remained using mainly the serial strategy instead (Figure 3.9B).
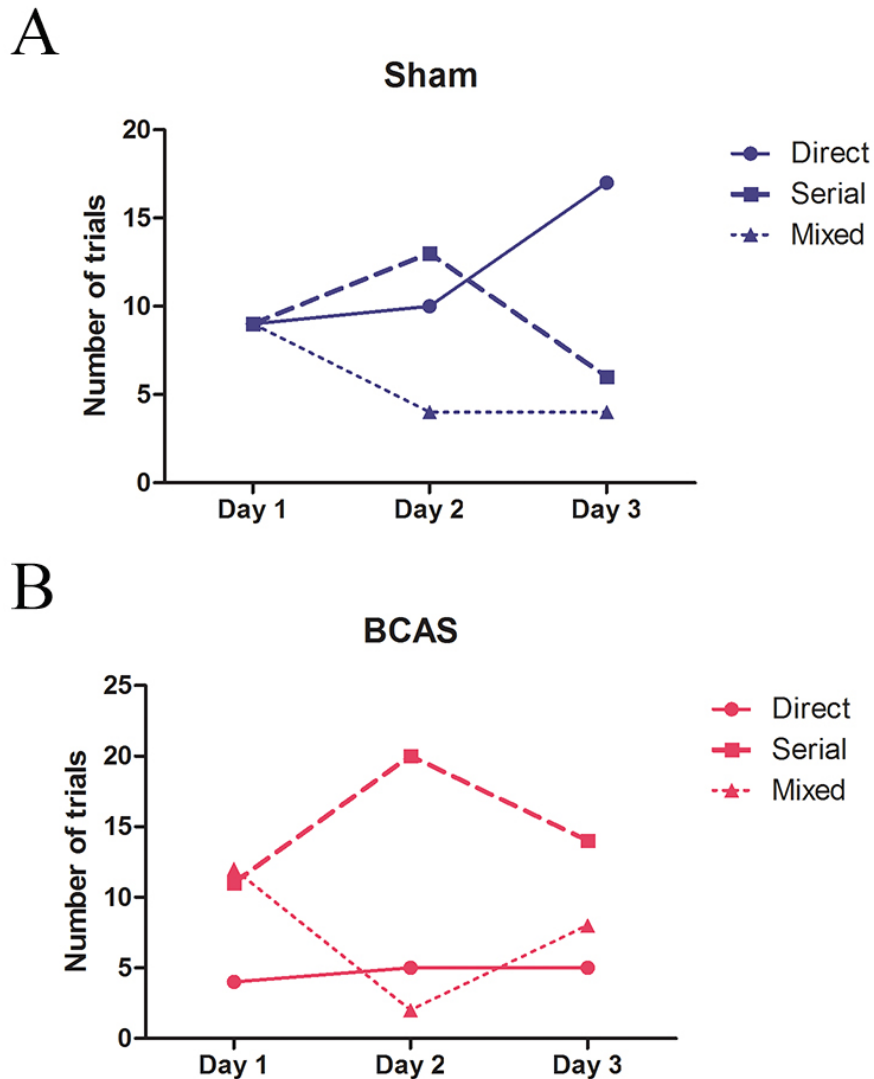
Figure 3.9 Searching strategies used by the sham and BCAS mice during acquisition phase
A, Searching strategy of sham-operated mice **B**, Searching strategy of BCAS mice. Fisher's exact test was used on the Day 3, showing a significant association between the strategy and the group (sham and BCAS), $P < 0.005$. N=27.

Fisher's exact test shows that on the third training day, the searching strategies chosen by the mice were significantly associated with the group difference. These observations suggested that though sham-operated mice and BCAS mice have both learnt to escape from the maze during 3 days' training, only sham-operated mice solved the task using spatial memory. BCAS mice improved their performance by searching the holes along the perimeters quickly instead of going directly to the target hole.

Probe trial was conducted 24 h after the last section of acquisition phase to test the memory of the mouse. Mice were exposed to the Barnes maze with the target hole being covered and allowed to explore the maze for 2 minutes. Setting of the 5 zones was demonstrated in Chapter 2, section 4.5.2 as shown by Figure 2.3B. Two-way repeated ANOVA shown significant different preferences of the zones by sham and BCAS mice (Figure. 3.10A), $F(2,16) = 5.3$. Notably, sham-operated mice strongly prefer to stay in Zone 1 where the target hole was located with the duration spent in Zone 1 being about 4-fold longer than the duration spent in any other zone (Figure 3.10A). In contrast, the time spent in Zone 1 by the BCAS mice was only about half of that of the sham-operated mice. Besides, Figure 3.10B showed that the BCAS mice made significantly more total errors than the sham-operated mice due to that BCAS mice tended to explore other holes, while sham-operated mice preferred to stay around the target holes. These observations suggested that sham-operated mice had a better memory about the location of escape box while the BCAS showed a deficit memory. Searching strategy (before the mouse reaching the target hole for the first time) analysis showed

to similar to acquisition phase, sham-operated mice prefer direct strategy while BCAS mice remained using serial or mixed strategy (Figrue 3.10C).

Therefore, it could be concluded that BCAS mice showed cognitive impairment characterized with impaired spatial memory.
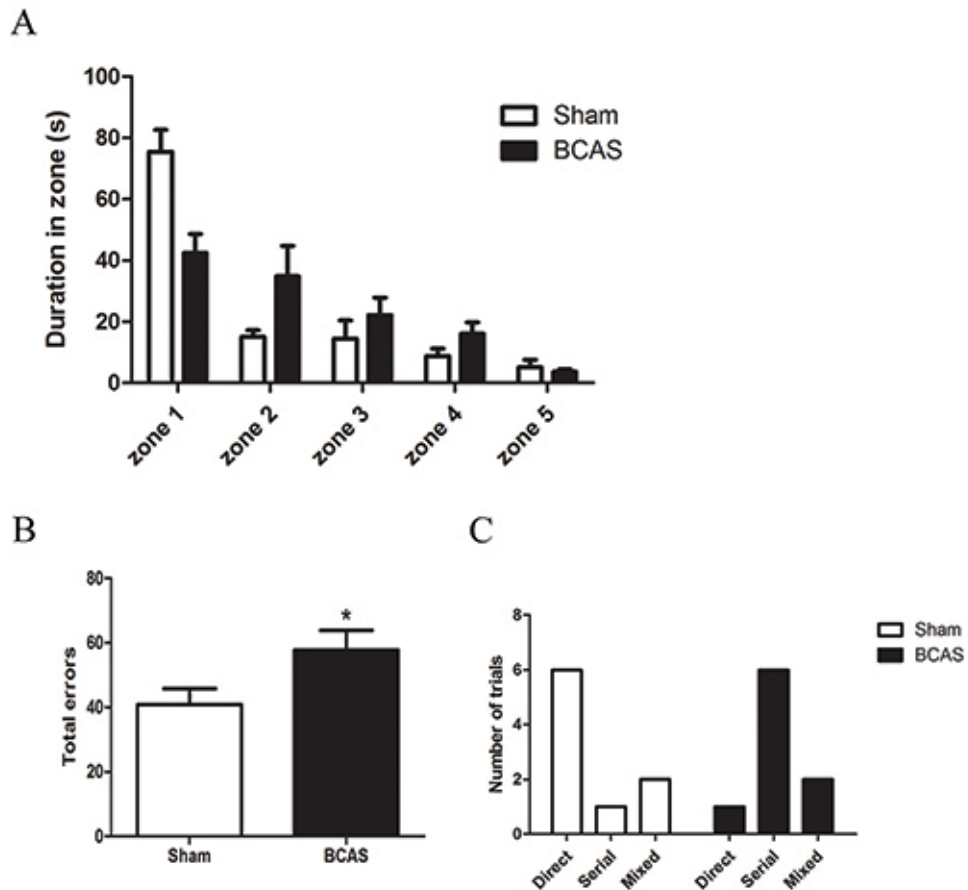
Figure 3.10 Barnes Maze performance in the probe trial
A, Total time spent in Zone 1-5. Duration time in 5 zones were significantly different between sham and BCAS group, by two-way repeated ANOVA, $F_{(2, 16)} = 5.3$, $p < 0.05$, N=9. **B**, Total error made during the 2 min of probe trial, *$p < 0.05$ by student's t test. N=9, t=2.2. **C**, Searching strategies for sham-operated and BCAS group. Fisher's exact Test shows a significant association between the strategies and the group difference. $P < 0.05$, N=9 per group.

3.2.4 Lipids alterations

3.2.4.1 Effects of hypoperfusion on sphingolipids

The total amount of sphingolipid was not changed by hypoperfusion in BCAS. But significant reduction in the total amount of glycoceramides was

93

observed in WMT of BCAS as shown in Figure 3.11. The total amounts of

Cer and SM did not appear to be affected by hypoperfusion (Figure 3.11).
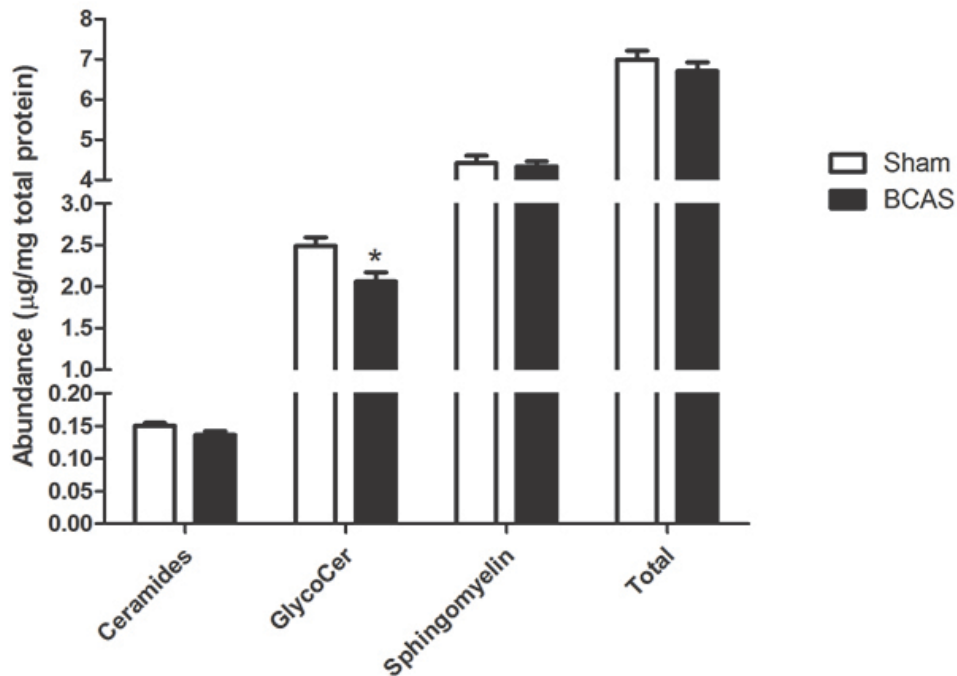
Figure 3.11 Changes in amounts of sphingolipids for cerebral WML
The amounts major subclasses of sphingolipids, including Ceramide, sphingomyelin and glycoceramides (GlycoCer) are expressed as mean±S.E.M, normalized to the total protein concentration. *P<0.05 by Student's t- test, t=2.2. N=6.

In glycoceramides profiling (Figure 3.12), monohexosylceramides (MHC) are shown to be the predominant components, which include both galactosylceramides (CalCer) and glucosylceramides (GluCer). On the other hand, the dihexosylceramides (DHC), which includes the lactosylceramides (LacCer), consist only less than 0.3% of total glycoceramides. Profiles of individual glycoceramides (Figure.3.12) showed a decreasing trend for all 7 species analyzed here, though only MHC 22:0 and MHC 24:1 showed statistically significant decreases.
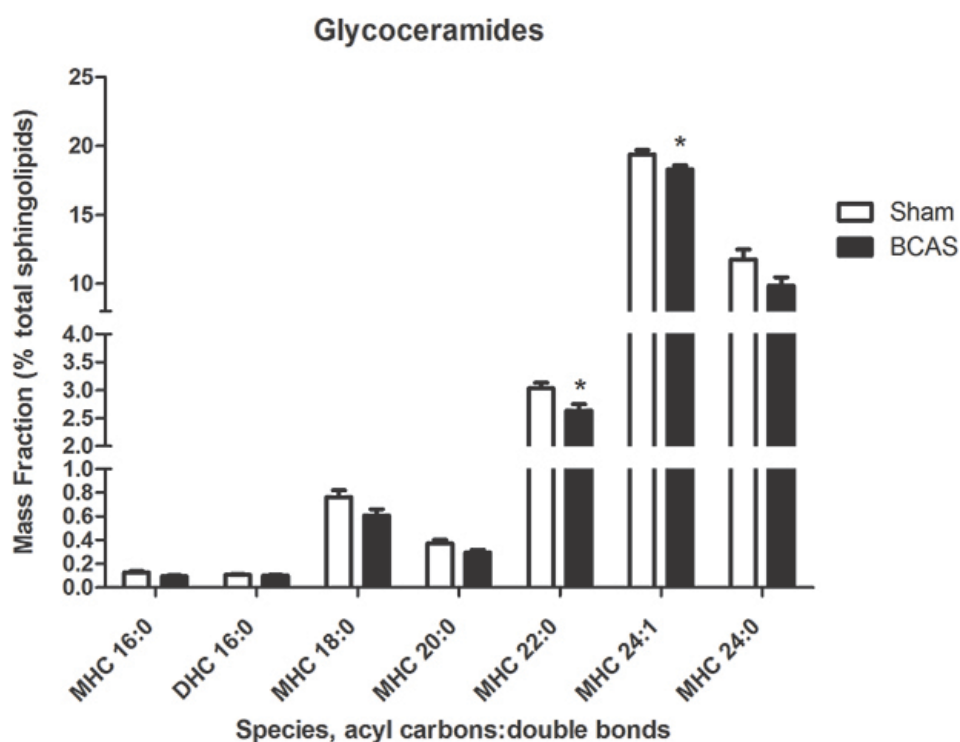
Figure 3.12 Comparative glycoceramides profiles in WMT of Sham and BCAS

Individual species of glycoceramides are expressed as mass fractions of total amount sphingolipids. *P<0.05 by Student's t- test, t=2.6 for MHC 22:0 and t=2.5 for MHC 24:1. N=6. Abbreviations: MHC, monohexolceramide; DHC, dihexolceramide.

It is interesting that though the total amount of Cer and SM remained unchanged, the individual species compositions altered. As shown in Fig 3.13, there were notable reductions in the mass fractions of Cer d18:1/C24:1, Cer d18:0/C24:0 and SM 42:1, while significant elevations in SM 34:1, SM 36:1 were observed (Figure 3.14). When separating the sphingolipid species by the carbon numbers of their acyl chain, it is noted that the accumulative amount of C22, C24-sphingolipids decreased while C16, 18 increased (Figure 3.15).
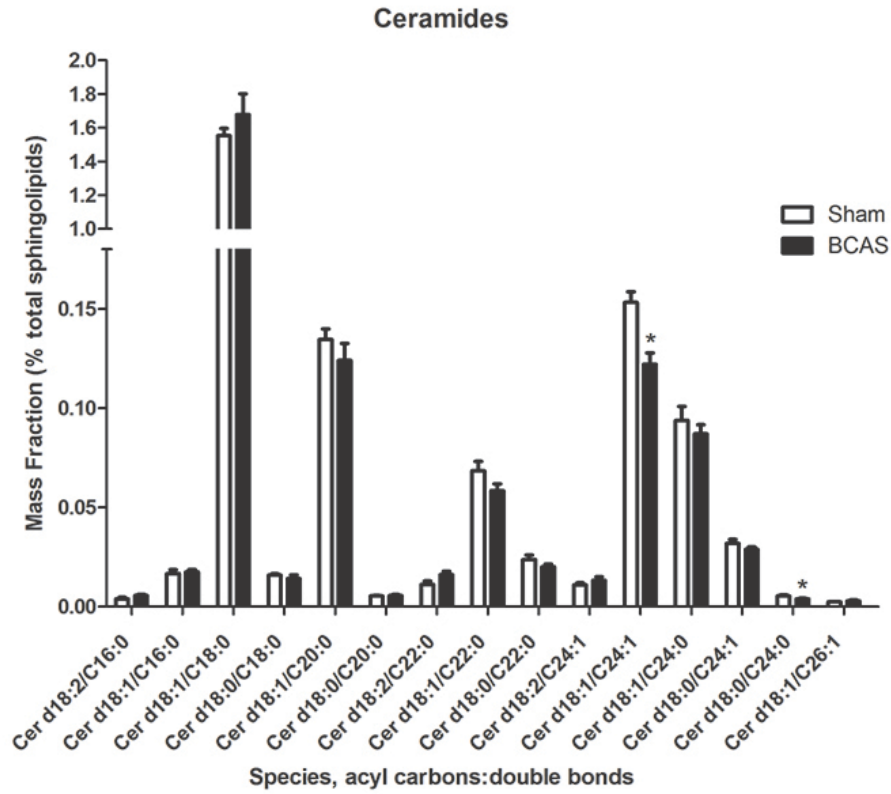
Figure 3.13 Comparative ceramides profiles in WMT of Sham and BCAS

Individual species are expressed as mass fractions of sphingolipids total amount. *P<0.05 by Student's t- test, t=2.8 for Cer d18:1/C24:1and t=2.2 for Cer d18:0/C24:0. N=6. Abbreviations: Cer, ceramide.
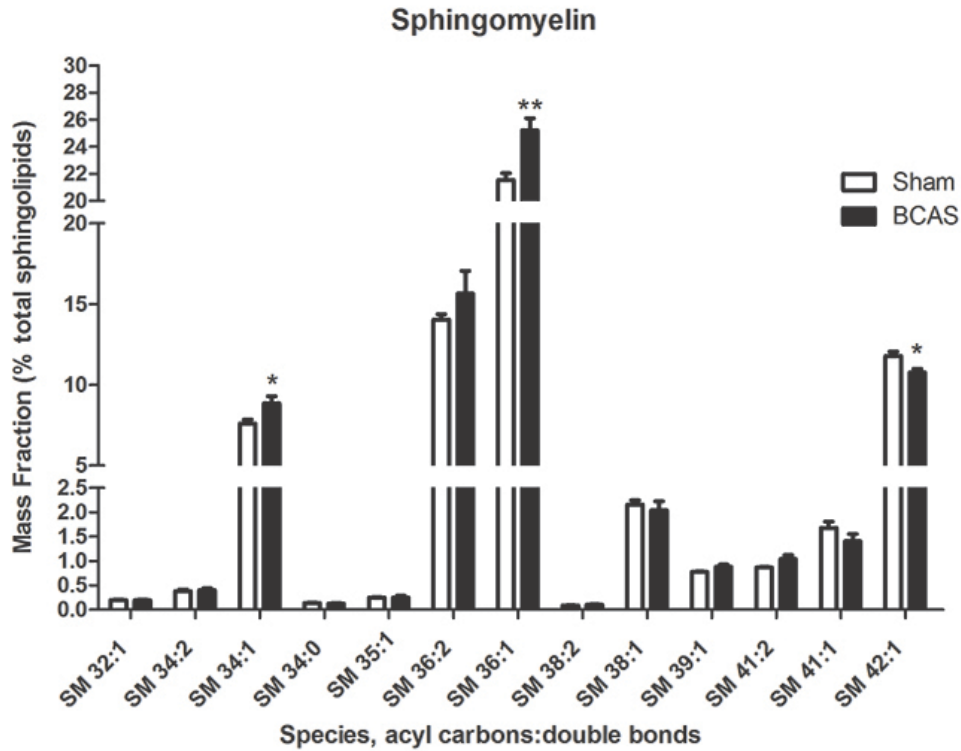
Figure 3.14 Comparative sphingomyelins profiles in WMT of Sham and BCAS

Individual species are expressed as mass fractions of sphingolipids total amount. *P<0.05, **P<0.01 by Student's t- test, t=2.4 for SM 34:1, t=3.6 for SM 36:1, and t=3.0 for SM 42:1, N=6.
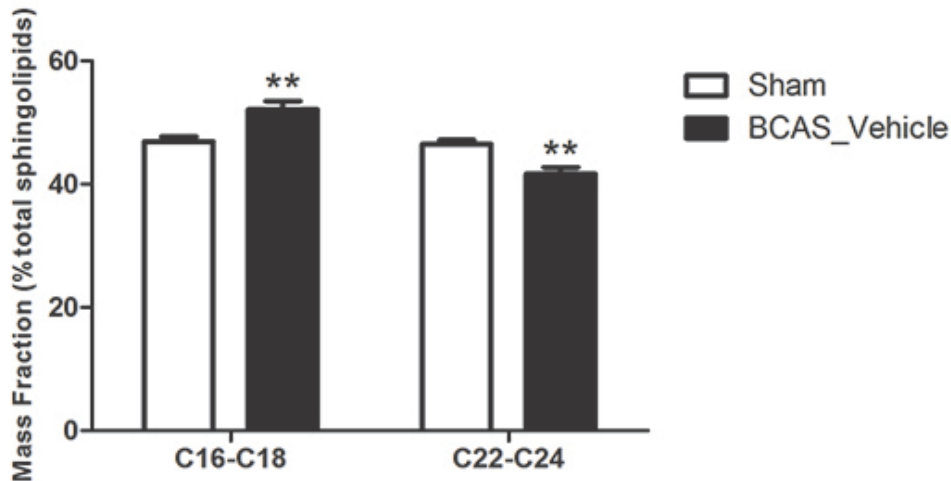
Figure 3.15 Changes of C16-18 sphingolipids and C22-24 sphingolipids in WML

Data are expressed as mass fractions of total amount sphingolipids. **P<0.0 by Student's t- test, t=3.3 for C16-18-sphingolipids; t=3.8 for C22-24-sphingolipids, N=6.

3.2.4.2 Effects of hypoperfusion on phospholipids

As shown by Figure 3.16, appreciable elevations in PS and PG in BCAS mice were found to be of statistical significance both at ~1.3 to 1.4-fold increase. The total amounts of LPC, PC, LPE, PE, PI did not appear to change. Since PC and PE are the predominant phospholipid subclasses, the amount of overall phospholipid also did not change. All the 7 individual species of PS were elevated significantly (Figure 3.17A) and 2 species of PG (16:0/18:1; 18:1/18:1) increased notably (Figure 3.16B) in BCAS. Most individual species, especially the predominant species of LPC, PC, LPE, PE, and PI remained unchanged.
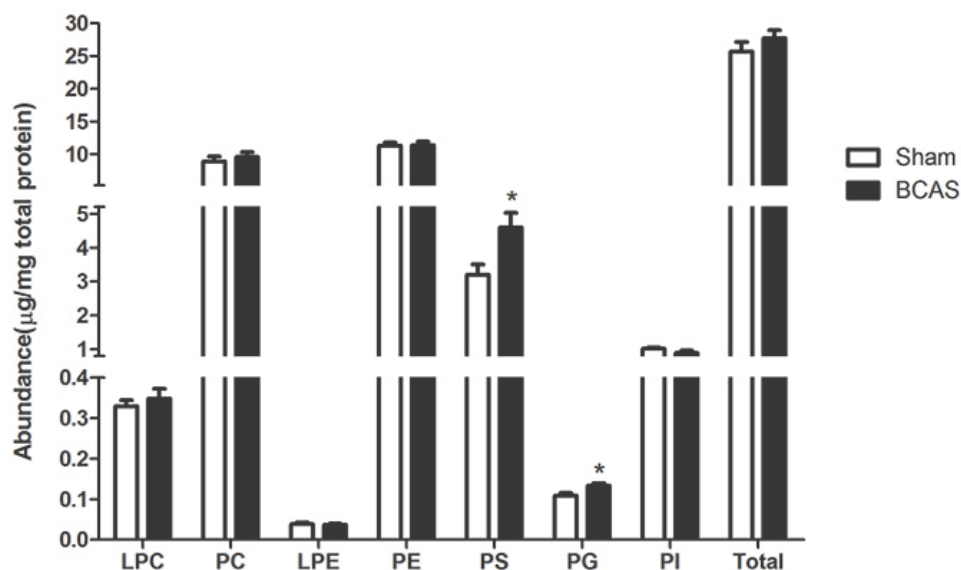
Figure 3.16 Changes in amounts of phospholipids for cerebral WML
Amounts of individual subclasses were normalized to the total protein concentration. *P<0.05 by Student's t- test, t=2.7 for PS and t=2.6 for PG, N=6. Abbreviations: LPC, lysophosphatidylcholine; PC, phosphatidylcholine; LPE, lysophosphatidylethanolamine; PE, phosphatidylethanolamine; PS, phosphatidylserine; PG, phosphatidyglycerol; PI, phosphatidylinositol.
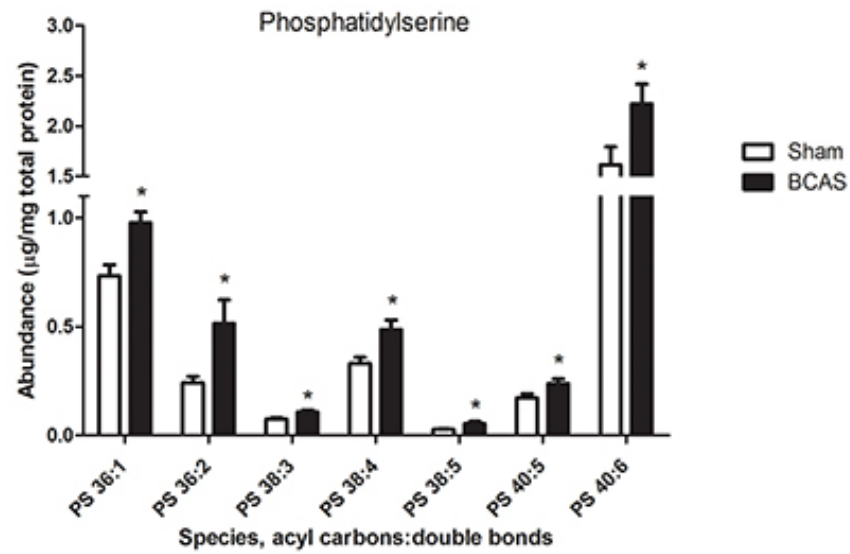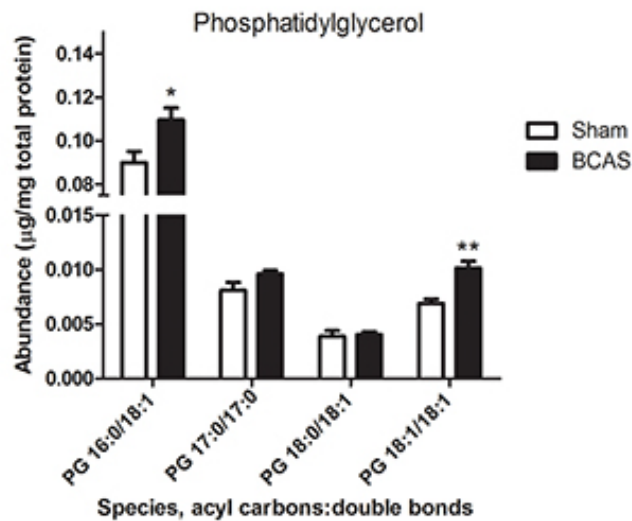
Figure 3.17 Profiles of PS and PG in WMT for Sham and BCAS mice
A, Profile of PS, *P<0.05 by Student's t-test, respectively PS 36:1, t=3.4; PS 36:2, t=2.4; PS 38:3, t=3.0; PS 38:4, t=3.0; PS 38:5, t=2.5; PS 40:5, t=2.3, PS 40:6, t=2.3. N=6. **B**, Profile of PG, *P<0.05, t= 2.6 for PG 16:0/18:1; **P<0.01, t= 4.4 for PG18:1/18:1.

3.2.4.3 Effects of hypoperfusion on cholesterol

As we can see from Figure 3.18, the cholesterol levels in sham-operated mice and BCAS mice were 21.8±1.3 and 21.7±1.3 μg/mg total protein respectively, suggesting that chronic hypoperfusion did not affect the cholesterol levels in WM.
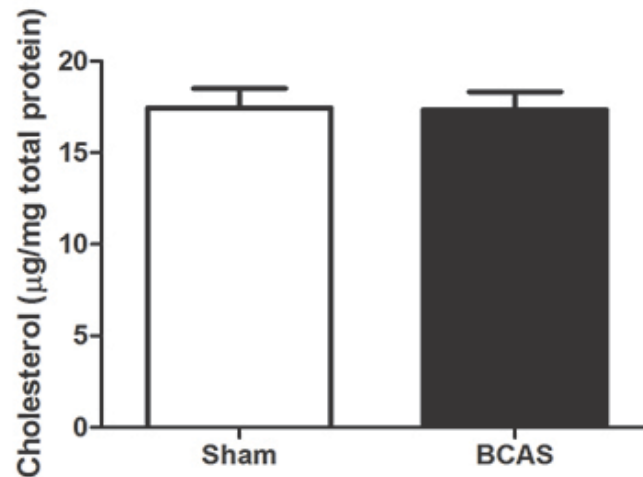
Figure 3.18 Amounts of total cholesterol in WMT for Sham and BCAS mice
Amounts of cholesterol were normalized to total protein. No significance was detected by Student's t-test. N=6.

3.3   Discussion

3.3.1   Hypoperfusion caused long-lasting hypoxia

Cerebral hypoperfusion is usually quantified by CBF (D'Haeseleer et al. 2015). In this study, the CBF was measured by laser-doppler flowmetry as described previously (Shibata et al. 2004). Shibata et al. have demonstrated that BCAS reduced the global CBF to a minimum (~70% of the baseline) two hours after the BCAS, which is close to our observation ($62.8 \pm 2.4\%$) at 15 mins, and then the CBF slowly recovered by 10% at 14 days. Hypoxia-inducible factor 1(HIF-1) is a very important factor that respond to hypoxia.

Its alpha subunit (HIF-1α) level determines the transcriptional activity of HIF1. Under well-oxygenated conditions, HIF1-α is degraded rapidly by an ubiquitin ligase. While in hypoxic conditions, the degradation is inhibited and thus HIF-1α level raises, inducing down-stream gene transcription (Adams et al. 2009; Semenza 2012). Thus HIF-1α level is usually used as a marker for hypoxia. Chronic cerebral hypoperfusion in rats induced significant long-lasting HIF-1α accumulation in the brain has been demonstrated (Yang et al. 2013; Marquez-Martin et al. 2012), indicating the long-lasting hypoxic conditions induced by chronic hypoperfusion. Similarly, we also revealed significant immunofluorescent intensity increases of HIF1-α both in cortex and CC as well as elevated HIF-1α protein level in WMT. Therefore, the reduced CBF and global elevation of HIF-1α at 15 days suggested BCAS has successfully induced cerebral chronic hypoperfusion and a long-lasting global hypoxic condition in cerebral WM.

3.3.2 Selective white matter lesions

WMLs in the brain appear as hypodensities on computed tomography or as hyperintensities in T2-weighted and proton density MRI(Pantoni and Garcia 1995).The neuropathological changes in these lesions are characterized by diffused myelin sheath rarefaction, loss of oligodendrocytes and glia activation (Englund 2002).

Kluver-Barrera staining was firstly described by Kluver and Barrera (Kluver and Barrera 1953). It is a combined myelin stain by Luxol Fast Blue that has strong affinity for lipoproteins in myelin sheath and Nissl stain by cresyl violet. Under the stain, myelin fibres appear blue and Nissl substance and nuclei appear pink to purple. It is widely used in studies involved with

white matters (Nakaji et al. 2006) (Huynh et al. 2014). MBP, exclusively expressed by mature OLG, is a major protein in myelin which accounts for about 30% of the total protein in CNS myelin (Quarles 2005). It plays an essential role in maintaining the compact myelin by adhering the cytoplasmic leaflets of the OLG membrane together, and thus reduced MBP indicated myelin damage and has been observed in demyelination diseases (Harauz and Boggs 2013). Therefore, our results demonstrate that BCAS induced by implantation of microcoils with an inner diameter of 0.18mm cause selective WML without apparent damage to cortical and hippocampus neurons as shown by crysel violet staining of KB staining in Figure 3.6 and immunoblot of NeuN in Figure 3.7, which is consistent with previous research (Shibata et al. 2004). More severe cerebral chronic hypoperfusion in mice induced by implantation smaller microcoils (inner diameter: 0.16mm), producing a reduction in CBF by ~70%, have been reported to cause infarcts and neuron loss in cortex and hippocampus (Shibata et al. 2004). Permanent bilateral CCAs occlusion in rat, also called '2-VO', could produce a reduction in CBF by 50% -70% (Hainsworth and Markus 2008) and induce not only white matter lesions but also neuronal damage in CA3 hippocampus (Kawaguchi et al. 2002). These observations suggest that white matters are more vulnerable to mild chronic hypoperfusion. However, the reasons are not fully understood. One possibility is that WM receives most of its blood supply through long penetrating arteries from the surface of the brain and anastomoses between the penetrating arteries are scarce or absent. This lack of collaterals may cause the WM to be more sensitive to hypoperfusion (Pantoni and Garcia 1997b). Besides, OLGs are believed to be extremely

vulnerable to ischemia (Dewar, Underhill, and Goldberg 2003). Mechanisms of the OLG's vulnerability are not fully understood yet. OLG is sensitive to oxidative stress due to its high lipid content, high iron and limited antioxidants (Juurlink, Thorburne, and Hertz 1998). Chronic hypoperfusion has been reported to induce oxidative stress in white matters (Miyamoto, Maki, et al. 2013). Therefore, the vulnerability to oxidative stress may contribute to OLG's vulnerability to hypoperfusion. Thus, to better understand the pathological aspects and development of WML, it is important to study the lipidome and its alteration in WML induced by hypoperfusion.

3.3.3 Cognitive impairment induced by hypoperfusion shown by Barnes Maze

Although both sham-operated mice and BCAS mice showed clear reductions in the primary path length, latency and errors during acquisition phase, different strategies were preferred by the two groups, indicating that BCAS mice did not switch to a direct searching strategy as evidenced in the sham-operated mice (Figure. 3.9). This may suggest that BCAS mice learnt the fact that there was an escape box through training, but they had not learnt to locate the escape box with spatial cue or they may not remember precisely the location of the, and thus causing the failure to switch strategies. This is confirmed by the result that BCAS mice spent much less time Zone 1 where the target hole was located and tended to explore the wrong holes resulting a significant more total errors during probe trials. Though some studies have used primary latency to evaluate the performance in Barnes Maze (Yamada et al. 2011; Sunyer et al. 2007), Harrison et al. have also reported that escape

strategy is more informative than primary latency in assessing the performance in Barnes Maze (Harrison et al. 2006). Thus, it is reasonable to conclude that BCAS mice showed impairment spatial memory in this experiment. As we have demonstrated that only selective WML was induced in BCAS mice without neuronal injury in cortex or hippocampus, our results indicate that global chronic hypoperfusion causes cognitive impairment through WML, providing evidence that BCAS is suitable as an animal model in studying the mechanism and therapy to WML in vascular dementia.

3.3.4   Sphingolipids alterations

3.3.4.1 Reduction in glycoceramides

In the present study, we have demonstrated all the sphingolipid species that are more than 0.1% of total mass fraction. Among the three major subclasses of sphingolipids, only glycoceramides showed a significant reduction of overall content due to the decreases of each individual species in WML. Lipid profiles of the white matters from the temporal cortex of patients with subcortical ischemic vascular dementia (SIVD) have been reported by Lam et al. (Lam et al. 2014), in which a similar reduction of GluCer and GalCer was indicated. It has been shown that the concentrations of glycoceramides in white matters and in myelin are respectively about 5-fold and 10-fold higher than it is in grey matters (O'Brien and Sampson 1965). Therefore, the reduction of glycoceramides is consistent with the expected myelin loss in WML of BCAS. Glycoceramides are important components of membrane structures, clustered in "lipid rafts" instead of a uniform distribution in the membranes (Westerlund and Slotte 2009). Due to their biophysical properties, decrease in glycosphingolipids in membranes

will increase the membrane fluidity (Curatolo 1987b). Thus they are crucial for the long-term stability of the tightly packed myelin sheaths (Curatolo 1987a). GalCer is the predominant glycosphingolipid in myelin. GalCer is used as a marker for myelinating OLG as they are synthesised in parallel to the expression of MBP and PLP (Raff et al. 1978). Anti-CalCer antibodies reversibly inhibit the differentiation of OPC (Bansal and Pfeiffer 1989) (Ranscht, Wood, and Bunge 1987) and change organization of OLG membrane sheets in culture (Dyer and Benjamins 1988). These studies have suggested that CalCer plays essential role in the development of oligodendrocyte and myelination. When white matter damage occurs, OPCs respond quickly to proliferate, migrate and differentiate into myelin sheath-forming, mature OLGs (Miyamoto et al., 2010). However, the extent and outcome of endogenous repair is limited in diseases with chronic WML (Alizadeh, Dyck, and Karimi-Abdolrezaee 2015). There is growing evidence that the failure to form new myelin sheaths due to disruption of OPC differentiation is one factor underlying chronic white matter damage (Alizadeh, Dyck, and Karimi-Abdolrezaee 2015) (Miyamoto, Maki, et al. 2013; Miyamoto, Pham, et al. 2013). Therefore, reduced CalCer in BCAS may contribute to the WML by impeding OPC differentiation and remyelination as well, although further investigation is needed to elucidate this possibility.

3.3.4.2 Acyl chain length alterations of sphingolipids

C22-C26 and C16-C18 acyl chain sphingolipids have been defined as very long chain (VLC)-sphingolipids and long-chain (LC)-sphingolipids respectively according to previous studies (Spassieva et al. 2009)Imgrund,

2009 #248}. Although the overall amounts of Cer and SM were not significantly altered in WML, it is interesting to note the observed tendency of a decrease in VLC-sphingolipids an increase in LC-sphingolipids (Figure 3.15). Similar changes have also been observed in the white matter tissues from the temporal cortex of SIVD patients (Lam et al. 2014). Besides, the lipidome of ceramides synthases 2 (CerS2)-null mice has been reported to have a similar profile with reductions in VLC-Cer and VLC-SM while elevated LC-Cer and LC-SM and an overall reduction in hexosylCer in the brain, without significant variations in phospholipid and cholesterol. CerS2-null mice exhibit intensive and progressive myelin and MBP loss (Imgrund et al. 2009). CerS2 belongs to a family of six ceramide synthases (CerS1-6). Each of the six CerS has their own preference for acyl-CoA when the acyl chain is introduced to sphingosine in the formation of ceramides. CerS2 is the enzyme that prefers VLC acyl-CoA (Laviad et al. 2008). Therefore it seemed that VLC-sphingolipid aberrations are associated with the myelin loss in WML in BCAS as well as WML in SIVD patients. Mechanisms of the demyelination pathologies induced by reduction of VLC are not understood. It is known that ceramide with different acyl chain lengths has different biophysical properties (Pinto et al. 2008). Similarly, LC-sphingolipids have lower melting temperature, contributing to higher membrane fluidity (Niemela, Hyvonen, and Vattulainen 2006). It has been reported that depleting VLC-sphingolipids by depleting CerS2 caused biophysical property alterations such as fluidity and curvature, and morphology changes in cellular membrane in the brain, leading to compromised cellular processes(Silva et al. 2012).

Aside from the structural roles in cellular membrane and myelin, several sphingolipid species are also known as bioactive lipids that participate in various cell signalling pathways. Ceramide has been well reviewed for its role in regulating apoptosis. While Kroesen et al. showed that LC-Cer and VLC-Cer differentially regulate the apoptosis processes (Kroesen et al. 2003). Accumulation of LC-sphingolipids has been found to cause autophagy through arresting cell growth and inducing unfolded protein response (Spassieva et al. 2009), a cellular stress response related to the endoplasmic reticulum (ER) (Hetz 2012). Moreover, Zigdon et al. reported that depleting VLC-sphingolipid or exogenously added LC-ceramides could disrupt mitochondrial functions, inducing oxidative stress both in vivo and in vitro (Zigdon et al. 2013). Thus further studies are needed to elucidate how the alteration of acyl chain lengths associates with demyelination in WMLs. Besides, it is not clear that if CerS2 is involved in the WML with a vascular origin. Interestingly, Laviad et al.(Laviad et al. 2008) have observed that S1P specifically inhibited CerS2 activity non-competitively in vitro while having no effects on the other CerS (1, 3, 4, 5, and 6). S1P has been known as an important bioactive sphingolipid in the past decade (Spiegel and Milstien 2003). A number of studies have found that it was associated with the oligodendroglial lineage cell survival and development (Novgorodov et al. 2007; Cui et al. 2014; Jaillard et al. 2005). This may imply the involvement of S1P in the sphingolipids changes of WML.

3.3.5   Phospholipids alterations

Phosphatidylserine (PS) is the third abundant subclass of phospholipids in mouse brain after PC and PE. In addition of its important role as a

structural component in biological membranes, regulating surface charge and protein localization (Yeung et al. 2008), PS has also been reported to act as modulators of several signalling pathways (Kim, Huang, and Spector 2014). PS is exclusively located at the inner side of the membrane bilayer in normal cells. Pathological conditions such as apoptosis induce the translocation of PS to the outside of the membrane bilayer (PS exposure), resulting in cells uptake and removal of the apoptotic cells via a PS-recognizing receptor on phagocytic cells (Zwaal, Comfurius, and Bevers 2005). PS is also a critical modulator for activation of Akt, Raf-1 and protein kinase C, supporting neuronal survival (Kim, Huang, and Spector 2014). Besides, PS modulates several receptors including the AMPA glutamate receptors, benzodiazepine receptors and cannabinoid type 2 receptors in relation to its function in regulating membrane surface potential (Kim, Huang, and Spector 2014). Interestingly, PS has been shown to stimulate both SphK1 and SphK2 activity in Swiss 3T3 fibroblast lysates in a dose-dependent manner (Liu, Sugiura, et al. 2000) due to the PS binding sites in these kinases (Weigert et al. 2010). Mozzi et al. (Mozzi, Andreoli, and Horrocks 1993) have shown that hypoxia could induce PS synthesis in tissue slices or homogenates of rat cerebral cortex. A number of studies have observed PS exposure induced by hypoxia (Slone, Pope, and Fleming 2015) or hypoxic mimic agent $CoCl_2$ (Gotoh et al. 2012) (Karovic et al. 2007). Morever, PS elevation was also observed in the postmortem brain sample of SIVD patients (Lam et al. 2014). These observations suggest that the PS augmentation in WML of BCAS mice is associated with the hypoxia induced by hypoperfusion. Two major routes for PS synthesis have been summarized: acylation of lysophosphatidyl

serine (LPS) via a lysophospholipid acyltransferase or base exchanging reactions with PE and PC in microsomes and phosphatidic acid-dependent pathway (Kim, Huang, and Spector 2014). Besides, direct decarboxylation of PS in mitochondria has been reported to contribute at least 7% of PE in the brain, which may be important in myelination in the early stages of brain development (Bradbury 1984). According to the result of LC-MS/MS analysis in this study, the content of PE or PC did not alter in WML under chronic hypoperfusion, thus the elevation of PS seemed to be associated with the acylation of LPS. LPS profiling should provide further useful information.

Phosphatidylglycerol (PG) in mouse brain is actually quite low, consisting of 0.4-0.6% of total phospholipids according to our results. Consistently, lipidome of postmortem white matter tissues demonstrated an increase of PG in the SIVD patients compared to control cohort (Lam et al. 2014). PG is reported to be exclusively component of mitochondrial membrane (Schenkel and Bakovic 2014). It can be formed by a transfer of the phosphatidyl moiety of PC to free glycerol (Sastry 1985). PG is synthesised from phosphatidic acid via cytidine diphosphate diacylglycerol (CDP-DAG) and glycerol-3-phosphate (G3P) (Sastry 1985) and can be degraded back to DAG and G3P by PG specific phospholipase Pgc1p (Pokorna et al. 2015). Mutating Pgc1p in yeasts could induce PG accumulation that results in mitochondrial membrane fragmentation and a striking increase in mitochondrial respiration as indicated by a 2-fold higher O_2 consumption as well as Complex IV (Pokorna et al. 2015). This suggests that it is essential to degrade excess PG in maintaining the morphology and

function of the mitochondrial membrane. Researches have shown that mitochondrial dysfunction is associated with demyelination diseases. For example, increased complex IV activity has been observed in a mouse model of hypomyelination induced by MBP gene knockout (Andrews et al. 2006), or in the white matter lesions of multiple sclerosis (Mahad et al. 2009). Loss of myelin sheaths is observed in primary mitochondrial diseases such as Kearns-Sayre syndrome and Leber's hereditary optic neuritis (Campbell and Mahad 2012). Chronic hypoperfusion has been shown to induce mitochondrial dysfunction (Du et al. 2013) (Guang and Du 2006). However, it is not clear that how the mitochondrial dysfunction induced by hypoperfusion is associated with WML. Our observation of PG elevation in BCAS mice may provide a hint on the direction of future work.

3.3.6 Unchanged cholesterol

Cholesterol is well known for its role in myelin biogenesis because of its role in lipid rafts. Interference with cholesterol synthesis would results in defects of myelination (Mielke et al. 2005). In addition, depletion of cholesterol has been found in white matters of multiple sclerosis (MS) patients. The lipidomics study on the white matters of SIVD patients has also indicated a decrease in cholesterol. However, it is interesting to find that the overall level of cholesterol remained unchanged in the hypoperfusion-induced WML. This might be due to that the white matter lesion in SIVD patients are more severe than the WML in the mouse model, suggesting that reduction in cholesterol may occur in a later stage of development of hypoperfusion-induced WML.

3.3.7 Summary of lipid changes

It has been reported in this chapter that chronic cerebral hypoperfusion induced selective WML characterized by significant MBP loss, myelin sheaths rarefaction and vast alterations of the WM lipid including overall reduction of glycoceramides and sphingosine, VLC-sphingolipids decrease accompanied with LC-sphingolipids accumulation and elevations of PS and PG. Due to the distinct biophysical properties of myelin proteins and lipids, they form a delicate balance of forces maintaining the stable structure of normal myelin. Ohler et al. (Ohler et al. 2004) have depicted a physical model considering the forces, indicating that increases of myelin fluidity, decreases of myelin adhesion and increases of membrane curvature contribute to demyelination. These authors suggested that MBP and glycoceramides reduction could increase myelin fluidity; PS elevation could decrease the intermembrane adhesion because of their negative charges; the accumulation of LC-sphingolipids could increase the membrane curvature. Hypoperfusion induces lipid changes in WM that profoundly disturb the myelin structure stability and may interfere with signaling pathways involving bioactive lipids such as CalCer, PG, and thus results the WML characterized with MBP and myelin loss and cognitive impairment in BCAS mice.

CHAPTER 4 SPHINGOSINE KINASE INHIBITION AMELIORATES CHRONIC HYPOPERFUSION-INDUCED WHITE MATTER LESIONS

4.1 Introduction

OLGs form sail-like extensions of their cytoplasmic membrane which wrap around the axon up to 150 layers thick to form myelin sheaths. This process is dynamic even in the mature CNS where oligodendrocyte progenitor cells (OPCs) still persist (Nishiyama et al. 2009). When white matter damage occurs, OPCs respond quickly to proliferate, migrate and differentiate into myelin sheath-forming, mature OLGs (Miyamoto et al. 2010). However, the extent and outcome of endogenous repair is limited in diseases with chronic WML (Alizadeh, Dyck, and Karimi-Abdolrezaee 2015). There is growing evidence that the failure to form new myelin sheaths due to disruption of OPC differentiation is one factor underlying chronic white matter damage (Alizadeh, Dyck, and Karimi-Abdolrezaee 2015; Miyamoto, Maki, et al. 2013; Miyamoto, Pham, et al. 2013). In addition, a condition induced by prolonged $CoCl_2$ incubation that mimicked chronic hypoxic state in primary cultured OPCs has been reported to cause HIF-1α stabilization in OPCs and inhibition of OPC maturation (Miyamoto, Pham, et al. 2013). Sphingolipids especially ceramide, sphingosine, and sphingosine-1-phosphate (S1P) have been recognized as important regulators of cellular functions,   (Hannun and Obeid 2008). S1P was previously reported to act as a second messenger in cell proliferation (Olivera and Spiegel 1993) and an

anti-apoptotic messenger (Cuvillier et al. 1996). It has been reviewed that relative expression and activation of S1P receptors differentially regulate various physiological and pathological processes in the CNS such as ischemia (Hasegawa et al. 2010) and demyelination diseases (Matloubian et al. 2004). Previous reports have demonstrated the involvement of the S1P signalling pathway regulating OLG lineage-cell survival, proliferation, membrane dynamics and differentiation (Jung et al. 2007; Miron et al. 2008; Cui et al. 2014).However, little is known about the role of SphK/S1P signalling and FTY720 in hypoxia- or hypoperfusion-associated WML. Therefore, sphingosine and S1P and associated signalling pathways, including SphK and HIF-1α, in relation to the development of WML were measured using the BCAS model. Furthermore, the role of S1P on OPC differentiation into OLG was investigated in vitro using $CoCl_2$ prolonged incubation to elucidate the possible roles of SphK/S1P/S1PR in hypoperfusion-induced WMLs

4.2   Results

4.2.1   Effects of SKI-II on BCAS-induced S1P changes

Lipid extracts in WMT were analysed by LC-MS/MS. Four species of S1P, namely, S1P (d18:2), S1P (d18:1), S1P (d18:0) and S1P (d20:1), were uniformly increased with the total S1P level elevated (11.3±0.8 nmol /mg total protein) significantly by nearly 40% compared to sham-operated mice (8.1±0.2 nmol /mg total protein) (Figure 4.1). It can be seen that d18:1 S1P is the predominant species.
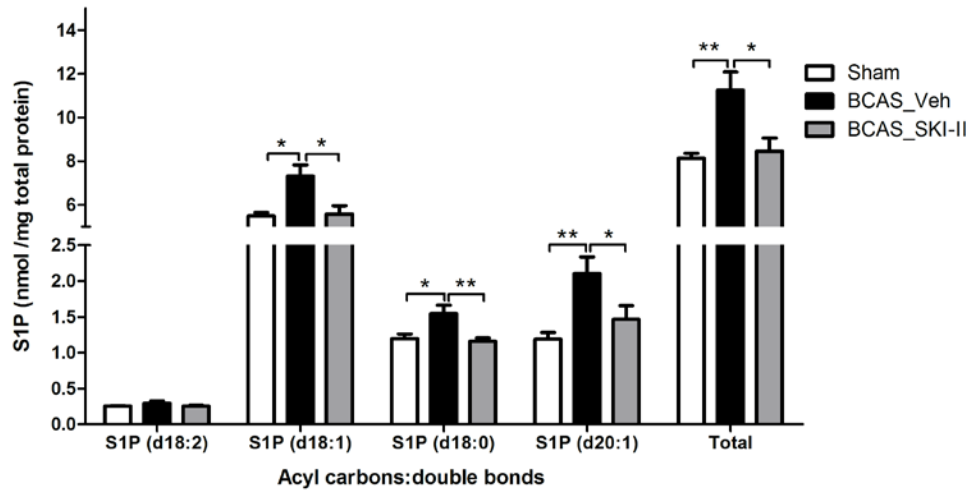
Figure 4.1 Effects of SKI-II on BCAS-induced S1P in WML

S1P profiles of individual species in WML expressed as molar concentrations to total protein in Sham, BCAS (Vehicle) and BCAS with SKI-II treatment. One-way ANOVA $F_{(2,16)}=7.3$ for S1P (d18:1) $F_{(2,16)}=$ 6.9 for S1P (d18:0); $F_{(2,16)}= 6.7$ for S1P (d20:1); $F_{(2,16)}=8.2$ for total S1P, N=6. *$P<0.05$, **$P<0.01$ with post-hoc Bonferroni correction. Abbreviations: Veh, vehicle-treated.
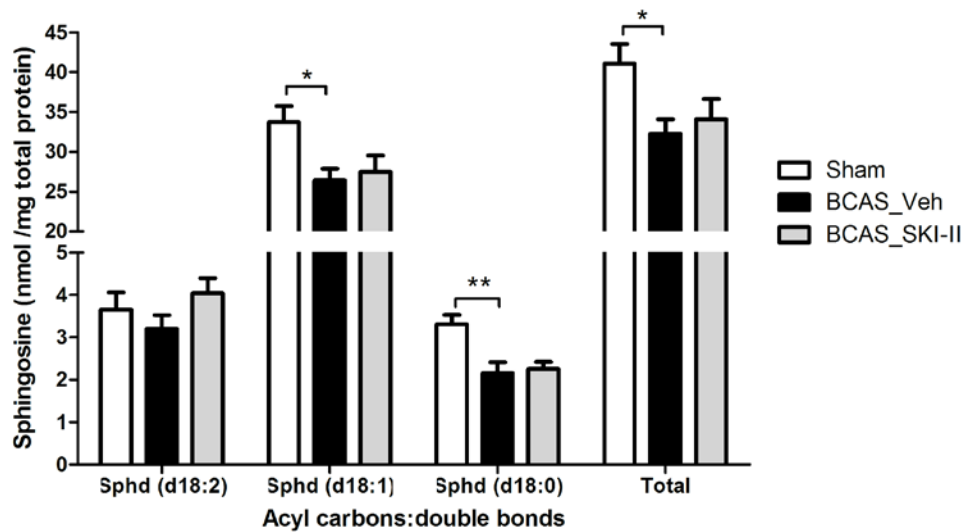
Figure 4.2 Effects of SKI-II on BCAS-induced sphingosine changes in WML

Sphingosine profile of individual species in WM expressed as molar concentrations to total protein in Sham, BCAS (Vehicle) and BCAS with SKI-II treatment. One-way ANOVA $F_{(2,16)}=4.4$ for Sph (d18:1) $F_{(2,16)}=$ 8.5 for Sph (d18:0); $F_{(2,16)}=4.1$ for total Sph, N=6. *$P<0.05$, **$P<0.01$ with post-hoc Bonferroni correction. Abbreviations: Sph, sphingosine.

Three species of sphingosine, namely Sphd 18:2, Sphd 18:1, Sphd 18:0 was demonstrated in Figure 4.2. Sphd 18:1 and Sphd 18:0 decreased significantly in BCAS mice. On the contrary, Sphd 18:2 did not decrease in BCAS. Since Sphd 18:1 was the predominant species in cerebral WMT, the overall sphingosine in BCAS (32.3±1.8 nmol) diminished to ~77% of that in sham-operated mice (41.1±2.5 nmol /mg total protein).

Not surprisingly, i.p. injection of the dual SphK1/SphK2 inhibitor SKI-II at a dose of 50mg/kg every other day abolished the BCAS-induced elevations in S1P as indicated in Figure 4.1. However, the BCAS-induced decreases in the levels of sphingosine were not affected by the treatment of SKI-II as shown in Figure 4.2.
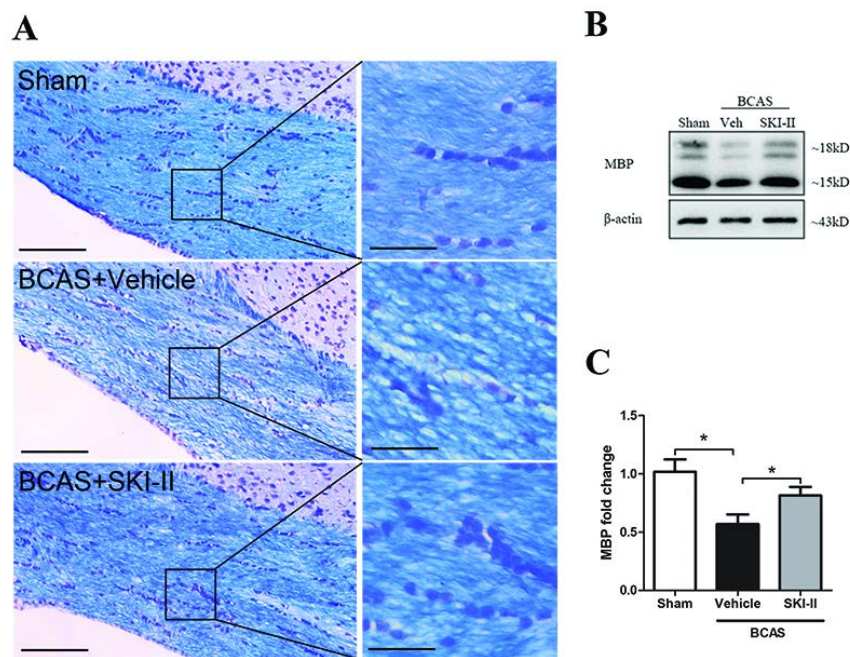
Figure 4.3 SKI-II treatment reversed WML and the loss of MBP in BCAS mice
A, Representative images of Kluver-Barrera staining. Scale bars = 120 µm. Panel on the right show high magnification images of the areas defined by the black squares on the left panels, Scale bars = 30 µm. **B**, Representative immunoblot and C, bar graph of white matter tissue myelin basic protein (MBP) immunoreactivity (as mean ± S.E.M. fold-change relative to mean value of sham animals). One-way ANOVA, $F_{(2, 16)} = 9.7$, $*p < 0.05$ with *post-hoc* Bonferroni correction. Veh =Vehicle.

4.2.2 SKI-II attenuates WML in BCAS mice

Furthermore, SKI-II partially attenuated the white matter damage as shown by the reductions in myelin loss and vacuolation in corpus callosum as shown by KB staining (Figure 4.3A) as well as partial recovery of MBP immunoreactivity (Figure 4.3B,C).

4.2.3 Effects of SKI-II on BCAS-induced changes in SphK and oligodendroglial markers

Interestingly, SphK2, but not SphK1 was up-regulated in BCAS, suggesting that SphK2 may be the main isoform responsible for the observed S1P increase (Figure 4.4A-C). Additionally, SphK2 increase was reversed by SKI-II treatment (Figure 4.4C). Levels of the proteoglycan NG2, a marker for OPCs known to be up-regulated after white matter damage (Nishiyama et al. 2009; Wigley et al. 2007) was increased in BCAS, but attenuated in BCAS with SKI-II treatment (Figure 4.4A and 4.4D). Taken together with the previously described changes in MBP (see Figure 4.3C,D), present results suggest that BCAS may disrupt the differentiation of OPC to mature oligodendrocytes, and that co-treatment with SKI-II restores this maturation process (characterized by decreasing NG2 and increasing MBP (Miyamoto, Pham, et al. 2013; Polito and Reynolds 2005)). On the other hand, the up-regulation of hypoxia marker HIF-1α in BCAS was not affected by SKI-II, suggesting that S1P and SphK changes are downstream of HIF-1α-mediated pathways (Figure 4.4E).
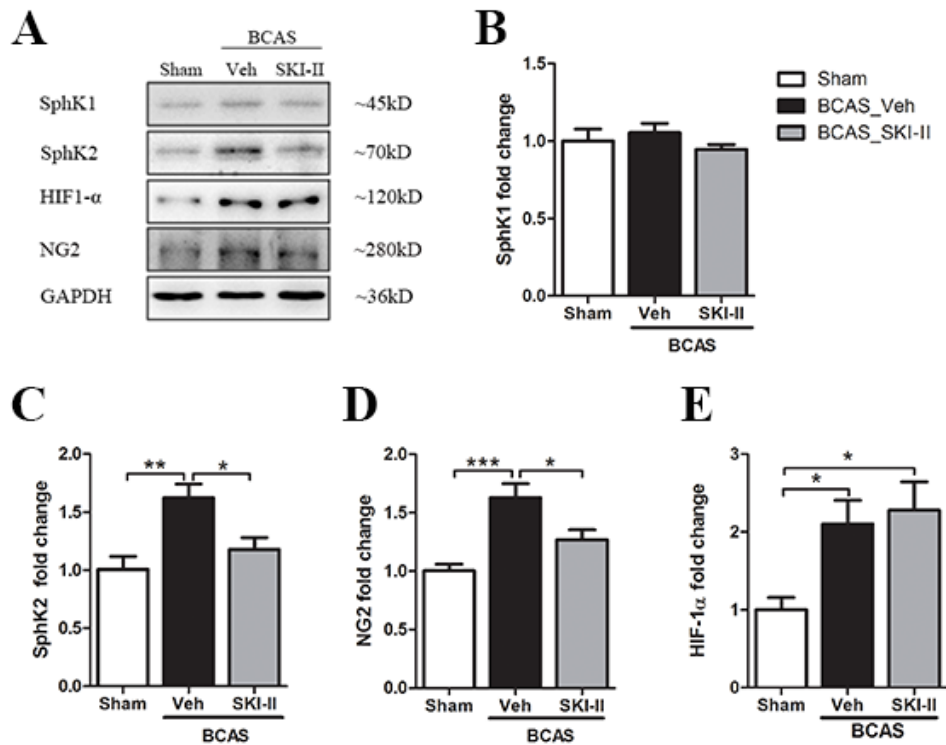
Figure 4.4 Effects of SKI-II on BCAS-induced changes in sphingosine kinase, NG2 and HIF-1α immunoreactivities.
A, Representative immunoblots and bar graphs (as mean ± S.E.M. fold-change relative to mean value of sham operated animals) of **B**, SphK1; **C**, SphK2; **D**, NG2 and **E**, HIF-1α immunoreactivities, $N = 5$ per group. One-way ANOVA, $F_{(2,12)}=$ 0.8 (SphK1); 8.2 (SphK2); 11.0 (NG2); and 5.7 (HIF-1α), $*p < 0.05$, $**p < 0.01$ and $***p < 0.005$ with *post-hoc* Bonferroni correction.

4.2.4 SKI-II attenuates the inhibition of OPC differentiation by hypoxia-mimetic CoCl₂ in vitro

To further investigate the involvement of HIF-1α-SphK in regulating OPC differentiation, SKI-II was added to cultured rat primary OPC in chemical hypoxia induced by $CoCl_2$ as described previously (Piret et al. 2002). OLG differentiation was induced by switching OPC medium to OLG medium as described in Chapter 2. $CoCl_2$ or SKI-II was added accordingly to OLG medium for treatment.
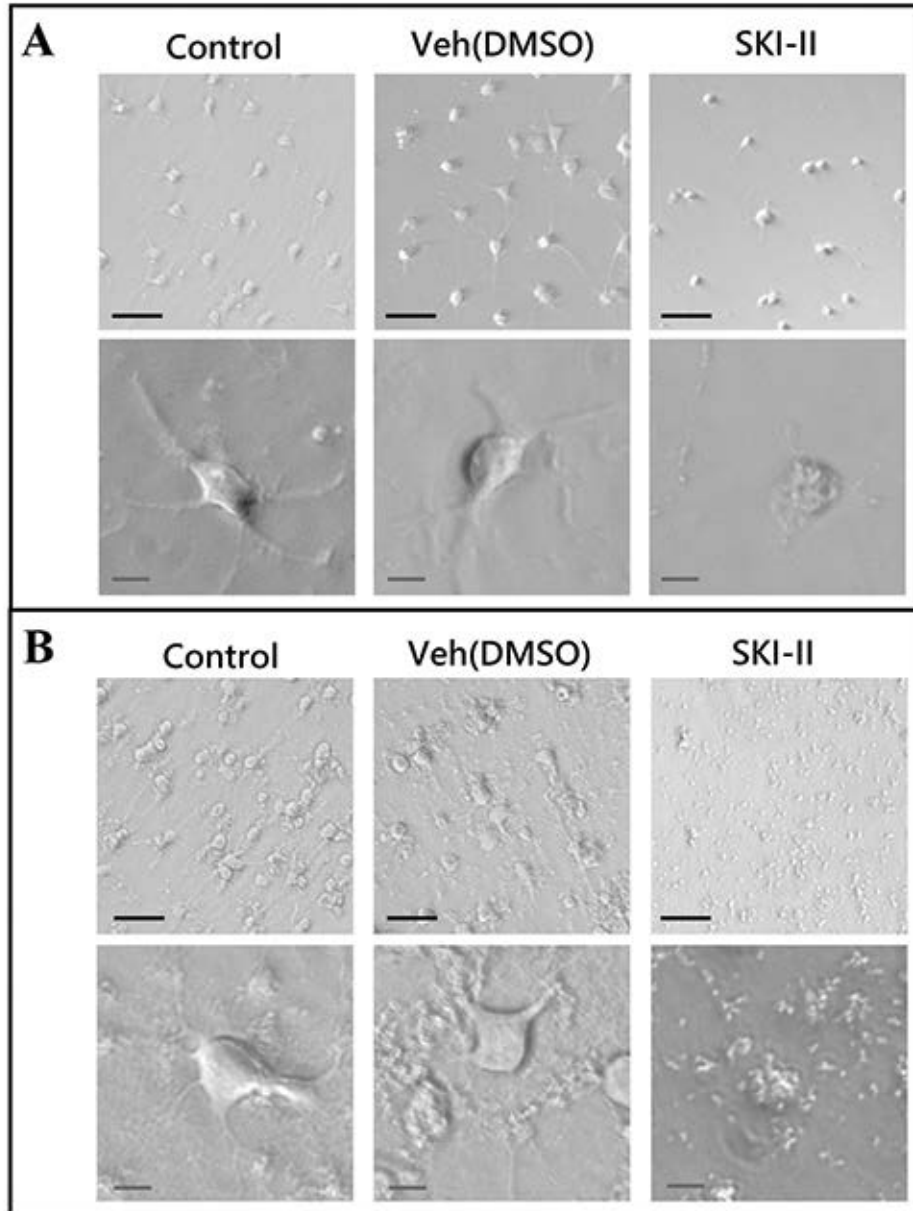
Figure 4.5 Effects of SKI-II on OPC and OLG under non-hypoxic conditions
Representative phase contrast images of A, OPC and B, OLG treated with vehicle DMSO and 0.2 µm SKI-II for 72 h. Upper panels: 10X magnifications, scale bar= 50µm. Lower panels: 40X, scale bar =10 µm.

Figure 4.5A shows the phase contrast images of OPC treated with the existence of 0.1% vehicle (DMSO) alone or 0.2µM SKI-II under normal condition. OPC incubated with control or vehicle medium showed typical bipolar or tripolar morphologies for OPC. It can be seen that SKI-II

treatment for 72 h under non-hypoxic conditions caused the outgrowth of the OPC to diminish. After swifting the OPC medium to OLG medium and incubated for 72 h, the OPC differentiated into OLG, showing the typical multiple processes morphology for OLG (Figure 4.5B). Similarly, high cell death was observed with OLG treated with SKI-II. These results suggest that SphK activities are essential for the survival and development of OPC and OLG.

On the other hand, hypoxic conditions induced by $CoCl_2$ (up to 50μM) for up to 72 h did not have any significant effects on cell viability of OPC (Figure 4.6).
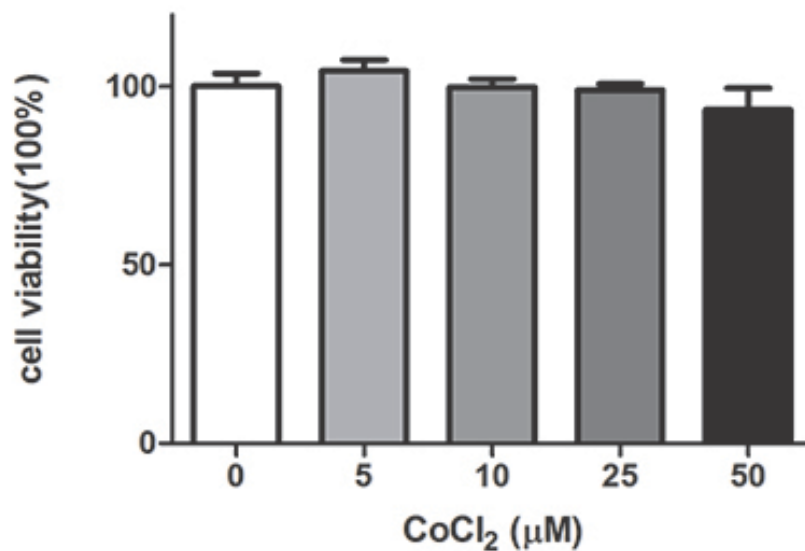
Figure 4.6 OLG cell viability measured by MTT assays
After treatment with $CoCl_2$ (up to 50 μM) for 72 hours ($p > 0.05$ for all concentrations compared to untreated, one-way ANOVA with *post-hoc* Dunnett's tests). N=3

However, increase in HIF-1α was evident as shown by the average intensity of HIF-1α immunofluorescence staining in cells treated with 25 μM CoCl$_2$ (Figure 4.7).

A

B
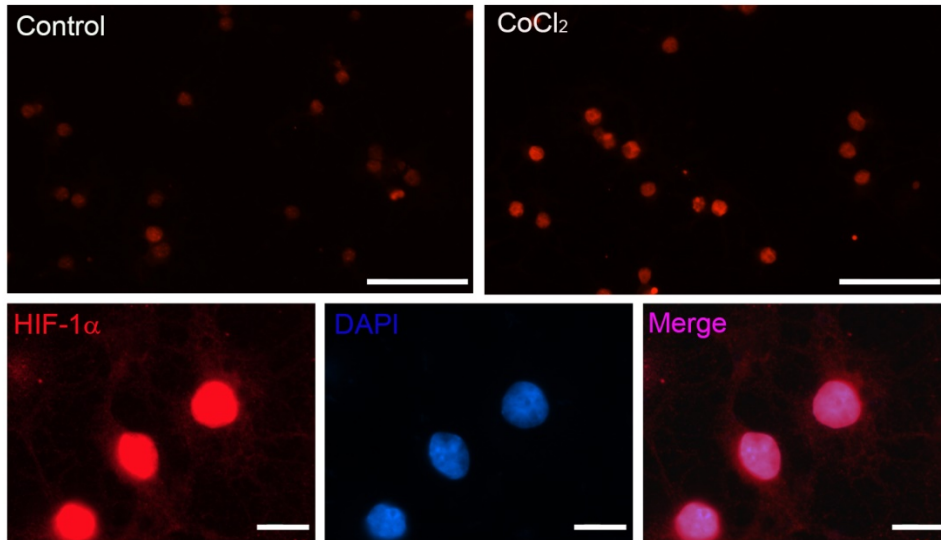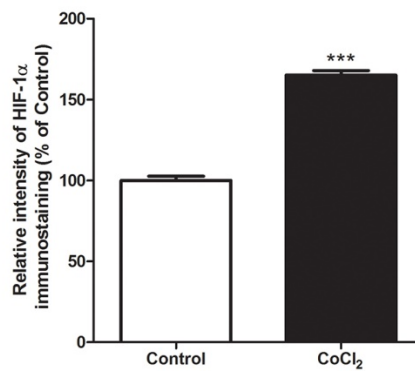
Figure 4.7 HIF-1α levels in OLG treated with CoCl$_2$ in vitro
A, top: representative HIF-1α immunofluorescence (IF) staining (red) in untreated and CoCl$_2$-treated (25 μM, 72 h) OPC. Scale bar = 50 μm. Bottom: Higher magnification IF images of HIF-1α, DAPI and merged. Scale bar = 10 μm. **B**, Quantification of HIF-1α immunostaining intensity with the cell bodies shown in the percentage of control. N=3

Moreover, immunoblots of SphK2 in primary OPC incubated with OLG medium together with $CoCl_2$ (25 μM) for 72 h increased to ~1.5 fold compared with incubation cells in the control OLG medium, suggesting that HIF-1α could stimulate the SphK2 expression in primary OLG (Figure 4.8).
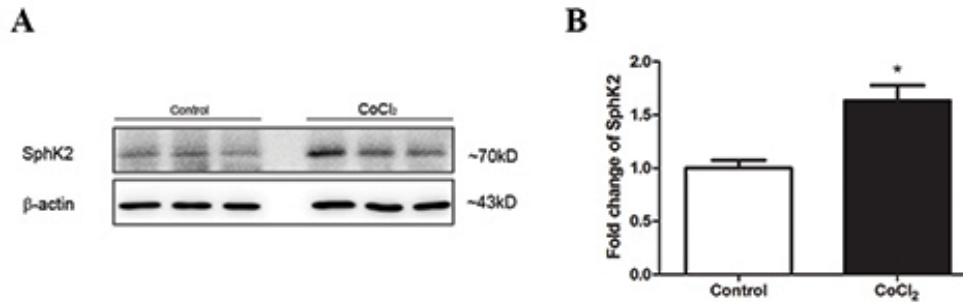
Figure 4.8 Effect of hypoxia on SphK2 expression in OLG in vitro
A, Immunoblots and **B**, bar graphs (as mean ± S.E.M. fold-change relative to mean value of control) of SphK2 in oligodendrocytes (OLG) after treatment with $CoCl_2$ (25 μM) for 72 h. *$P < 0.05$ by student's t-test, t= 3.9, N=3.

Figure 4.9A showed the immunofluorescence staining of OPCs (NG2-positive cells, green) and OLGs (MBP-positive cells, red). The ratio of OLGs to OPCs in hypoxic conditions induced by treatment with 25 μM $CoCl_2$ were obtained and shown in Figure 4.9B. Hypoxia caused the OLG/OPC ratio to fall by more than half, indicating that hypoxia inhibited OPC differentiation into OLG. SKI-II (0.1 or 0.2 μM) was able to reverse this inhibition concentration dependently and completely at the higher concentration. These results strongly suggested that under hypoxic conditions, HIF-1α-induced inhibition of OPC differentiation is mediated via SphK.

A
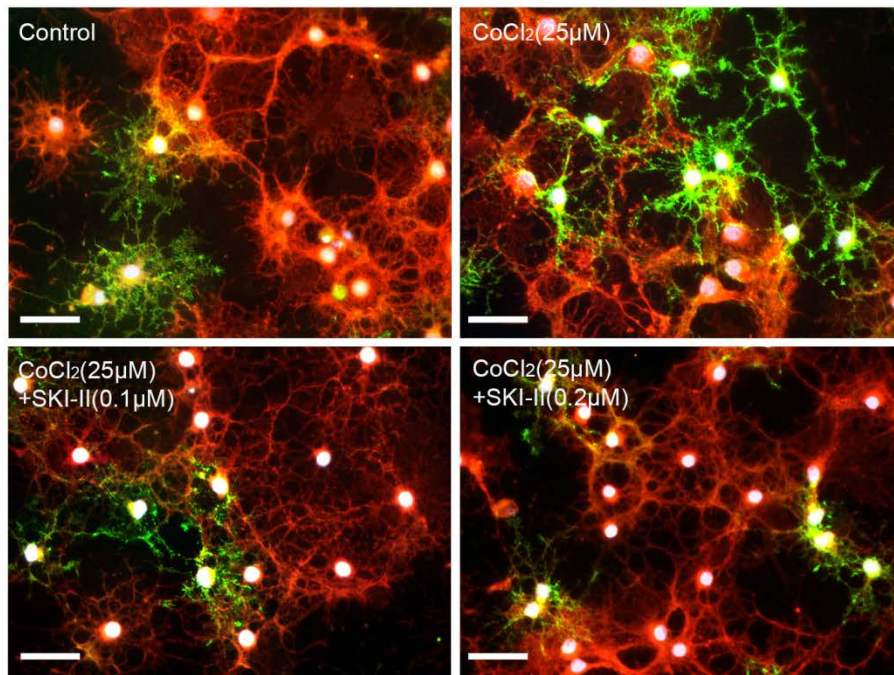
B
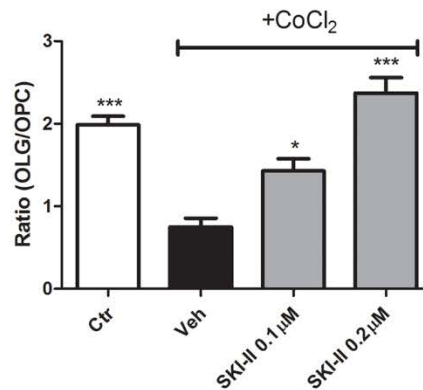
Figure 4.9 Effects of SKI-II on inhibition of OPC differentiation by hypoxia-mimetic CoCl$_2$ in vitro
A, Merged IF representative images for NG2 (green, marker for OPC), MBP (red, marker for OLG) and DAPI (blue, nucleus) in untreated and CoCl$_2$-treated cells with and without co-treatment with SKI-II, Scale bar = 30μm. **B,** ratio of OLG (MBP+ cells in E) to OPC (NG2+ cells after 72 h treatment (The method of quantification has been descried in Chapter 2). F (3, 16) = 25.0 by One-way ANOVA with *post-hoc Bonferroni*'s tests (compared with Veh). N=5, *P<0.05, ***P<0.001.

4.3   Discussion

Here, the profiles of sphingosine and S1P in the normal mice brain under hypoperfusion condition were revealed for the first time. Although S1P and sphingosine are present in relatively small amounts in the brain when compared to other sphingolipids and phospholipids, they are two important bioactive sphingolipids that are gaining more and more attention in the past 20 years. A number of studies have reported an overall S1P elevation in ischemic or hypoxic conditions. Schnizer et al. found that S1P was induced significantly in A549 cells following hypoxia for 2-4 h (Schnitzer et al. 2009). A similar elevation of S1P in microendothelial cells subjected to oxygen-deprivation (OD) was observed by Fernando et al. (Testai et al. 2014). Sphingosine is an important intermediate, providing the backbone of most sphingolipids. Sphingosine kinases (SphK) catalyse the ATP-dependent phosphorylation of sphingosine and produce S1P. SphK is critical to the regulation of S1P levels (Spiegel and Milstien 2003; Pulkoski-Gross, Donaldson, and Obeid 2015). The elevated expression of SphK2 in BCAS mice (Figure 4.4C) was shown in this study, which explained the increase of S1P and reduction of sphingosine.

SKI-II has been shown to be a SphK1/SphK2 dual inhibitor with a slightly higher potency towards SphK2 (IC50=20μM) than towards SphK1 (IC50 =35μM) (Gao et al. 2012). X-ray crystallography revealed that SKI-II binds to the sphingosine binding site (Gustin et al. 2013), which explains that it shows no inhibition towards other kinases such as ERK2 or PKC-α (French, Schrecengost et al. 2003). Recently Cingolani et al. (Cingolani et al. 2014) found that SKI-II inhibits dihydroceramide desaturase (Des1) activity

at a concentration of 10μM without reduction in Des1 protein, resulting in an accumulation of dihydroceramides in HGC 27 cells. The concentration of 10μM SKI-II that exhibits Des1 inhibition is actually quite high compared to its usual concentration of 0.3 - 1μM applied to inhibit SphKs in primary culture of neurons (Yung et al. 2012) or in bronchial epithelial cell line (Mercado et al. 2014). In fact, IC50 concentration of SKI-II in JC cells is below 1μM (French et al. 2006). These observations suggest that though SKI-II might inhibit Des1 at high concentration, it is still reasonably acceptable as a selective SphKs inhibitor considering the low concentration we used for SphK inhibition. Besides, we have not observed any accumulation of dihydroceramides in WML under chronic hypoperfusion in vivo, and thus it is highly unlikely that Des1 was inhibited by SKI-II at the low concentrations used in these experiments. Moreover, SKI-II has already been shown to have SphK inhibitory effects in mouse kidneys (Kim et al. 2007), airway smooth muscles (Chiba et al. 2010), and the brain (Yung et al. 2012) when administered either by i.p. injection or oral gavage. Thus, it is suitable to use SKI-II in the present study as a SphK inhibitor. And indeed SKI-II reversed the S1P and SphK2 elevation in WML. Notably, SKI-II did not significantly induce the sphingosine recovery though a slight increase could be seen. This may be due to the large discrepancy between the physiological amounts of sphingosine and S1P. Besides, the level of sphingosine is also regulated by CerS which synthases ceramides from sphingosine.

We observed that SphK2, not SphK1, increased significantly in white matter extracts during global hypoperfusion, which explains the S1P

elevation in white matter lesions. Besides, a similar SphK2 elevation in hypoxic-mimetic primary OLG culture (Figure 4.8). Given that chronic cerebral hypoperfusion induced hypoxia as indicated by increased HIF-1α expression, our finding that hypoperfusion induces SphK2 expression is consistent with previous findings (Wacker, Park, and Gidday 2009; Yung et al. 2012) that brain SphK2 protein expression and activity were up-regulated in mice subjected to hypoxic preconditioning, while SphK1 remained unchanged. Schnizer et al. (Schnitzer et al. 2009) also reported the same in A549 lung cancer cells.

Therefore, the effects of attenuated WML and S1P by the non-isozyme-specific SKI-II may be mediated mainly via the inhibition of SphK2, but follow-up confirmatory studies with SphK2-specific inhibitors are needed. It is also unclear as to why expression of SphK2, but not SphK1 was affected by BCAS and SKI-II treatment. Though the two isozymes SphK1 and SphK2 share five conserved domains, they differed in their N terminus and have different kinetic properties, distribution and certain opposing functions (Bryan et al. 2008; Liu, Sugiura, et al. 2000; Maceyka et al. 2005). SphK2 has several transmembrane domains and also nuclear localization signal at its N terminus. Thus Sphk2 can be expressed in the cellular membrane, cytosol and nucleus in cell type-specific manners (Bryan et al. 2008). Compared to SphK2, SphK1 lacks the transmembrane domain and thus has mainly a cytosolic localization (Bryan et al. 2008). SphK1 has been reported to pro-survival effects, while SphK2 is known to inhibit cell growth, induce apoptosis, and is upregulated in metabolically stressful conditions such as serum starvation (Liu et al. 2003; Maceyka et al. 2005). Another possible

explanation of the selective up-regulation of SphK2 expression in BCAS is that SphK2 is the predominant isoform in the brain over SphK1 (Blondeau et al. 2007) and therefore the more functionally "active" form. Further investigations are needed to elucidate the basis for the isoform-specific changes in SphK2 under hypoxic conditions.

Contrary to findings in this study that SKI-II attenuated the up-regulation of SphK2 activity under hypoxic conditions without reducing the expression of SphK1 in vivo or in vitro, a few studies reported that 10µM SKI-II not only inhibits SphK1 activity but also reduces the protein expression by enhancing the degradation of this enzyme via an ubiquitin-proteasomal pathway and/or activation of the proteasome in various cell lines (Cingolani et al. 2014; Loveridge et al. 2010; Ren et al. 2010). The reason why SphK1 expression was not reduced in the present study may due to a number of differences in experimental systems, for examples, differences between rat primary oligodendrocyte cultures and immortalized cell lines; possible differences in the relative expression of SphK1 and SphK2 in these cells; as well as differences in the general experimental conditions.

The present data indicated that with a dose of 50mg/kg intraperitoneally injected every other day, SKI-II only partially inhibits the SphKs, reversing the S1P elevation to the normal physiological level in vivo. Treatment with 0.2 µM SKI-II for 72 h was able to partially inhibit the $CoCl_2$-induced SphK2 up-regulation. However the mechanism of how SKI-II reduces SphK2 protein level remains to be elucidated. It has been reported that in common with SphK1, SphK2 was also regulated by the ubiquitin-proteasomal pathway (Lim et al. 2011). Therefore it is possible that SKI-II

induced increase in SphK2 degradation via the similar ubiquitin-proteasomal pathway, although further work is required to confirm the presence of this process in the brain, as it may not occur in all cell types (Watson et al. 2013).

It is not surprising that HIF-1α was found to be involved in the S1P/SphK signalling pathways in hypoxic conditions. Wacker et al. (Wacker, Perfater, and Gidday 2012) reported that chemical induction of HIF-1α was protective against ischemic injuries in SphK2$^{+/+}$ mice but was ineffective in SphK2$^{-/-}$ mice. This is consistent with the current findings which show that BCAS-induced HIF-1α was not affected by SKI-II (Figure 4.4). The HIF-1α stabilizer CoCl$_2$ induced SphK2 elevation in vitro (Figure 4.8) indicating that HIF-1α signals upstream of SphK. CoCl$_2$ is a hypoxia-mimetic agent which can stabilize HIF-1α by inactivating the prolyl hydroxylases through binding to the iron-binding centre of the enzyme and blocking HIF-1α binding with pVHL(Yuan et al. 2003). However, Yung et al. (Yung et al. 2012) found that isoflurane preconditioning induced HIF-1α only in SphK2$^{+/+}$ but not the SphK2$^{-/-}$ mice, suggesting potentially complex, bi-directional regulation between HIF-1α and SphK, similar to those found for SphK1 in cancer cells (Anelli et al. 2008; Anelli et al. 2005). Further work is therefore required to elucidate the molecular pathways underlying HIF-1α and SphK regulation.

In addition to astrocytes, microglia and oligodendrocytes, there exists another glial cell population that is characterized by the expression of NG2 (Ong and Levine 1999). NG2-positive cells, also known as polydendrocytes, have the potential of proliferation or differentiation into mature OLG (Nishiyama 2007; Ong and Levine 1999). Although NG2 cells are reported to have astroglial fate and neuronal fate as well, the astrogenic and neuronal

potential is limited to a subset of embryonic NG2 cells (Huang et al. 2014).

In adult CNS, cells express PDGFRα also express NG2 (Dawson et al. 2003).

In addition, progeny of NG2 cells in white matters are either polydendrocyte

or OLG (Nishiyama et al. 2009). As NG2 cells differentiate into mature OLG,

they stop expressing NG2 and begin to express oligodendrocyte myelin

antigens such as O4 and MBP. Therefore it is now widely accepted to use

NG2 as a marker for oligodendrocyte progenitor cells (OPCs). OPCs are

activated rapidly in response to various demyelinating injuries. They

proliferate and migrate to the lesion areas (Polito and Reynolds 2005). OPC

number decreases upon onset and progression of remyelination concomitant

with appearance of BrdU+ mature oligodendrocytes have been reported

(Watanabe, Toyama, and Nishiyama 2002; Reynolds et al. 2002), suggesting

at least a part of OPCs differentiation into mature OLG. However the extent

and outcome of endogenous remyelination may be limited in chronic WML.

There is growing evidence that the failure to form new myelin sheaths due to

disruption of OPC differentiation is one factor underlying chronic white

matter damage (Alizadeh, Dyck, and Karimi-Abdolrezaee 2015; Miyamoto,

Pham, et al. 2013). It has been presently demonstrated, both in chronically

hypoperfused BCAS mouse brains as well as in cultured cells treated with

the hypoxia-mimetic $CoCl_2$, that these conditions result in decreased MBP

and increased NG2 .Furthermore, co-treatment with SKI-II was able to

reverse MBP and NG2 alternations in both BCAS brains (Figure 4.3, 4.4)

and $CoCl_2$–treated cells (Figure 4.9). These data, taken together with

observations of SKI-II's amelioration of BCAS-induced WML (Figure 4.3)

and S1P (Figure 4.1), as well as data from previous studies showing

disrupted OPC differentiation in chronic white matter damage (Alizadeh, Dyck, and Karimi-Abdolrezaee 2015) (Miyamoto, Maki, et al. 2013; Miyamoto, Pham, et al. 2013) strongly suggest that one mechanism underlying hypoperfusion-related WML is the inhibition of OPC differentiation induced by elevated S1P levels.

More recently, S1P receptors have been described (Spiegel and Milstien 2002). These receptors are all G protein-coupled receptors, which exist in 5 subtypes namely $S1P_1$-$S1P_5$. It has been reported that cultured OPCs and OLGs expressed $S1P_1$, $S1P_2$, $S1P_3$, $S1P_5$ (Yu et al. 2004; Novgorodov et al. 2007). Table 4.1 shows some previous publications about complex functions of S1P receptors in different stages of oligodendroglial lineage cells. FTY720P is a potent agonist for $S1P_1$, $S1P_3$, $S1P_4$, $S1P_5$. It has been reported that FTY720P inhibited rat OPC differentiation into OLG at concentrations 0.1-1μM for 72h while a low concentration of 10nM led to an increase in the percentage of mature OLG (Jung et al. 2007). However, the effect of FTY720P on OPC differentiation seems to be controversial. Hu et al. (Hu et al. 2011) reported that 10nM FTY720P inhibited OPC maturation as evident by the retraction of oligodendrocyte processes and promote the proliferation during 98h of treatment. Additionally, $S1P_5$ receptor activation has been reported to impede OPC migration (Novgorodov et al. 2007) and regulate process retraction in pre-oligodendrocytes (Jaillard et al. 2005), both of which may hinder OLG terminal differentiation and therefore attenuate remyelination after white matter injury (Keirstead and Blakemore 1999). In contrast, the $S1P_1$-specific agonist SEW2871 seemed to have no effect on OPC differentiation (Jung et al. 2007). According to them, S1P1 is related

129

with promoting OPC proliferation via PDGF-induced mitogenesis of rat OPC (Jung et al. 2007). However, a very recent study showed that S1P1 receptor knockout led to delayed maturation of mouse pre-OLG to OLG (Dukala and Soliven 2016). These controversial seem to indicate that S1P receptors may have different roles in different stages of oligodendroglial lineage cells. Results in the present study have clearly showed that the terminal differentiation of OPC was disrupted by SphK-induced S1P elevation. However, current data and previous publications mentioned above are not enough to determine the role of specific S1P receptors in hypoxia-induced OPC differentiation disruption. Therefore receptor specific agonist or antagonist may provide further understanding of S1P signalling pathway in hypoxia-induced OPC differentiation disruption in future studies.

Table 4.1 Function of S1P receptors in oligodendroglial lineage cells

Receptor	Function	Reference
S1P1	Promotes OPC proliferation	Jung et al, 2007
	Morphological maturation and early myelination	Dukala et al, 2016
S1P5	Promotes the survival of mature rat OLG	Jaillard et al, 2005
	Inhibits OPC migration	Novgorodov et al, 2007
	Regulates process retraction in pre-OLG	Miron et al, 2008
FTY720P*	Enhances OPC differentiation at low concentration, inhibits OPC differentiation at high concentration	Jung et al, 2007
	Promotes the proliferation but inhibites the differentiation	Hu et al, 2011

* FTY720P, a potent agonist of S1P1, S1P3, S1P4 and S1P5

As shown in Chapter 3, hypoperfusion caused a reduction of VLC-sphingolipid and an increase of LC-sphingolipid (Figure 3.15). CerS2 was the enzyme that synthases VLC-ceramides. S1P has been reported to

specifically inhibited CerS2 activity non-competitively in vitro while having no effects on the other CerS (1, 3, 4, 5, and 6) (Laviad et al. 2008). According to this publication, there are two $S1P_1$ receptor-like motifs in CerS2. The corresponding residues in $S1P_1$ were identified as essential for S1P binding. Mutation either of the two $S1P_1$ receptor-like residues in CerS2 abolishes the S1P inhibition without affecting CerS2 activity (Laviad et al. 2008). Thus, the current observation of elevated S1P levels may explain the acyl chain length alteration in WML, suggesting again the involvement of CerS2 in hypoperfusion. However, further investigations on the interplay between the elevation of S1P and alteration of sphingolipids induced by hypoperfusion are needed.

In summary, the data presented in this chapter show that chronic hypoperfusion-induced WML and associated disruption of OPC differentiation may involve HIF-1α/SphK2/S1P/S1PR and that the SphK inhibitor, SKI-II, can ameliorate the WML along with hypoperfusion-induced changes in S1P, SphK2 and OPC differentiation without affecting HIF-1α levels. SphK / S1P may be potential targets for the treatment of ischemic white matter disease.

CHAPTER 5   CONCLUSION, LIMITATIONS AND FUTURE WORKS

5.1   Conclusion

I have presented in this thesis data that demonstrated that chronic hypoperfusion induced by BCAS causes global CBF reduction in the mouse brain, leading to cerebral WML characterized by myelin loss, MBP reduction and OPC activation without apparent damage to cerebral grey matters. These BCAS mice showed deficits in learning and spatial memory as indicated by worse performance in a spatial memory test (Barnes Maze) when compared to the sham-operated mice. There are also changes in the lipidomes of cerebral white matters in the BCAS mice. Of the lipid molecules belonging to the 3 major lipid classes, namely sphingolipids, phospholipids and cholesterols, there are overall content reductions in glycosphingolipids and sphingosine but increases in S1P, PS and PG. More detailed analysis showed that the sphingolipid composition in the white matters altered with a reduction in very long acyl chain-sphingolipids whereas and an elevation in long acyl chain-sphingolipid. Cholesterol levels in white matters remained unchanged in the BCAS mice. These lipid alterations may affect the biophysical properties of the cellular membrane and thus may introduce instability in the myelin structure. Besides, lipid alterations are mainly observed in sphingolipids, indicating the essential roles of sphingolipids in maintaining WM integrity.

In addition, the data revealed that a HIF-1α/SphK2/S1P signaling pathway is involved in chronic hypoperfusion-induced WML. Global

chronic hypoperfusion increases SphK2 activity and expression via stabilizing HIF-1α, resulting notable S1P elevation in white matter tissues. Chemical hypoxia induced by HIF-1α stabilizer CoCl2 in primary OPC culture also can cause elevation of SphK2 and impede OPC differentiation in vitro. SKI-II, an inhibitor of SphK, can both attenuate the WML in vivo and release the inhibition of OPC differentiation in vitro, suggesting that SphK2/S1P activation in WML impairs the endogenous remyelination in response to white matter injury through the disruption OPC differentiation into OLG. Figure 5.1 shows a summary diagram of the main findings for this whole study.

Collectively, chronic hypoperfusion induces an explosion of lipid alterations in white matters which may affect myelin stability resulting in demyelination and WML. Hypoperfusion activates HIF-1α/SphK2/S1P signaling contributing to WML through disrupting myelin repair and sphingolipid metabolism. Therefore, the data suggest that SphK / S1P may be potential targets for the treatment of ischemic WML.
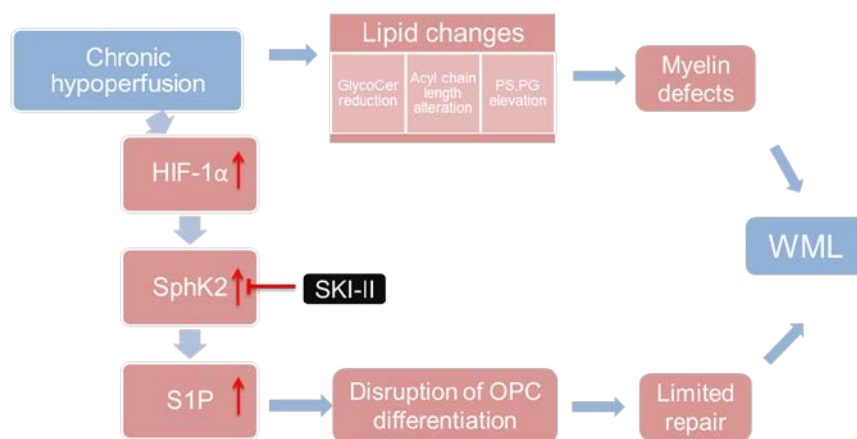
Figure 5.1 A summary diagram for the mechanism of hypoperfusion-induced WML

5.2 Significance

Firstly, this study has demonstrated the lipidome of hypoperfusion-induced WML in mouse for the first time. Characteristics of the lipidome of hypoperfusion-induced WML in mouse have been shown to be similar with the cerebral white matter lipidome in SIVD patients (Lam et al. 2014). Alterations in several structural lipids as well as bioactive lipids such as PS, PG, ceramide, sphingosine and S1P have been shown. Therefore, it provides valuable references for future studies in WML. Secondly, although previous studies have demonstrated the involvement of S1P and its receptors in regulating oligodendroglial lineage cells(Jung et al. 2007; Miron et al. 2008; Dukala and Soliven 2016) and that hypoxia induces inhibition of OPC differentiation (Miyamoto, Pham, et al. 2013), this study showed that hypoxia-induced inhibition of OPC differentiation is mediated via HIF-1α/SphK/S1P pathway for the first time. Thirdly, SphK inhibition has been indicated to ameliorate hypoperfusion-induced WML in mouse. Though a dual SphK1 and SphK2 inhibitor SKI-II was used in this study, it has been shown that only SphK2 is up-regulated by hypoxia in the brain, which is consistent with previous report that SphK2 is the predominant isoform in the brain (Blondeau et al. 2007). ABC294640 is a selective SphK2 competitive inhibitor(Gao et al. 2012). It also has oral bioavailability in a rat model of diabetic retinopathy (Maines et al. 2006). ABC294640 exhibits anti-tumour activity in various types of cancer cells due to SphK2 inhibition(French et al. 2010; Beljanski, Knaak, and Smith 2010) and is now in the early-phase clinical trial under the name YELIVA for treating solid tumor. Recently the RedHill Biopharma announced positive top-line results that YELIVA

successfully met its primary and secondary endpoints, demonstrating that the drug is well tolerated and can be safely administered to cancer patients at doses that provide circulating drug levels that are predicted to have therapeutic activity Therefore, YELIVA has clearly demonstrated that specific SphK2 inhibition may have potential in the treatment of ischemic WML.

5.3   Limitations and Future works

However, there are several limitations of the present study. We did not distinguish the GluCer and GalCer when analyze the glycoceramides. Except for the structural role of CalCer in myelin membrane, it is reported to regulate OPC differentiation and thus play a role in the development of oligodendrocyte and myelination (Bansal and Pfeiffer 1989; Ranscht, Wood, and Bunge 1987). To investigate GalCer alterations in WMLs could provide a better understanding of WML pathology and mechanisms. In addition, sulfatide or 3-O-sulfogalactosylceramide, is an important subclasses of sphingolipids in myelin. Although less abundant than GalCer, it accounts for up 4% of total myelin lipids (Takahashi and Suzuki 2012) and is exclusively expressed in myelin (Kirschning, Rutter, and Hohenberg 1998). Sulfatide has been reported to negatively regulate the oligodendrocyte terminal differentiation (Hirahara et al. 2004) and enhance oligodendroglia cell proliferation (Shroff et al. 2009). Therefore, inclusion of sulfatide will be an improvement in the lipidomic study.

Although only SphK2 expression was observed to be up-regulated in hypoperfusion, the involvement of SphK1 cannot be completely excluded. Several studies have shown that SphK1 can be activated during hypoxia

(Anelli et al. 2005; Schwalm et al. 2008). Moreover, SphK1 and SphK2 are reported to have opposite functions in sphingolipid metabolism (Maceyka et al. 2005). However, SKI-II is a dual inhibitor of both SphK1 and SphK2. Therefore, in order to elucidate the specific roles played by SphK1 and SphK2 respectively in ischemic WML, selective SphK inhibitor can be used in future work. CB5468139 or SKI-I, is a potent selective SphK1 inhibitor with a Ki of 0.3 µM which decreased kidney adenocarcinoma A498 proliferation (Gao et al. 2012). ABC294640 is a selective SphK2 competitive inhibitor with a Ki of 7.3µM (Gao et al. 2012). No effect was observed on SphK1, or the closely related diacylglycerol kinase, at concentrations up to 100 µM (French et al. 2010).

CerS2 is the enzyme that prefers VLC-CoA to synthesize VLC-ceramides in mammals. It is a key enzyme in ceramides metabolism and myelin formation. Cers2$^{-/-}$ mice show severe myelin defects in cerebral white matters, characterized with the reduction of VLC-ceramides, accumulation of LC-ceramides and thus showing severe myelin defects in cerebral white matters (Imgrund et al. 2009). Since a decrease of VLC-sphingolipids and an increase of LC-sphingolipids have been demonstrated in this study (Chapter 3), it is interesting to investigate if the acyl chain length alteration in sphingolipids is related to CerS2.

Sphingolipid metabolism is complex. Bioactive sphingolipid molecules and related enzymes can regulate the level of other sphingolipids. For example, degradation of S1P by Spl is the only exit point of sphingolipid metabolism. SphK1 and SphK2 have been found to regulate ceramide biosynthesis oppositely (Maceyka et al. 2005). Besides, S1P can inhibit

CerS2 activity and thus affect ceramide composition (Laviad et al. 2008). As demonstrated, SKI-II partially reverses the sphingolipids chain length alterations in WML but more work is needed in order to understand the mechanism of SphK/S1P in hypoperfusion-induced sphingolipid changes.

In addition, mitochondrial dysfunction may possibly be involved in the pathophysiology of WML as indicated by the PG elevation and LC-sphingolipid accumulation. Thus, it will be interesting to investigate the relationship between lipid changes and the alteration of mitochondria functions in WML.

REFERENCE

Adams, J. M., L. T. Difazio, R. H. Rolandelli, J. J. Lujan, G. Hasko, B. Csoka, Z. Selmeczy, and Z. H. Nemeth. 2009. 'HIF-1: a key mediator in hypoxia', *Acta Physiol Hung*, 96: 19-28.

Ader, I., C. Gstalder, P. Bouquerel, M. Golzio, G. Andrieu, S. Zalvidea, S. Richard, R. A. Sabbadini, B. Malavaud, and O. Cuvillier. 2015. 'Neutralizing S1P inhibits intratumoral hypoxia, induces vascular remodelling and sensitizes to chemotherapy in prostate cancer', *Oncotarget*, 6: 13803-21.

Ader, I., B. Malavaud, and O. Cuvillier. 2009. 'When the sphingosine kinase 1/sphingosine 1-phosphate pathway meets hypoxia signaling: new targets for cancer therapy', *Cancer Res*, 69: 3723-6.

Aderem, A., and R. J. Ulevitch. 2000. 'Toll-like receptors in the induction of the innate immune response', *Nature*, 406: 782-7.

Aggarwal, S., L. Yurlova, and M. Simons. 2011. 'Central nervous system myelin: structure, synthesis and assembly', *Trends Cell Biol*, 21: 585-93.

Aharon-Peretz, J., E. Daskovski, and T. Mashiach. 2002. 'Natural history of dementia associated with lacunar infarctions', *2nd International Congress on Vascular Dementia*: 17-20.

Ahmad, M., J. S. Long, N. J. Pyne, and S. Pyne. 2006. 'The effect of hypoxia on lipid phosphate receptor and sphingosine kinase expression and mitogen-activated protein kinase signaling in human pulmonary smooth muscle cells', *Prostaglandins Other Lipid Mediat*, 79: 278-86.

Akiguchi, I., H. Tomimoto, T. Suenaga, H. Wakita, and H. Budka. 1997. 'Alterations in glia and axons in the brains of Binswanger's disease patients', *Stroke*, 28: 1423-29.

Alizadeh, A., S. M. Dyck, and S. Karimi-Abdolrezaee. 2015. 'Myelin damage and repair in pathologic CNS: challenges and prospects', *Front Mol Neurosci*, 8: 35.

Andersen, K., L. J. Launer, M. E. Dewey, L. Letenneur, A. Ott, J. R. M. Copeland, J. F. Dartigues, P. Kragh-Sorensen, M. Baldereschi, C. Brayne, A. Lobo, J. M. Martinez-Lage, T. Stijnen, A. Hofman, and EURODEM Incidence Res Grp. 1999. 'Gender differences in the incidence of AD and vascular dementia - The EURODEM Studies', *Neurology*, 53: 1992-97.

Andrews, H., K. White, C. Thomson, J. Edgar, D. Bates, I. Griffiths, D. Turnbull, and P. Nichols. 2006. 'Increased axonal mitochondrial activity as an adaptation to myelin deficiency in the Shiverer mouse', *Journal of Neuroscience Research*, 83: 1533-9.

Anelli, V., R. Bassi, G. Tettamanti, P. Viani, and L. Riboni. 2005. 'Extracellular release of newly synthesized sphingosine-1-phosphate by cerebellar granule cells and astrocytes', *J Neurochem*, 92: 1204-15.

Anelli, V., C. R. Gault, A. B. Cheng, and L. M. Obeid. 2008. 'Sphingosine kinase 1 is up-regulated during hypoxia in U87MG glioma cells. Role of hypoxia-inducible factors 1 and 2', *J Biol Chem*, 283: 3365-75.

Anstey, K. J., C. von Sanden, A. Salim, and R. O'Kearney. 2007. 'Smoking as a risk factor for dementia and cognitive decline: a meta-analysis of prospective studies', *Am J Epidemiol*, 166: 367-78.

Artavanis-Tsakonas, S., M. D. Rand, and R. J. Lake. 1999. 'Notch signaling: cell fate control and signal integration in development', *Science*, 284: 770-6.

Ayata, C. 2010. 'CADASIL: experimental insights from animal models', *Stroke*, 41: S129-34.

Baerwald, K. D., and B. Popko. 1998. 'Developing and mature oligodendrocytes respond differently to the immune cytokine interferon-gamma', *Journal of Neuroscience Research*, 52: 230-39.

Bansal, R., and S. E. Pfeiffer. 1989. 'Reversible inhibition of oligodendrocyte progenitor differentiation by a monoclonal antibody against surface galactolipids', *Proc Natl Acad Sci U S A*, 86: 6181-5.

Baumann, N., and D. Pham-Dinh. 2001. 'Biology of oligodendrocyte and myelin in the mammalian central nervous system', *Physiol Rev*, 81: 871-927.

Beljanski, V., C. Knaak, and C. D. Smith. 2010. 'A novel sphingosine kinase inhibitor induces autophagy in tumor cells', *J Pharmacol Exp Ther*, 333: 454-64.

Berg JM, Tymoczko JL, Stryer L. 2002. *Biochemistry* (W H Freeman: New York).

Biessels, G. J. 2015. 'Diagnosis and treatment of vascular damage in dementia', *Biochim Biophys Acta*.

Black, S., G. C. Roman, D. S. Geldmacher, S. Salloway, J. Hecker, A. Burns, C. Perdomo, D. Kumar, R. Pratt, and Group Donepezil 307 Vascular Dementia Study. 2003. 'Efficacy and tolerability of donepezil in vascular dementia: positive results of a 24-week, multicenter, international, randomized, placebo-controlled clinical trial', *Stroke*, 34: 2323-30.

Blondeau, N., Y. Lai, S. Tyndall, M. Popolo, K. Topalkara, J. K. Pru, L. Zhang, H. Kim, J. K. Liao, K. Ding, and C. Waeber. 2007. 'Distribution of sphingosine kinase activity and mRNA in rodent brain', *J Neurochem*, 103: 509-17.

Boggs, J. M., and K. M. Koshy. 1994. 'Do the long fatty acid chains of sphingolipids interdigitate across the center of a bilayer of shorter chain symmetric phospholipids?', *Biochim Biophys Acta*, 1189: 233-41.

Bogousslavsky, J., and F. Regli. 1992. 'Centrum Ovale Infarcts - Subcortical Infarction in the Superficial Territory of the Middle Cerebral-Artery', *Neurology*, 42: 1992-98.

Bradbury, K. 1984. 'Ethanolamine glycerophospholipid formation by decarboxylation of serine glycerophospholipids in myelinating organ cultures of cerebellum', *J Neurochem*, 43: 382-7.

Bradl, M. 1999. 'Myelin dysfunction/degradation in the central nervous system: why are myelin sheaths susceptible to damage?', *J Neural Transm Suppl*, 55: 9-17.

Brown, W. R., D. M. Moody, V. R. Challa, C. R. Thore, and J. A. Anstrom. 2002. 'Apoptosis in leukoaraiosis lesions', *J Neurol Sci*, 203-204: 169-71.

Brown, W. R., D. M. Moody, C. R. Thore, and V. R. Challa. 2000. 'Apoptosis in leukoaraiosis', *AJNR Am J Neuroradiol*, 21: 79-82.

Bruck, W. 2005. 'The pathology of multiple sclerosis is the result of focal inflammatory demyelination with axonal damage', *Journal of Neurology*, 252 Suppl 5: v3-9.

Bryan, L., T. Kordula, S. Spiegel, and S. Milstien. 2008. 'Regulation and functions of sphingosine kinases in the brain', *Biochim Biophys Acta*, 1781: 459-66.

Bugiani, O. 2004. 'A beta-related cerebral amyloid angiopathy', *Neurological Sciences*, 25: S1-S2.

Campbell, G. R., and D. J. Mahad. 2012. 'Mitochondrial changes associated with demyelination: consequences for axonal integrity', *Mitochondrion*, 12: 173-9.

Casaccia-Bonnefil, P. 2000. 'Cell death in the oligodendrocyte lineage: a molecular perspective of life/death decisions in development and disease', *Glia*, 29: 124-35.

Cavalieri, M., R. Schmidt, C. Chen, V. Mok, G. R. de Freitas, S. Song, Q. Yi, S. Ropele, A. Grazer, N. Homayoon, C. Enzinger, K. Loh, K. S. Wong, A. Wong, Y. Xiong, H. M. Chang, M. C. Wong, F. Fazekas, J. W. Eikelboom, G. J. Hankey, and Vitatops Trial Study Group. 2012. 'B vitamins and magnetic resonance imaging-detected ischemic brain lesions in patients with recent transient ischemic attack or stroke: the VITAmins TO Prevent Stroke (VITATOPS) MRI-substudy', *Stroke*, 43: 3266-70.

Chabriat, H., A. Joutel, M. Dichgans, E. Tournier-Lasserve, and M. G. Bousser. 2009. 'Cadasil', *Lancet Neurology*, 8: 643-53.

Chen, Y., V. Balasubramaniyan, J. Peng, E. C. Hurlock, M. Tallquist, J. Li, and Q. R. Lu. 2007. 'Isolation and culture of rat and mouse oligodendrocyte precursor cells', *Nat Protoc*, 2: 1044-51.

Chiba, Y., H. Takeuchi, H. Sakai, and M. Misawa. 2010. 'SKI-II, an inhibitor of sphingosine kinase, ameliorates antigen-induced bronchial smooth muscle hyperresponsiveness, but not airway inflammation, in mice', *J Pharmacol Sci*, 114: 304-10.

Cho, S. Y., S. Cho, E. Park, B. Kim, E. J. Sohn, B. Oh, E. O. Lee, H. J. Lee, and S. H. Kim. 2014. 'Coumestrol suppresses hypoxia inducible factor 1alpha by inhibiting ROS mediated sphingosine kinase 1 in hypoxic PC-3 prostate cancer cells', *Bioorg Med Chem Lett*, 24: 2560-4.

Choi, E. K., D. Park, T. K. Kim, S. H. Lee, D. K. Bae, G. Yang, Y. H. Yang, J. Kyung, D. Kim, W. R. Lee, J. G. Suh, E. S. Jeong, S. U. Kim, and Y. B. Kim. 2011. 'Animal models of periventricular leukomalacia', *Lab Anim Res*, 27: 77-84.

Cingolani, F., M. Casasampere, P. Sanllehi, J. Casas, J. Bujons, and G. Fabrias. 2014. 'Inhibition of dihydroceramide desaturase activity by the sphingosine kinase inhibitor SKI II', *J Lipid Res*, 55: 1711-20.

Cui, Q. L., J. Fang, T. E. Kennedy, G. Almazan, and J. P. Antel. 2014. 'Role of p38MAPK in S1P receptor-mediated differentiation of human oligodendrocyte progenitors', *Glia*, 62: 1361-75.

Cukierman-Yaffe, T., H. C. Gerstein, J. D. Williamson, R. M. Lazar, L. Lovato, M. E. Miller, L. H. Coker, A. Murray, M. D. Sullivan, S. M.

Marcovina, L. J. Launer, and Investigators Action to Control Cardiovascular Risk in Diabetes-Memory in Diabetes. 2009. 'Relationship between baseline glycemic control and cognitive function in individuals with type 2 diabetes and other cardiovascular risk factors: the action to control cardiovascular risk in diabetes-memory in diabetes (ACCORD-MIND) trial', *Diabetes Care*, 32: 221-6.

Curatolo, W. 1987a. 'Glycolipid function', *Biochim Biophys Acta*, 906: 137-60.

———. 1987b. 'The physical properties of glycolipids', *Biochim Biophys Acta*, 906: 111-36.

Cuvillier, O., G. Pirianov, B. Kleuser, P. G. Vanek, O. A. Coso, S. Gutkind, and S. Spiegel. 1996. 'Suppression of ceramide-mediated programmed cell death by sphingosine-1-phosphate', *Nature*, 381: 800-3.

Czabotar, P. E., G. Lessene, A. Strasser, and J. M. Adams. 2014. 'Control of apoptosis by the BCL-2 protein family: implications for physiology and therapy', *Nature Reviews Molecular Cell Biology*, 15: 49-63.

D'Arrigo, P., and S. Servi. 2010. 'Synthesis of lysophospholipids', *Molecules*, 15: 1354-77.

D'Haeseleer, M., S. Hostenbach, I. Peeters, S. E. Sankari, G. Nagels, J. De Keyser, and B. D'Hooghe M. 2015. 'Cerebral hypoperfusion: a new pathophysiologic concept in multiple sclerosis?', *J Cereb Blood Flow Metab*, 35: 1406-10.

Dawson, M. R., A. Polito, J. M. Levine, and R. Reynolds. 2003. 'NG2-expressing glial progenitor cells: an abundant and widespread population of cycling cells in the adult rat CNS', *Mol Cell Neurosci*, 24: 476-88.

de Groot, J. C., F. E. de Leeuw, M. Oudkerk, A. Hofman, J. Jolles, and M. M. Breteler. 2001. 'Cerebral white matter lesions and subjective cognitive dysfunction: the Rotterdam Scan Study', *Neurology*, 56: 1539-45.

de Groot, J. C., F. E. de Leeuw, M. Oudkerk, J. van Gijn, A. Hofman, J. Jolles, and M. M. B. Breteler. 2002. 'Periventricular cerebral white matter lesions predict rate of cognitive decline', *Annals of Neurology*, 52: 335-41.

de Leeuw, F. E., J. C. de Groot, E. Achten, M. Oudkerk, L. M. Ramos, R. Heijboer, A. Hofman, J. Jolles, J. van Gijn, and M. M. Breteler. 2001. 'Prevalence of cerebral white matter lesions in elderly people: a population based magnetic resonance imaging study. The Rotterdam Scan Study', *J Neurol Neurosurg Psychiatry*, 70: 9-14.

de Leeuw, F. E., J. C. de Groot, M. Oudkerk, J. C. Witteman, A. Hofman, J. van Gijn, and M. M. Breteler. 2002. 'Hypertension and cerebral white matter lesions in a prospective cohort study', *Brain*, 125: 765-72.

Debette, S., J. C. Bis, M. Fornage, H. Schmidt, M. A. Ikram, S. Sigurdsson, G. Heiss, M. Struchalin, A. V. Smith, A. van der Lugt, C. DeCarli, T. Lumley, D. S. Knopman, C. Enzinger, G. Eiriksdottir, P. J. Koudstaal, A. L. DeStefano, B. M. Psaty, C. Dufouil, D. J. Catellier, F. Fazekas, T. Aspelund, Y. S. Aulchenko, A. Beiser, J. I. Rotter, C. Tzourio, D. K. Shibata, M. Tscherner, T. B. Harris, F. Rivadeneira, L. D. Atwood,

K. Rice, R. F. Gottesman, M. A. van Buchem, A. G. Uitterlinden, M. Kelly-Hayes, M. Cushman, Y. C. Zhu, E. Boerwinkle, V. Gudnason, A. Hofman, J. R. Romero, O. Lopez, C. M. van Duijn, R. Au, S. R. Heckbert, P. A. Wolf, T. H. Mosley, S. Seshadri, M. M. B. Breteler, R. Schmidt, L. J. Launer, and W. T. Longstreth. 2010. 'Genome-Wide Association Studies of MRI-Defined Brain Infarcts Meta-Analysis From the CHARGE Consortium', *Stroke*, 41: 210-17.

Dewar, D., and D. Dawson. 1995. 'Tau protein is altered by focal cerebral ischaemia in the rat: an immunohistochemical and immunoblotting study', *Brain Res*, 684: 70-8.

Dewar, D., S. M. Underhill, and M. P. Goldberg. 2003. 'Oligodendrocytes and ischemic brain injury', *J Cereb Blood Flow Metab*, 23: 263-74.

Dong, Y. F., K. Kataoka, K. Toyama, D. Sueta, N. Koibuchi, E. Yamamoto, K. Yata, H. Tomimoto, H. Ogawa, and S. Kim-Mitsuyama. 2011. 'Attenuation of brain damage and cognitive impairment by direct renin inhibition in mice with chronic cerebral hypoperfusion', *Hypertension*, 58: 635-42.

Du, J., M. Ma, Q. Zhao, L. Fang, J. Chang, Y. Wang, R. Fei, and X. Song. 2013. 'Mitochondrial bioenergetic deficits in the hippocampi of rats with chronic ischemia-induced vascular dementia', *Neuroscience*, 231: 345-52.

Dukala, D. E., and B. Soliven. 2016. 'S1P1 deletion in oligodendroglial lineage cells: Effect on differentiation and myelination', *Glia*, 64: 570-82.

Dyer, C. A., and J. A. Benjamins. 1988. 'Antibody to galactocerebroside alters organization of oligodendroglial membrane sheets in culture', *J Neurosci*, 8: 4307-18.

Edsall, L. C., O. Cuvillier, S. Twitty, S. Spiegel, and S. Milstien. 2001. 'Sphingosine kinase expression regulates apoptosis and caspase activation in PC12 cells', *J Neurochem*, 76: 1573-84.

Edsall, L. C., and S. Spiegel. 1999. 'Enzymatic measurement of sphingosine 1-phosphate', *Anal Biochem*, 272: 80-6.

Endo, K., Y. Igarashi, M. Nisar, Q. H. Zhou, and S. I. Hakomori. 1991. 'Cell-Membrane Signaling as Target in Cancer-Therapy - Inhibitory Effect of N,N-Dimethyl and N,N,N-Trimethyl Sphingosine Derivatives on Invitro and Invivo Growth of Human Tumor-Cells in Nude-Mice', *Cancer Research*, 51: 1613-18.

Englund, E. 2002. 'Neuropathology of white matter lesions in vascular cognitive impairment', *Cerebrovasc Dis*, 13 Suppl 2: 11-5.

Erkinjuntti, T., D. Inzitari, L. Pantoni, A. Wallin, P. Scheltens, K. Rockwood, G. C. Roman, H. Chui, and D. W. Desmond. 2000. 'Research criteria for subcortical vascular dementia in clinical trials', *J Neural Transm Suppl*, 59: 23-30.

Erkinjuntti, T., A. Kurz, S. Gauthier, R. Bullock, S. Lilienfeld, and C. V. Damaraju. 2002. 'Efficacy of galantamine in probable vascular dementia and Alzheimer's disease combined with cerebrovascular disease: a randomised trial', *Lancet*, 359: 1283-90.

Erkinjuntti, T., G. Roman, S. Gauthier, H. Feldman, and K. Rockwood. 2004. 'Emerging therapies for vascular dementia and vascular cognitive impairment', *Stroke*, 35: 1010-7.

Eskes, R., S. Desagher, B. Antonsson, and J. C. Martinou. 2000. 'Bid induces the oligomerization and insertion of Bax into the outer mitochondrial membrane', *Molecular and Cellular Biology*, 20: 929-35.

Falvey, C. M., C. Rosano, E. M. Simonsick, T. Harris, E. S. Strotmeyer, S. Satterfield, K. Yaffe, and A. B. C. Study Health. 2013. 'Macro- and microstructural magnetic resonance imaging indices associated with diabetes among community-dwelling older adults', *Diabetes Care*, 36: 677-82.

Fannon, A. M., and M. A. Moscarello. 1991. 'Characterization of myelin basic protein charge isomers from adult mouse brain', *Neuroreport*, 2: 135-8.

Farkas, E., G. Donka, R. A. I. de Vos, A. Mihaly, F. Bari, and P. G. M. Luiten. 2004. 'Experimental cerebral hypoperfusion induces white matter injury and microglial activation in the rat brain', *Acta Neuropathologica*, 108: 57-64.

Fassbender, K., O. Mielke, T. Bertsch, B. Nafe, S. Froschen, and M. Hennerici. 1999. 'Homocysteine in cerebral macroangiography and microangiopathy', *Lancet*, 353: 1586-7.

Feghali, C. A., and T. M. Wright. 1997. 'Cytokines in acute and chronic inflammation', *Front Biosci*, 2: d12-26.

Fern, R., and T. Moller. 2000. 'Rapid ischemic cell death in immature oligodendrocytes: a fatal glutamate release feedback loop', *J Neurosci*, 20: 34-42.

Ferrara, N., H. P. Gerber, and J. LeCouter. 2003. 'The biology of VEGF and its receptors', *Nature Medicine*, 9: 669-76.

Ferrer, I. 2010. 'Cognitive impairment of vascular origin: neuropathology of cognitive impairment of vascular origin', *J Neurol Sci*, 299: 139-49.

Fitzpatrick, A. L., L. H. Kuller, O. L. Lopez, P. Diehr, E. S. O'Meara, W. T. Longstreth, Jr., and J. A. Luchsinger. 2009. 'Midlife and late-life obesity and the risk of dementia: cardiovascular health study', *Arch Neurol*, 66: 336-42.

Forette. 2003. 'The prevention of dementia with antihypertensive treatment: New evidence from the systolic hypertension in Europe (Syst-Eur) study (vol 162, pg 2046, 2002)', *Archives of Internal Medicine*, 163: 241-41.

Franklin, R. J. 2002. 'Why does remyelination fail in multiple sclerosis?', *Nat Rev Neurosci*, 3: 705-14.

French, K. J., R. S. Schrecengost, B. D. Lee, Y. Zhuang, S. N. Smith, J. L. Eberly, J. K. Yun, and C. D. Smith. 2003. 'Discovery and evaluation of inhibitors of human sphingosine kinase', *Cancer Res*, 63: 5962-9.

French, K. J., J. J. Upson, S. N. Keller, Y. Zhuang, J. K. Yun, and C. D. Smith. 2006. 'Antitumor activity of sphingosine kinase inhibitors', *J Pharmacol Exp Ther*, 318: 596-603.

French, K. J., Y. Zhuang, L. W. Maines, P. Gao, W. Wang, V. Beljanski, J. J. Upson, C. L. Green, S. N. Keller, and C. D. Smith. 2010. 'Pharmacology and antitumor activity of ABC294640, a selective inhibitor of sphingosine kinase-2', *J Pharmacol Exp Ther*, 333: 129-39.

Frost, S. B., S. Barbay, M. L. Mumert, A. M. Stowe, and R. J. Nudo. 2006. 'An animal model of capsular infarct: endothelin-1 injections in the rat', *Behav Brain Res*, 169: 206-11.

Fukuda, Y., Y. Aoyama, A. Wada, and Y. Igarashi. 2004. 'Identification of PECAM-1 association with sphingosine kinase 1 and its regulation by agonist-induced phosphorylation', *Biochim Biophys Acta*, 1636: 12-21.

Gallo, V., and B. Deneen. 2014. 'Glial development: the crossroads of regeneration and repair in the CNS', *Neuron*, 83: 283-308.

Gao, P., Y. K. Peterson, R. A. Smith, and C. D. Smith. 2012. 'Characterization of isoenzyme-selective inhibitors of human sphingosine kinases', *PLoS One*, 7: e44543.

Gielen, E., W. Baron, M. Vandeven, P. Steels, D. Hoekstra, and M. Ameloot. 2006. 'Rafts in oligodendrocytes: Evidence and structure-function relationship', *Glia*, 54: 499-512.

Ginsberg, M. D., E. T. Hedleywhyte, and E. P. Richardson. 1976. 'Hypoxic-Ischemic Leukoencephalopathy in Man', *Archives of Neurology*, 33: 5-14.

Gold, G., E. Kovari, F. R. Herrmann, A. Canuto, P. R. Hof, J. P. Michel, C. Bouras, and P. Giannakopoulos. 2005. 'Cognitive consequences of thalamic, basal ganglia, and deep white matter lacunes in brain aging and dementia', *Stroke*, 36: 1184-88.

Gorelick, P. B. 1997. 'Status of risk factors for dementia associated with stroke', *Stroke*, 28: 459-63.

Gorelick, P. B., A. Scuteri, S. E. Black, C. Decarli, S. M. Greenberg, C. Iadecola, L. J. Launer, S. Laurent, O. L. Lopez, D. Nyenhuis, R. C. Petersen, J. A. Schneider, C. Tzourio, D. K. Arnett, D. A. Bennett, H. C. Chui, R. T. Higashida, R. Lindquist, P. M. Nilsson, G. C. Roman, F. W. Sellke, S. Seshadri, Council on Epidemiology American Heart Association Stroke Council, Council on Cardiovascular Nursing Council on Cardiovascular Radiology Prevention, Intervention, Surgery Council on Cardiovascular, and Anesthesia. 2011. 'Vascular contributions to cognitive impairment and dementia: a statement for healthcare professionals from the american heart association/american stroke association', *Stroke*, 42: 2672-713.

Gotoh, M., K. Sano-Maeda, H. Murofushi, and K. Murakami-Murofushi. 2012. 'Protection of neuroblastoma Neuro2A cells from hypoxia-induced apoptosis by cyclic phosphatidic acid (cPA)', *PLoS One*, 7: e51093.

Greer, J. M. 2013. 'Autoimmune T-cell reactivity to myelin proteolipids and glycolipids in multiple sclerosis', *Mult Scler Int*, 2013: 151427.

Greer, J. M., and M. B. Lees. 2002. 'Myelin proteolipid protein--the first 50 years', *Int J Biochem Cell Biol*, 34: 211-5.

Griffiths, I., M. Klugmann, T. Anderson, D. Yool, C. Thomson, M. H. Schwab, A. Schneider, F. Zimmermann, M. McCulloch, N. Nadon, and K. A. Nave. 1998. 'Axonal swellings and degeneration in mice lacking the major proteolipid of myelin', *Science*, 280: 1610-3.

Guang, H. M., and G. H. Du. 2006. 'Protections of pinocembrin on brain mitochondria contribute to cognitive improvement in chronic cerebral hypoperfused rats', *Eur J Pharmacol*, 542: 77-83.

Gustin, D. J., Y. Li, M. L. Brown, X. Min, M. J. Schmitt, M. Wanska, X. Wang, R. Connors, S. Johnstone, M. Cardozo, A. C. Cheng, S. Jeffries, B. Franks, S. Li, S. Shen, M. Wong, H. Wesche, G. Xu, T. J. Carlson, M. Plant, K. Morgenstern, K. Rex, J. Schmitt, A. Coxon, N. Walker, F. Kayser, and Z. Wang. 2013. 'Structure guided design of a series of sphingosine kinase (SphK) inhibitors', *Bioorg Med Chem Lett*, 23: 4608-16.

Hachinski, V., C. Iadecola, R. C. Petersen, M. M. Breteler, D. L. Nyenhuis, S. E. Black, W. J. Powers, C. DeCarli, J. G. Merino, R. N. Kalaria, H. V. Vinters, D. M. Holtzman, G. A. Rosenberg, A. Wallin, M. Dichgans, J. R. Marler, and G. G. Leblanc. 2006. 'National Institute of Neurological Disorders and Stroke-Canadian Stroke Network vascular cognitive impairment harmonization standards', *Stroke*, 37: 2220-41.

Hagberg, H., D. Peebles, and C. Mallard. 2002. 'Models of white matter injury: comparison of infectious, hypoxic-ischemic, and excitotoxic insults', *Ment Retard Dev Disabil Res Rev*, 8: 30-8.

Hainsworth, A. H., and H. S. Markus. 2008. 'Do in vivo experimental models reflect human cerebral small vessel disease? A systematic review', *J Cereb Blood Flow Metab*, 28: 1877-91.

Hait, N. C., A. Bellamy, S. Milstien, T. Kordula, and S. Spiegel. 2007. 'Sphingosine kinase type 2 activation by ERK-mediated phosphorylation', *J Biol Chem*, 282: 12058-65.

Hait, N. C., C. A. Oskeritzian, S. W. Paugh, S. Milstien, and S. Spiegel. 2006. 'Sphingosine kinases, sphingosine 1-phosphate, apoptosis and diseases', *Biochim Biophys Acta*, 1758: 2016-26.

Hait, N. C., S. Sarkar, H. Le Stunff, A. Mikami, M. Maceyka, S. Milstien, and S. Spiegel. 2005. 'Role of sphingosine kinase 2 in cell migration toward epidermal growth factor', *J Biol Chem*, 280: 29462-9.

Hannun, Y. A., and L. M. Obeid. 2002. 'The Ceramide-centric universe of lipid-mediated cell regulation: stress encounters of the lipid kind', *J Biol Chem*, 277: 25847-50.

———. 2008. 'Principles of bioactive lipid signalling: lessons from sphingolipids', *Nat Rev Mol Cell Biol*, 9: 139-50.

Harauz, G., and J. M. Boggs. 2013. 'Myelin management by the 18.5-kDa and 21.5-kDa classic myelin basic protein isoforms', *J Neurochem*, 125: 334-61.

Harauz, G., V. Ladizhansky, and J. M. Boggs. 2009. 'Structural polymorphism and multifunctionality of myelin basic protein', *Biochemistry*, 48: 8094-104.

Harkewicz, R., and E. A. Dennis. 2011. 'Applications of mass spectrometry to lipids and membranes', *Annu Rev Biochem*, 80: 301-25.

Harrison, F. E., R. S. Reiserer, A. J. Tomarken, and M. P. McDonald. 2006. 'Spatial and nonspatial escape strategies in the Barnes maze', *Learn Mem*, 13: 809-19.

Hartman, B. K., H. C. Agrawal, D. Agrawal, and S. Kalmbach. 1982. 'Development and maturation of central nervous system myelin: comparison of immunohistochemical localization of proteolipid protein and basic protein in myelin and oligodendrocytes', *Proc Natl Acad Sci U S A*, 79: 4217-20.

Harvey, R. J., M. Skelton-Robinson, and M. N. Rossor. 2003. 'The prevalence and causes of dementia in people under the age of 65 years', *Journal of Neurology Neurosurgery and Psychiatry*, 74: 1206-09.

Hasegawa, Y., H. Suzuki, T. Sozen, W. Rolland, and J. H. Zhang. 2010. 'Activation of sphingosine 1-phosphate receptor-1 by FTY720 is neuroprotective after ischemic stroke in rats', *Stroke*, 41: 368-74.

Hassan, A., B. J. Hunt, M. O'Sullivan, R. Bell, R. D'Souza, S. Jeffery, J. M. Bamford, and H. S. Markus. 2004. 'Homocysteine is a risk factor for cerebral small vessel disease, acting via endothelial dysfunction', *Brain*, 127: 212-9.

Hayashi, S., T. Okada, N. Igarashi, T. Fujita, S. Jahangeer, and S. Nakamura. 2002. 'Identification and characterization of RPK118, a novel sphingosine kinase-1-binding protein', *J Biol Chem*, 277: 33319-24.

Hetz, C. 2012. 'The unfolded protein response: controlling cell fate decisions under ER stress and beyond', *Nat Rev Mol Cell Biol*, 13: 89-102.

Hirahara, Y., R. Bansal, K. Honke, K. Ikenaka, and Y. Wada. 2004. 'Sulfatide is a negative regulator of oligodendrocyte differentiation: development in sulfatide-null mice', *Glia*, 45: 269-77.

Hu, Y., X. Lee, B. Ji, K. Guckian, D. Apicco, R. B. Pepinsky, R. H. Miller, and S. Mi. 2011. 'Sphingosine 1-phosphate receptor modulator fingolimod (FTY720) does not promote remyelination in vivo', *Mol Cell Neurosci*, 48: 72-81.

Huang, W., N. Zhao, X. Bai, K. Karram, J. Trotter, S. Goebbels, A. Scheller, and F. Kirchhoff. 2014. 'Novel NG2-CreERT2 knock-in mice demonstrate heterogeneous differentiation potential of NG2 glia during development', *Glia*, 62: 896-913.

Hughes, P. M., D. C. Anthony, M. Ruddin, M. S. Botham, E. L. Rankine, M. Sablone, D. Baumann, A. K. Mir, and V. H. Perry. 2003. 'Focal lesions in the rat central nervous system induced by endothelin-1', *J Neuropathol Exp Neurol*, 62: 1276-86.

Huwiler, A., F. Doll, S. Ren, S. Klawitter, A. Greening, I. Romer, S. Bubnova, L. Reinsberg, and J. Pfeilschifter. 2006. 'Histamine increases sphingosine kinase-1 expression and activity in the human arterial endothelial cell line EA.hy 926 by a PKC-alpha-dependent mechanism', *Biochim Biophys Acta*, 1761: 367-76.

Huynh, J. L., P. Garg, T. H. Thin, S. Yoo, R. Dutta, B. D. Trapp, V. Haroutunian, J. Zhu, M. J. Donovan, A. J. Sharp, and P. Casaccia. 2014. 'Epigenome-wide differences in pathology-free regions of multiple sclerosis-affected brains', *Nat Neurosci*, 17: 121-30.

Igarashi, N., T. Okada, S. Hayashi, T. Fujita, S. Jahangeer, and S. Nakamura. 2003. 'Sphingosine kinase 2 is a nuclear protein and inhibits DNA synthesis', *J Biol Chem*, 278: 46832-9.

Igarashi, Y., S. Hakomori, T. Toyokuni, B. Dean, S. Fujita, M. Sugimoto, T. Ogawa, K. el-Ghendy, and E. Racker. 1989. 'Effect of chemically well-defined sphingosine and its N-methyl derivatives on protein kinase C and src kinase activities', *Biochemistry*, 28: 6796-800.

Igarashi, Y., K. Kitamura, T. Toyokuni, B. Dean, B. Fenderson, T. Ogawass, and S. Hakomori. 1990. 'A specific enhancing effect of N,N-dimethylsphingosine on epidermal growth factor receptor

autophosphorylation. Demonstration of its endogenous occurrence (and the virtual absence of unsubstituted sphingosine) in human epidermoid carcinoma A431 cells', *J Biol Chem*, 265: 5385-9.

Ikram, M. A., S. Seshadri, J. C. Bis, M. Fornage, A. L. DeStefano, Y. S. Aulchenko, S. Debette, T. Lumley, A. R. Folsom, E. G. van den Herik, M. J. Bos, A. Beiser, M. Cushman, L. J. Launer, E. Shahar, M. Struchalin, Y. Du, N. L. Glazer, W. D. Rosamond, F. Rivadeneira, M. Kelly-Hayes, O. L. Lopez, J. Coresh, A. Hofman, C. DeCarli, S. R. Heckbert, P. J. Koudstaal, Q. Yang, N. L. Smith, C. S. Kase, K. Rice, T. Haritunians, G. Roks, P. L. de Kort, K. D. Taylor, L. M. de Lau, B. A. Oostra, A. G. Uitterlinden, J. I. Rotter, E. Boerwinkle, B. M. Psaty, T. H. Mosley, C. M. van Duijn, M. M. Breteler, W. T. Longstreth, Jr., and P. A. Wolf. 2009. 'Genomewide association studies of stroke', *N Engl J Med*, 360: 1718-28.

Imgrund, S., D. Hartmann, H. Farwanah, M. Eckhardt, R. Sandhoff, J. Degen, V. Gieselmann, K. Sandhoff, and K. Willecke. 2009. 'Adult ceramide synthase 2 (CERS2)-deficient mice exhibit myelin sheath defects, cerebellar degeneration, and hepatocarcinomas', *J Biol Chem*, 284: 33549-60.

Inzitari, D., M. Simoni, G. Pracucci, A. Poggesi, A. M. Basile, H. Chabriat, T. Erkinjuntti, F. Fazekas, J. M. Ferro, M. Hennerici, P. Langhorne, J. O'Brien, F. Barkhof, M. C. Visser, L. O. Wahlund, G. Waldemar, A. Wallin, L. Pantoni, and Ladis Study Group. 2007. 'Risk of rapid global functional decline in elderly patients with severe cerebral age-related white matter changes: the LADIS study', *Arch Intern Med*, 167: 81-8.

Irving, E. A., K. Yatsushiro, J. McCulloch, and D. Dewar. 1997. 'Rapid alteration of tau in oligodendrocytes after focal ischemic injury in the rat: involvement of free radicals', *J Cereb Blood Flow Metab*, 17: 612-22.

Jaillard, C., S. Harrison, B. Stankoff, M. S. Aigrot, A. R. Calver, G. Duddy, F. S. Walsh, M. N. Pangalos, N. Arimura, K. Kaibuchi, B. Zalc, and C. Lubetzki. 2005. 'Edg8/S1P5: an oligodendroglial receptor with dual function on process retraction and cell survival', *J Neurosci*, 25: 1459-69.

Jalal, F. Y., Y. Yang, J. Thompson, A. C. Lopez, and G. A. Rosenberg. 2012. 'Myelin Loss Associated With Neuroinflammation in Hypertensive Rats', *Stroke*, 43: 1115-U359.

Jellinger, K. A., and J. Attems. 2005. 'Prevalence and pathogenic role of cerebrovascular lesions in Alzheimer disease', *Journal of the Neurological Sciences*, 229: 37-41.

Jendiroba, D. B., J. Klostergaard, A. Keyhani, L. Pagliaro, and E. J. Freireich. 2002. 'Effective cytotoxicity against human leukemias and chemotherapy-resistant leukemia cell lines by N-N-dimethylsphingosine', *Leuk Res*, 26: 301-10.

Jennemann, R., M. Rabionet, K. Gorgas, S. Epstein, A. Dalpke, U. Rothermel, A. Bayerle, F. van der Hoeven, S. Imgrund, J. Kirsch, W. Nickel, K. Willecke, H. Riezman, H. J. Grone, and R. Sandhoff. 2012. 'Loss of ceramide synthase 3 causes lethal skin barrier disruption', *Hum Mol Genet*, 21: 586-608.

Jiwa, N. S., P. Garrard, and A. H. Hainsworth. 2010. 'Experimental models of vascular dementia and vascular cognitive impairment: a systematic review', *Journal of Neurochemistry*, 115: 814-28.

Joutel, A., C. Corpechot, A. Ducros, K. Vahedi, H. Chabriat, P. Mouton, S. Alamowitch, V. Domenga, M. Cecillion, E. Marechal, J. Maciazek, C. Vayssiere, C. Cruaud, E. A. Cabanis, M. M. Ruchoux, J. Weissenbach, J. F. Bach, M. G. Bousser, and E. TournierLasserve. 1996. 'Notch3 mutations in CADASIL, a hereditary adult-onset condition causing stroke and dementia', *Nature*, 383: 707-10.

Joutel, A., M. Monet-Lepretre, C. Gosele, C. Baron-Menguy, A. Hammes, S. Schmidt, B. Lemaire-Carrette, V. Domenga, A. Schedl, P. Lacombe, and N. Hubner. 2010. 'Cerebrovascular dysfunction and microcirculation rarefaction precede white matter lesions in a mouse genetic model of cerebral ischemic small vessel disease', *J Clin Invest*, 120: 433-45.

Jung, C. G., H. J. Kim, V. E. Miron, S. Cook, T. E. Kennedy, C. A. Foster, J. P. Antel, and B. Soliven. 2007. 'Functional consequences of S1P receptor modulation in rat oligodendroglial lineage cells', *Glia*, 55: 1656-67.

Juskewitch, J. E., B. E. Knudsen, J. L. Platt, K. A. Nath, K. L. Knutson, G. J. Brunn, and J. P. Grande. 2012. 'LPS-induced murine systemic inflammation is driven by parenchymal cell activation and exclusively predicted by early MCP-1 plasma levels', *Am J Pathol*, 180: 32-40.

Juurlink, B. H., S. K. Thorburne, and L. Hertz. 1998. 'Peroxide-scavenging deficit underlies oligodendrocyte susceptibility to oxidative stress', *Glia*, 22: 371-8.

Kajimoto, T., T. Okada, H. Yu, S. K. Goparaju, S. Jahangeer, and S. Nakamura. 2007. 'Involvement of sphingosine-1-phosphate in glutamate secretion in hippocampal neurons', *Molecular and Cellular Biology*, 27: 3429-40.

Kalaria, R. N., G. E. Maestre, and R. Arizaga. 2008. 'Alzheimer's disease and vascular dementia in developing countries: prevalence, management, and risk factors (vol 7, pg 812, 2008)', *Lancet Neurology*, 7: 867-67.

Kalaria, R. N., G. E. Maestre, R. Arizaga, R. P. Friedland, D. Galasko, K. Hall, J. A. Luchsinger, A. Ogunniyi, E. K. Perry, F. Potocnik, M. Prince, R. Stewart, A. Wimo, Z. X. Zhang, P. Antuono, and Group World Federation of Neurology Dementia Research. 2008. 'Alzheimer's disease and vascular dementia in developing countries: prevalence, management, and risk factors', *Lancet Neurol*, 7: 812-26.

Karovic, O., I. Tonazzini, N. Rebola, E. Edstrom, C. Lovdahl, B. B. Fredholm, and E. Dare. 2007. 'Toxic effects of cobalt in primary cultures of mouse astrocytes. Similarities with hypoxia and role of HIF-1alpha', *Biochem Pharmacol*, 73: 694-708.

Kawaguchi, C., S. Takizawa, K. Niwa, T. Iwamoto, I. Kuwahira, H. Kato, and Y. Shinohara. 2002. 'Regional vulnerability to chronic hypoxia and chronic hypoperfusion in the rat brain', *Pathophysiology*, 8: 249-53.

Keirstead, H. S., and W. F. Blakemore. 1999. 'The role of oligodendrocytes and oligodendrocyte progenitors in CNS remyelination', *Adv Exp Med Biol*, 468: 183-97.

Kerr, J. F., A. H. Wyllie, and A. R. Currie. 1972. 'Apoptosis: a basic biological phenomenon with wide-ranging implications in tissue kinetics', *Br J Cancer*, 26: 239-57.

Kim, H. Y., B. X. Huang, and A. A. Spector. 2014. 'Phosphatidylserine in the brain: metabolism and function', *Prog Lipid Res*, 56: 1-18.

Kim, K. W., J. C. Youn, M. K. Han, N. J. Paik, T. J. Lee, J. H. Park, S. B. Lee, I. H. Choo, D. Y. Lee, J. H. Jhoo, and J. I. Woo. 2008. 'Lack of association between apolipoprotein E polymorphism and vascular dementia in Koreans', *J Geriatr Psychiatry Neurol*, 21: 12-7.

Kim, M., M. Kim, N. Kim, V. D. D'Agati, C. W. Emala, Sr., and H. T. Lee. 2007. 'Isoflurane mediates protection from renal ischemia-reperfusion injury via sphingosine kinase and sphingosine-1-phosphate-dependent pathways', *Am J Physiol Renal Physiol*, 293: F1827-35.

Kimura, A., T. Ohmori, R. Ohkawa, S. Madoiwa, J. Mimuro, T. Murakami, E. Kobayashi, Y. Hoshino, Y. Yatomi, and Y. Sakata. 2007. 'Essential roles of sphingosine 1-phosphate/S1P(1) receptor axis in the migration of neural stem cells toward a site of spinal cord injury', *Stem Cells*, 25: 115-24.

Kinney, H. C., J. Karthigasan, N. I. Borenshteyn, J. D. Flax, and D. A. Kirschner. 1994. 'Myelination in the developing human brain: biochemical correlates', *Neurochem Res*, 19: 983-96.

Kirschning, E., G. Rutter, and H. Hohenberg. 1998. 'High-pressure freezing and freeze-substitution of native rat brain: suitability for preservation and immunoelectron microscopic localization of myelin glycolipids', *Journal of Neuroscience Research*, 53: 465-74.

Kluver, H., and E. Barrera. 1953. 'A method for the combined staining of cells and fibers in the nervous system', *J Neuropathol Exp Neurol*, 12: 400-3.

Knopman, D. S., J. E. Parisi, B. F. Boeve, R. H. Cha, H. Apaydin, A. Salviati, S. D. Edland, and W. A. Rocca. 2003. 'Vascular dementia in a population-based autopsy study', *Arch Neurol*, 60: 569-75.

Kohama, T., A. Olivera, L. Edsall, M. M. Nagiec, R. Dickson, and S. Spiegel. 1998. 'Molecular cloning and functional characterization of murine sphingosine kinase', *J Biol Chem*, 273: 23722-8.

Kroesen, B. J., S. Jacobs, B. J. Pettus, H. Sietsma, J. W. Kok, Y. A. Hannun, and L. F. de Leij. 2003. 'BcR-induced apoptosis involves differential regulation of C16 and C24-ceramide formation and sphingolipid-dependent activation of the proteasome', *J Biol Chem*, 278: 14723-31.

Kumar, S. 2007. 'Caspase function in programmed cell death', *Cell Death Differ*, 14: 32-43.

Lam, S. M., Y. Wang, X. Duan, M. R. Wenk, R. N. Kalaria, C. P. Chen, M. K. Lai, and G. Shui. 2014. 'Brain lipidomes of subcortical ischemic vascular dementia and mixed dementia', *Neurobiol Aging*, 35: 2369-81.

Launer, L. J., K. Masaki, H. Petrovitch, D. Foley, and R. J. Havlik. 1995. 'The association between midlife blood pressure levels and late-life

cognitive function. The Honolulu-Asia Aging Study', *JAMA*, 274: 1846-51.

Laviad, E. L., L. Albee, I. Pankova-Kholmyansky, S. Epstein, H. Park, A. H. Merrill, Jr., and A. H. Futerman. 2008. 'Characterization of ceramide synthase 2: tissue distribution, substrate specificity, and inhibition by sphingosine 1-phosphate', *J Biol Chem*, 283: 5677-84.

Lee, M. J., S. Thangada, K. P. Claffey, N. Ancellin, C. H. Liu, M. Kluk, M. Volpi, R. I. Sha'afi, and T. Hla. 1999. 'Vascular endothelial cell adherens junction assembly and morphogenesis induced by sphingosine-1-phosphate', *Cell*, 99: 301-12.

Levine, J. M., R. Reynolds, and J. W. Fawcett. 2001. 'The oligodendrocyte precursor cell in health and disease', *Trends in Neurosciences*, 24: 39-47.

Li, M. H., T. Hla, and F. Ferrer. 2013. 'FTY720 inhibits tumor growth and enhances the tumor-suppressive effect of topotecan in neuroblastoma by interfering with the sphingolipid signaling pathway', *Pediatr Blood Cancer*, 60: 1418-23.

Liao, D., L. Cooper, J. Cai, J. F. Toole, N. R. Bryan, R. G. Hutchinson, and H. A. Tyroler. 1996. 'Presence and severity of cerebral white matter lesions and hypertension, its treatment, and its control. The ARIC Study. Atherosclerosis Risk in Communities Study', *Stroke*, 27: 2262-70.

Lim, K. G., C. Sun, R. Bittman, N. J. Pyne, and S. Pyne. 2011. '(R)-FTY720 methyl ether is a specific sphingosine kinase 2 inhibitor: Effect on sphingosine kinase 2 expression in HEK 293 cells and actin rearrangement and survival of MCF-7 breast cancer cells', *Cell Signal*, 23: 1590-5.

Liu, H., M. Sugiura, V. E. Nava, L. C. Edsall, K. Kono, S. Poulton, S. Milstien, T. Kohama, and S. Spiegel. 2000. 'Molecular cloning and functional characterization of a novel mammalian sphingosine kinase type 2 isoform', *J Biol Chem*, 275: 19513-20.

Liu, H., R. E. Toman, S. K. Goparaju, M. Maceyka, V. E. Nava, H. Sankala, S. G. Payne, M. Bektas, I. Ishii, J. Chun, S. Milstien, and S. Spiegel. 2003. 'Sphingosine kinase type 2 is a putative BH3-only protein that induces apoptosis', *J Biol Chem*, 278: 40330-6.

Liu, Q. H., S. H. He, L. Groysman, D. Shaked, J. Russin, S. Cen, and W. J. Mack. 2013. 'White Matter Injury Due to Experimental Chronic Cerebral Hypoperfusion Is Associated with C5 Deposition', *PLoS One*, 8.

Liu, Y., R. Wada, T. Yamashita, Y. Mi, C. X. Deng, J. P. Hobson, H. M. Rosenfeldt, V. E. Nava, S. S. Chae, M. J. Lee, C. H. Liu, T. Hla, S. Spiegel, and R. L. Proia. 2000. 'Edg-1, the G protein-coupled receptor for sphingosine-1-phosphate, is essential for vascular maturation', *J Clin Invest*, 106: 951-61.

Lo, E. H. 2010. 'Degeneration and repair in central nervous system disease', *Nat Med*, 16: 1205-9.

Longstreth, W. T., Jr., R. Katz, J. Olson, C. Bernick, J. J. Carr, M. R. Malinow, D. L. Hess, M. Cushman, and S. M. Schwartz. 2004. 'Plasma total homocysteine levels and cranial magnetic resonance

imaging findings in elderly persons: the Cardiovascular Health Study', *Arch Neurol*, 61: 67-72.

Loveridge, C., F. Tonelli, T. Leclercq, K. G. Lim, J. S. Long, E. Berdyshev, R. J. Tate, V. Natarajan, S. M. Pitson, N. J. Pyne, and S. Pyne. 2010. 'The sphingosine kinase 1 inhibitor 2-(p-hydroxyanilino)-4-(p-chlorophenyl)thiazole induces proteasomal degradation of sphingosine kinase 1 in mammalian cells', *J Biol Chem*, 285: 38841-52.

Ma, Y., S. Pitson, T. Hercus, J. Murphy, A. Lopez, and J. Woodcock. 2005. 'Sphingosine activates protein kinase A type II by a novel cAMP-independent mechanism', *J Biol Chem*, 280: 26011-7.

Maceyka, M., V. E. Nava, S. Milstien, and S. Spiegel. 2004. 'Aminoacylase 1 is a sphingosine kinase 1-interacting protein', *FEBS Lett*, 568: 30-4.

Maceyka, M., H. Sankala, N. C. Hait, H. Le Stunff, H. Liu, R. Toman, C. Collier, M. Zhang, L. S. Satin, A. H. Merrill, Jr., S. Milstien, and S. Spiegel. 2005. 'SphK1 and SphK2, sphingosine kinase isoenzymes with opposing functions in sphingolipid metabolism', *J Biol Chem*, 280: 37118-29.

MacLennan, A. J., S. J. Benner, A. Andringa, A. H. Chaves, J. L. Rosing, R. Vesey, A. M. Karpman, S. A. Cronier, N. Lee, L. C. Erway, and M. L. Miller. 2006. 'The S1P(2) sphingosine 1-phosphate receptor is essential for auditory and vestibular function', *Hearing Research*, 220: 38-48.

MacLennan, A. J., P. R. Carney, W. J. Zhu, A. H. Chaves, J. Garcia, J. R. Grimes, K. J. Anderson, S. N. Roper, and N. Lee. 2001. 'An essential role for the H218/AGR16/Edg-5/LPB2 sphingosine 1-phosphate receptor in neuronal excitability', *European Journal of Neuroscience*, 14: 203-09.

Mahad, D. J., I. Ziabreva, G. Campbell, N. Lax, K. White, P. S. Hanson, H. Lassmann, and D. M. Turnbull. 2009. 'Mitochondrial changes within axons in multiple sclerosis', *Brain*, 132: 1161-74.

Maier, O., D. Hoekstra, and W. Baron. 2008. 'Polarity development in oligodendrocytes: sorting and trafficking of myelin components', *J Mol Neurosci*, 35: 35-53.

Maines, L. W., L. R. Fitzpatrick, K. J. French, Y. Zhuang, Z. Xia, S. N. Keller, J. J. Upson, and C. D. Smith. 2008. 'Suppression of ulcerative colitis in mice by orally available inhibitors of sphingosine kinase', *Dig Dis Sci*, 53: 997-1012.

Maines, L. W., L. R. Fitzpatrick, C. L. Green, Y. Zhuang, and C. D. Smith. 2010. 'Efficacy of a novel sphingosine kinase inhibitor in experimental Crohn's disease', *Inflammopharmacology*, 18: 73-85.

Maines, L. W., K. J. French, E. B. Wolpert, D. A. Antonetti, and C. D. Smith. 2006. 'Pharmacologic manipulation of sphingosine kinase in retinal endothelial cells: implications for angiogenic ocular diseases', *Invest Ophthalmol Vis Sci*, 47: 5022-31.

Malchnkhuu, E., K. Sato, T. Maehama, C. Mogi, H. Tomura, S. Ishiuchi, Y. Yoshimoto, H. Kurose, and F. Okajima. 2008. 'S1P(2) receptors mediate inhibition of glioma cell migration through Rho signaling pathways independent of PTEN', *Biochemical and Biophysical Research Communications*, 366: 963-68.

Manolio, T. A., G. L. Burke, D. H. O'Leary, G. Evans, N. Beauchamp, L. Knepper, and B. Ward. 1999. 'Relationships of cerebral MRI findings to ultrasonographic carotid atherosclerosis in older adults : the Cardiovascular Health Study. CHS Collaborative Research Group', *Arterioscler Thromb Vasc Biol*, 19: 356-65.

Marcoux, F. W., R. B. Morawetz, R. M. Crowell, U. Degirolami, and J. H. Halsey. 1982. 'Differential Regional Vulnerability in Transient Focal Cerebral-Ischemia', *Stroke*, 13: 339-46.

Marcus, J., S. Honigbaum, S. Shroff, K. Honke, J. Rosenbluth, and J. L. Dupree. 2006. 'Sulfatide is essential for the maintenance of CNS myelin and axon structure', *Glia*, 53: 372-81.

Marquez-Martin, A., F. Jimenez-Altayo, A. P. Dantas, L. Caracuel, A. M. Planas, and E. Vila. 2012. 'Middle cerebral artery alterations in a rat chronic hypoperfusion model', *J Appl Physiol (1985)*, 112: 511-8.

Marret, S., R. Mukendi, J. F. Gadisseux, P. Gressens, and P. Evrard. 1995. 'Effect of ibotenate on brain development: an excitotoxic mouse model of microgyria and posthypoxic-like lesions', *J Neuropathol Exp Neurol*, 54: 358-70.

Martin-Villalba, A., I. Herr, I. Jeremias, M. Hahne, R. Brandt, J. Vogel, J. Schenkel, T. Herdegen, and K. M. Debatin. 1999. 'CD95 ligand (Fas-L/APO-1L) and tumor necrosis factor-related apoptosis-inducing ligand mediate ischemia-induced apoptosis in neurons', *Journal of Neuroscience*, 19: 3809-17.

Martin, D. A., and K. B. Elkon. 2004. 'Mechanisms of apoptosis', *Rheum Dis Clin North Am*, 30: 441-54, vii.

Mastrandrea, L. D., S. M. Sessanna, and S. G. Laychock. 2005. 'Sphingosine kinase activity and sphingosine-1 phosphate production in rat pancreatic islets and INS-1 cells: response to cytokines', *Diabetes*, 54: 1429-36.

Matloubian, M., C. G. Lo, G. Cinamon, M. J. Lesneski, Y. Xu, V. Brinkmann, M. L. Allende, R. L. Proia, and J. G. Cyster. 2004. 'Lymphocyte egress from thymus and peripheral lymphoid organs is dependent on S1P receptor 1', *Nature*, 427: 355-60.

McCracken, E., D. Dewar, and A. J. Hunter. 2001. 'White matter damage following systemic injection of the mitochondrial inhibitor 3-nitropropionic acid in rat', *Brain Res*, 892: 329-35.

Mehlhorn, I. E., E. Florio, K. R. Barber, C. Lordo, and C. W. M. Grant. 1988. 'Evidence That Trans-Bilayer Interdigitation of Glycosphingolipid Long-Chain Fatty-Acids May Be a General Phenomenon', *Biochimica Et Biophysica Acta*, 939: 151-59.

Mercado, N., Y. Kizawa, K. Ueda, Y. Xiong, G. Kimura, A. Moses, J. M. Curtis, K. Ito, and P. J. Barnes. 2014. 'Activation of transcription factor Nrf2 signalling by the sphingosine kinase inhibitor SKI-II is mediated by the formation of Keap1 dimers', *PLoS One*, 9: e88168.

Mielke, M. M., P. P. Zandi, M. Sjogren, D. Gustafson, S. Ostling, B. Steen, and I. Skoog. 2005. 'High total cholesterol levels in late life associated with a reduced risk of dementia', *Neurology*, 64: 1689-95.

Miron, V. E., J. A. Hall, T. E. Kennedy, B. Soliven, and J. P. Antel. 2008. 'Cyclical and dose-dependent responses of adult human mature oligodendrocytes to fingolimod', *Am J Pathol*, 173: 1143-52.

Miyamoto, N., T. Maki, L. D. Pham, K. Hayakawa, J. H. Seo, E. T. Mandeville, J. B. Mandeville, K. W. Kim, E. H. Lo, and K. Arai. 2013. 'Oxidative stress interferes with white matter renewal after prolonged cerebral hypoperfusion in mice', *Stroke*, 44: 3516-21.

Miyamoto, N., L. D. Pham, K. Hayakawa, T. Matsuzaki, J. H. Seo, C. Magnain, C. Ayata, K. W. Kim, D. Boas, E. H. Lo, and K. Arai. 2013. 'Age-related decline in oligodendrogenesis retards white matter repair in mice', *Stroke*, 44: 2573-8.

Miyamoto, N., R. Tanaka, H. Shimura, T. Watanabe, H. Mori, M. Onodera, H. Mochizuki, N. Hattori, and T. Urabe. 2010. 'Phosphodiesterase III inhibition promotes differentiation and survival of oligodendrocyte progenitors and enhances regeneration of ischemic white matter lesions in the adult mammalian brain', *J Cereb Blood Flow Metab*, 30: 299-310.

Mozzi, R., V. Andreoli, and L. A. Horrocks. 1993. 'Phosphatidylserine synthesis in rat cerebral cortex: effects of hypoxia, hypocapnia and development', *Mol Cell Biochem*, 126: 101-7.

Mulder, C., P. Scheltens, F. Barkhof, C. Gundy, R. A. Verstraeten, and F. E. de Leeuw. 2005. 'Low vitamin B6 levels are associated with white matter lesions in Alzheimer's disease', *J Am Geriatr Soc*, 53: 1073-4.

Muller, C., N. M. Bauer, I. Schafer, and R. White. 2013. 'Making myelin basic protein - from mRNA transport to localized translation', *Frontiers in Cellular Neuroscience*, 7.

Mullershausen, F., L. M. Craveiro, Y. Shin, M. Cortes-Cros, F. Bassilana, M. Osinde, W. L. Wisbart, M. Thallmair, M. E. Schwab, R. Sivasankaran, K. Seuwen, and K. K. Dev. 2007. 'Phosphorylated FTY720 promotes astrocyte migration through sphingosine-1-phosphate receptors', *Journal of Neurochemistry*, 102: 1151-61.

Nakaji, K., M. Ihara, C. Takahashi, S. Itohara, M. Noda, R. Takahashi, and H. Tomimoto. 2006. 'Matrix metalloproteinase-2 plays a critical role in the pathogenesis of white matter lesions after chronic cerebral hypoperfusion in rodents', *Stroke*, 37: 2816-23.

Nava, V. E., J. P. Hobson, S. Murthy, S. Milstien, and S. Spiegel. 2002. 'Sphingosine kinase type 1 promotes estrogen-dependent tumorigenesis of breast cancer MCF-7 cells', *Experimental Cell Research*, 281: 115-27.

Ness, J. K., and T. L. Wood. 2002. 'Insulin-like growth factor I, but not neurotrophin-3, sustains Akt activation and provides long-term protection of immature oligodendrocytes from glutamate-mediated apoptosis', *Mol Cell Neurosci*, 20: 476-88.

Neubauer, H. A., and S. M. Pitson. 2013. 'Roles, regulation and inhibitors of sphingosine kinase 2', *FEBS J*, 280: 5317-36.

Neuropathology Group. Medical Research Council Cognitive, Function, and Study Aging. 2001. 'Pathological correlates of late-onset dementia in a multicentre, community-based population in England and Wales. Neuropathology Group of the Medical Research Council Cognitive Function and Ageing Study (MRC CFAS)', *Lancet*, 357: 169-75.

Ni, J., H. Ohta, K. Matsumoto, and H. Watanabe. 1994. 'Progressive cognitive impairment following chronic cerebral hypoperfusion

induced by permanent occlusion of bilateral carotid arteries in rats', *Brain Res*, 653: 231-6.

Niemela, P. S., M. T. Hyvonen, and I. Vattulainen. 2006. 'Influence of chain length and unsaturation on sphingomyelin bilayers', *Biophys J*, 90: 851-63.

Nishio, K., M. Ihara, N. Yamasaki, R. N. Kalaria, T. Maki, Y. Fujita, H. Ito, N. Oishi, H. Fukuyama, T. Miyakawa, R. Takahashi, and H. Tomimoto. 2010. 'A mouse model characterizing features of vascular dementia with hippocampal atrophy', *Stroke*, 41: 1278-84.

Nishiyama, A. 2007. 'Polydendrocytes: NG2 cells with many roles in development and repair of the CNS', *Neuroscientist*, 13: 62-76.

Nishiyama, A., M. Komitova, R. Suzuki, and X. Zhu. 2009. 'Polydendrocytes (NG2 cells): multifunctional cells with lineage plasticity', *Nat Rev Neurosci*, 10: 9-22.

Norton, W. T., and S. E. Poduslo. 1973. 'Myelination in rat brain: changes in myelin composition during brain maturation', *J Neurochem*, 21: 759-73.

Novgorodov, A. S., M. El-Alwani, J. Bielawski, L. M. Obeid, and T. I. Gudz. 2007. 'Activation of sphingosine-1-phosphate receptor S1P5 inhibits oligodendrocyte progenitor migration', *FASEB J*, 21: 1503-14.

O'Brien, J. S., and E. L. Sampson. 1965. 'Lipid composition of the normal human brain: gray matter, white matter, and myelin', *J Lipid Res*, 6: 537-44.

O'Brien, J. T., T. Erkinjuntti, B. Reisberg, G. Roman, T. Sawada, L. Pantoni, J. V. Bowler, C. Ballard, C. DeCarli, P. B. Gorelick, K. Rockwood, A. Burns, S. Gauthier, and S. T. DeKosky. 2003. 'Vascular cognitive impairment', *Lancet Neurol*, 2: 89-98.

Ohler, B., K. Graf, R. Bragg, T. Lemons, R. Coe, C. Genain, J. Israelachvili, and C. Husted. 2004. 'Role of lipid interactions in autoimmune demyelination', *Biochim Biophys Acta*, 1688: 10-7.

Ohta, H., H. Nishikawa, H. Kimura, H. Anayama, and M. Miyamoto. 1997. 'Chronic cerebral hypoperfusion by permanent internal carotid ligation produces learning impairment without brain damage in rats', *Neuroscience*, 79: 1039-50.

Ohtaki, H., T. Fujimoto, T. Sato, K. Kishimoto, M. Fujimoto, M. Moriya, and S. Shioda. 2006. 'Progressive expression of vascular endothelial growth factor (VEGF) and angiogenesis after chronic ischemic hypoperfusion in rat', *Acta Neurochir Suppl*, 96: 283-7.

Okada, T., G. Ding, H. Sonoda, T. Kajimoto, Y. Haga, A. Khosrowbeygi, S. Gao, N. Miwa, S. Jahangeer, and S. Nakamura. 2005. 'Involvement of N-terminal-extended form of sphingosine kinase 2 in serum-dependent regulation of cell proliferation and apoptosis', *J Biol Chem*, 280: 36318-25.

Olivera, A., T. Kohama, L. Edsall, V. Nava, O. Cuvillier, S. Poulton, and S. Spiegel. 1999. 'Sphingosine kinase expression increases intracellular sphingosine-1-phosphate and promotes cell growth and survival', *J Cell Biol*, 147: 545-58.

Olivera, A., and S. Spiegel. 1993. 'Sphingosine-1-phosphate as second messenger in cell proliferation induced by PDGF and FCS mitogens', *Nature*, 365: 557-60.

Olson, J. A. 1966. 'Lipid metabolism', *Annu Rev Biochem*, 35: 559-98.

Ong, W. Y., and J. M. Levine. 1999. 'A light and electron microscopic study of NG2 chondroitin sulfate proteoglycan-positive oligodendrocyte precursor cells in the normal and kainate-lesioned rat hippocampus', *Neuroscience*, 92: 83-95.

Osinde, M., F. Mullershausen, and K. K. Dev. 2007. 'Phosphorylated FTY720 stimulates ERK phosphorylation in astrocytes via S1P receptors', *Neuropharmacology*, 52: 1210-18.

Pantoni, L. 2002. 'Pathophysiology of age-related cerebral white matter changes', *Cerebrovasc Dis*, 13 Suppl 2: 7-10.

Pantoni, L., and J. H. Garcia. 1995. 'The significance of cerebral white matter abnormalities 100 years after Binswanger's report. A review', *Stroke*, 26: 1293-301.

———. 1997a. 'Pathogenesis of leukoaraiosis - A review', *Stroke*, 28: 652-59.

———. 1997b. 'Pathogenesis of leukoaraiosis: a review', *Stroke*, 28: 652-9.

Pantoni, L., J. H. Garcia, and J. A. Gutierrez. 1996. 'Cerebral white matter is highly vulnerable to ischemia', *Stroke*, 27: 1641-46.

Pantoni, L., D. Leys, F. Fazekas, W. T. Longstreth, Jr., D. Inzitari, A. Wallin, M. Filippi, P. Scheltens, T. Erkinjuntti, and V. Hachinski. 1999. 'Role of white matter lesions in cognitive impairment of vascular origin', *Alzheimer Dis Assoc Disord*, 13 Suppl 3: S49-54.

Pappas, B. A., J. C. de la Torre, C. M. Davidson, M. T. Keyes, and T. Fortin. 1996. 'Chronic reduction of cerebral blood flow in the adult rat: late-emerging CA1 cell loss and memory dysfunction', *Brain Res*, 708: 50-8.

Park, J. H., S. W. Seo, C. Kim, S. H. Kim, G. H. Kim, S. T. Kim, S. Jeon, J. M. Lee, S. J. Oh, J. S. Kim, Y. S. Choe, K. H. Lee, J. S. Shin, C. H. Kim, Y. Noh, H. Cho, C. W. Yoon, H. J. Kim, B. S. Ye, M. Ewers, M. W. Weiner, J. H. Lee, D. J. Werring, and D. L. Na. 2014. 'Effects of cerebrovascular disease and amyloid beta burden on cognition in subjects with subcortical vascular cognitive impairment', *Neurobiology of Aging*, 35: 254-60.

Patel, J., and R. Balabanov. 2012. 'Molecular Mechanisms of Oligodendrocyte Injury in Multiple Sclerosis and Experimental Autoimmune Encephalomyelitis', *International Journal of Molecular Sciences*, 13: 10647-59.

Paugh, S. W., S. G. Payne, S. E. Barbour, S. Milstien, and S. Spiegel. 2003. 'The immunosuppressant FTY720 is phosphorylated by sphingosine kinase type 2', *FEBS Lett*, 554: 189-93.

Pavlovic, A. M., T. Pekmezovic, R. Obrenovic, I. Novakovic, G. Tomic, M. Mijajlovic, and N. Sternic. 2011. 'Increased total homocysteine level is associated with clinical status and severity of white matter changes in symptomatic patients with subcortical small vessel disease', *Clin Neurol Neurosurg*, 113: 711-5.

Petito, C. K., J. P. Olarte, B. Roberts, T. S. Nowak, Jr., and W. A. Pulsinelli. 1998. 'Selective glial vulnerability following transient global ischemia in rat brain', *J Neuropathol Exp Neurol*, 57: 231-8.

Petty, Howard.R. 1993. *Molecular Biology of Membranes: Structure and Function* (Plenum Press: New York).

Pico, F., C. Dufouil, C. Levy, V. Besancon, A. de Kersaint-Gilly, C. Bonithon-Kopp, P. Ducimetiere, C. Tzourio, and A. Alperovitch. 2002. 'Longitudinal study of carotid atherosclerosis and white matter hyperintensities: the EVA-MRI cohort', *Cerebrovasc Dis*, 14: 109-15.

Pinto, S. N., L. C. Silva, R. F. de Almeida, and M. Prieto. 2008. 'Membrane domain formation, interdigitation, and morphological alterations induced by the very long chain asymmetric C24:1 ceramide', *Biophys J*, 95: 2867-79.

Piret, J. P., D. Mottet, M. Raes, and C. Michiels. 2002. 'CoCl2, a chemical inducer of hypoxia-inducible factor-1, and hypoxia reduce apoptotic cell death in hepatoma cell line HepG2', *Ann N Y Acad Sci*, 973: 443-7.

Pitman, M. R., D. H. Pham, and S. M. Pitson. 2012. 'Isoform-selective assays for sphingosine kinase activity', *Methods Mol Biol*, 874: 21-31.

Pitman, M. R., and S. M. Pitson. 2010. 'Inhibitors of the Sphingosine Kinase Pathway as Potential Therapeutics', *Current Cancer Drug Targets*, 10: 354-67.

Pitson, S. M., R. J. D'Andrea, L. Vandeleur, P. A. B. Moretti, P. Xia, J. R. Gamble, M. A. Vadas, and B. W. Wattenberg. 2000. 'Human sphingosine kinase: purification, molecular cloning and characterization of the native and recombinant enzymes', *Biochemical Journal*, 350: 429-41.

Pitson, S. M., P. A. Moretti, J. R. Zebol, H. E. Lynn, P. Xia, M. A. Vadas, and B. W. Wattenberg. 2003. 'Activation of sphingosine kinase 1 by ERK1/2-mediated phosphorylation', *EMBO J*, 22: 5491-500.

Podbielska, M., N. L. Banik, E. Kurowska, and E. L. Hogan. 2013. 'Myelin recovery in multiple sclerosis: the challenge of remyelination', *Brain Sci*, 3: 1282-324.

Pokorna, L., P. Cermakova, A. Horvath, M. G. Baile, S. M. Claypool, P. Griac, J. Malinsky, and M. Balazova. 2015. 'Specific degradation of phosphatidylglycerol is necessary for proper mitochondrial morphology and function', *Biochim Biophys Acta*, 1857: 34-45.

Polito, A., and R. Reynolds. 2005. 'NG2-expressing cells as oligodendrocyte progenitors in the normal and demyelinated adult central nervous system', *J Anat*, 207: 707-16.

Pulkoski-Gross, M. J., J. C. Donaldson, and L. M. Obeid. 2015. 'Sphingosine-1-phosphate metabolism: A structural perspective', *Crit Rev Biochem Mol Biol*: 1-16.

Pyne, S., S. C. Lee, J. Long, and N. J. Pyne. 2009. 'Role of sphingosine kinases and lipid phosphate phosphatases in regulating spatial sphingosine 1-phosphate signalling in health and disease', *Cell Signal*, 21: 14-21.

Quarles, Pierre Morell and Richard H. 1999. 'Characteristic Composition of Myelin.' in Agranoff BW Siegel GJ, Albers RW, et al (ed.), *Basic Neurochemistry: Molecular, Cellular and Medical Aspects* (Lippincott-Raven: Philadelphia).

Quarles, R. H. 2005. 'Comparison of CNS and PNS myelin proteins in the pathology of myelin disorders', *Journal of the Neurological Sciences*, 228: 187-89.

Raff, M. C., R. Mirsky, K. L. Fields, R. P. Lisak, S. H. Dorfman, D. H. Silberberg, N. A. Gregson, S. Leibowitz, and M. C. Kennedy. 1978. 'Galactocerebroside is a specific cell-surface antigenic marker for oligodendrocytes in culture', *Nature*, 274: 813-6.

Ranscht, B., P. M. Wood, and R. P. Bunge. 1987. 'Inhibition of in vitro peripheral myelin formation by monoclonal anti-galactocerebroside', *J Neurosci*, 7: 2936-47.

Ravaglia, G., P. Forti, A. Lucicesare, N. Pisacane, E. Rietti, M. Bianchin, and E. Dalmonte. 2008. 'Physical activity and dementia risk in the elderly: findings from a prospective Italian study', *Neurology*, 70: 1786-94.

Ren, S., C. Xin, J. Pfeilschifter, and A. Huwiler. 2010. 'A novel mode of action of the putative sphingosine kinase inhibitor 2-(p-hydroxyanilino)-4-(p-chlorophenyl) thiazole (SKI II): induction of lysosomal sphingosine kinase 1 degradation', *Cell Physiol Biochem*, 26: 97-104.

Reynolds, R., M. Dawson, D. Papadopoulos, A. Polito, I. C. Di Bello, D. Pham-Dinh, and J. Levine. 2002. 'The response of NG2-expressing oligodendrocyte progenitors to demyelination in MOG-EAE and MS', *J Neurocytol*, 31: 523-36.

Rocca, W. A., A. Hofman, C. Brayne, M. M. B. Breteler, M. Clarke, J. R. M. Copeland, J. F. Dartigues, K. Engedal, O. Hagnell, T. J. Heeren, C. Jonker, J. Lindesay, A. Lobo, A. H. Mann, P. K. Molsa, K. Morgan, D. W. Oconnor, A. D. Droux, R. Sulkava, D. W. K. Kay, and L. Amaducci. 1991. 'The Prevalence of Vascular Dementia in Europe - Facts and Fragments from 1980-1990 Studies', *Annals of Neurology*, 30: 817-24.

Roman, G. C., T. Erkinjuntti, A. Wallin, L. Pantoni, and H. C. Chui. 2002. 'Subcortical ischaemic vascular dementia', *Lancet Neurology*, 1: 426-36.

Roman, G. C., T. K. Tatemichi, T. Erkinjuntti, J. L. Cummings, J. C. Masdeu, J. H. Garcia, L. Amaducci, J. M. Orgogozo, A. Brun, A. Hofman, and et al. 1993. 'Vascular dementia: diagnostic criteria for research studies. Report of the NINDS-AIREN International Workshop', *Neurology*, 43: 250-60.

Roof, R. L., G. P. Schielke, X. Ren, and E. D. Hall. 2001. 'A comparison of long-term functional outcome after 2 middle cerebral artery occlusion models in rats', *Stroke*, 32: 2648-57.

Rosenberg, G. A. 2009. 'Inflammation and white matter damage in vascular cognitive impairment', *Stroke*, 40: S20-3.

Rosenberg, G. A., N. Sullivan, and M. M. Esiri. 2001. 'White matter damage is associated with matrix metalloproteinases in vascular dementia', *Stroke*, 32: 1162-67.

Rosenfeldt, H. M., J. P. Hobson, M. Maceyka, A. Olivera, V. E. Nava, S. Milstien, and S. Spiegel. 2001. 'EDG-1 links the PDGF receptor to Src and focal adhesion kinase activation leading to lamellipodia formation and cell migration', *FASEB J*, 15: 2649-59.

Ruitenberg, A., A. Ott, J. C. van Swieten, A. Hofman, and M. M. B. Breteler. 2001. 'Incidence of dementia: does gender make a difference?', *Neurobiology of Aging*, 22: 575-80.

Sachdev, P., R. Kalaria, J. O'Brien, I. Skoog, S. Alladi, S. E. Black, D. Blacker, D. G. Blazer, C. Chen, H. Chui, M. Ganguli, K. Jellinger, D. V. Jeste, F. Pasquier, J. Paulsen, N. Prins, K. Rockwood, G. Roman, P. Scheltens, Behavioral Internationlal Society for Vascular, and Disorders Cognitive. 2014. 'Diagnostic criteria for vascular cognitive disorders: a VASCOG statement', *Alzheimer Dis Assoc Disord*, 28: 206-18.

Saczynski, J. S., M. K. Jonsdottir, M. E. Garcia, P. V. Jonsson, R. Peila, G. Eiriksdottir, E. Olafsdottir, T. B. Harris, V. Gudnason, and L. J. Launer. 2008. 'Cognitive impairment: an increasingly important complication of type 2 diabetes: the age, gene/environment susceptibility--Reykjavik study', *Am J Epidemiol*, 168: 1132-9.

Sankala, H. M., N. C. Hait, S. W. Paugh, D. Shida, S. Lepine, L. W. Elmore, P. Dent, S. Milstien, and S. Spiegel. 2007. 'Involvement of sphingosine kinase 2 in p53-independent induction of p21 by the chemotherapeutic drug doxorubicin', *Cancer Res*, 67: 10466-74.

Sastry, P. S. 1985. 'Lipids of nervous tissue: composition and metabolism', *Prog Lipid Res*, 24: 69-176.

Sato, K., M. Ui, and F. Okajima. 2000. 'Differential roles of Edg-1 and Edg-5, sphingosine 1-phosphate receptors, in the signaling pathways in C6 glioma cells', *Molecular Brain Research*, 85: 151-60.

Schenkel, L. C., and M. Bakovic. 2014. 'Formation and regulation of mitochondrial membranes', *Int J Cell Biol*, 2014: 709828.

Schneider, J. A., R. S. Wilson, J. L. Bienias, D. A. Evans, and D. A. Bennett. 2004. 'Cerebral infarctions and the likelihood of dementia from Alzheimer disease pathology', *Neurology*, 62: 1148-55.

Schneider, J. A., R. S. Wilson, E. J. Cochran, J. L. Bienias, S. E. Arnold, D. A. Evans, and D. A. Bennett. 2003. 'Relation of cerebral infarctions to dementia and cognitive function in older persons', *Neurology*, 60: 1082-8.

Schnitzer, S. E., A. Weigert, J. Zhou, and B. Brune. 2009. 'Hypoxia enhances sphingosine kinase 2 activity and provokes sphingosine-1-phosphate-mediated chemoresistance in A549 lung cancer cells', *Mol Cancer Res*, 7: 393-401.

Schulze, T., S. Golfier, C. Tabeling, K. Rabel, M. H. Graler, M. Witzenrath, and M. Lipp. 2011. 'Sphingosine-1-phospate receptor 4 (S1P(4)) deficiency profoundly affects dendritic cell function and TH17-cell differentiation in a murine model', *FASEB J*, 25: 4024-36.

Schwalm, S., F. Doll, I. Romer, S. Bubnova, J. Pfeilschifter, and A. Huwiler. 2008. 'Sphingosine kinase-1 is a hypoxia-regulated gene that stimulates migration of human endothelial cells', *Biochem Biophys Res Commun*, 368: 1020-5.

Selhub, J. 1999. 'Homocysteine metabolism', *Annu Rev Nutr*, 19: 217-46.

Semenza, G. L. 2012. 'Hypoxia-Inducible Factors in Physiology and Medicine', *Cell*, 148: 399-408.

Shibata, M., S. Hisahara, H. Hara, T. Yamawaki, Y. Fukuuchi, J. Yuan, H. Okano, and M. Miura. 2000. 'Caspases determine the vulnerability of oligodendrocytes in the ischemic brain', *J Clin Invest*, 106: 643-53.

Shibata, M., R. Ohtani, M. Ihara, and H. Tomimoto. 2004. 'White matter lesions and glial activation in a novel mouse model of chronic cerebral hypoperfusion', *Stroke*, 35: 2598-603.

Shibata, M., N. Yamasaki, T. Miyakawa, R. N. Kalaria, Y. Fujita, R. Ohtani, M. Ihara, R. Takahashi, and H. Tomimoto. 2007. 'Selective impairment of working memory in a mouse model of chronic cerebral hypoperfusion', *Stroke*, 38: 2826-32.

Shimomura, T., F. Anan, Y. Umeno, N. Eshima, T. Saikawa, H. Yoshimatsu, M. Fujiki, and H. Kobayashi. 2008. 'Hyperhomocysteinaemia is a significant risk factor for white matter lesions in Japanese type 2 diabetic patients', *Eur J Neurol*, 15: 289-94.

Shroff, S. M., A. D. Pomicter, W. N. Chow, M. A. Fox, R. J. Colello, S. C. Henderson, and J. L. Dupree. 2009. 'Adult CST-null mice maintain an increased number of oligodendrocytes', *Journal of Neuroscience Research*, 87: 3403-14.

Shu, X., W. Wu, R. D. Mosteller, and D. Broek. 2002. 'Sphingosine kinase mediates vascular endothelial growth factor-induced activation of ras and mitogen-activated protein kinases', *Mol Cell Biol*, 22: 7758-68.

Shui, G., W. F. Cheong, I. A. Jappar, A. Hoi, Y. Xue, A. Z. Fernandis, B. K. Tan, and M. R. Wenk. 2011. 'Derivatization-independent cholesterol analysis in crude lipid extracts by liquid chromatography/mass spectrometry: applications to a rabbit model for atherosclerosis', *J Chromatogr A*, 1218: 4357-65.

Silva, L. C., O. Ben David, Y. Pewzner-Jung, E. L. Laviad, J. Stiban, S. Bandyopadhyay, A. H. Merrill, Jr., M. Prieto, and A. H. Futerman. 2012. 'Ablation of ceramide synthase 2 strongly affects biophysical properties of membranes', *J Lipid Res*, 53: 430-6.

Simons, K., and E. Ikonen. 1997. 'Functional rafts in cell membranes', *Nature*, 387: 569-72.

———. 2000. 'How cells handle cholesterol', *Science*, 290: 1721-6.

Singleton, P. A., S. M. Dudek, E. T. Chiang, and J. G. Garcia. 2005. 'Regulation of sphingosine 1-phosphate-induced endothelial cytoskeletal rearrangement and barrier enhancement by S1P1 receptor, PI3 kinase, Tiam1/Rac1, and alpha-actinin', *FASEB J*, 19: 1646-56.

Skoura, A., T. Sanchez, K. Claffey, S. M. Mandala, R. L. Proia, and T. Hla. 2007. 'Essential role of sphingosine 1-phosphate receptor 2 in pathological angiogenesis of the mouse retina', *Journal of Clinical Investigation*, 117: 2506-16.

Slone, E. A., M. R. Pope, and S. D. Fleming. 2015. 'Phospholipid scramblase 1 is required for beta2-glycoprotein I binding in hypoxia and reoxygenation-induced endothelial inflammation', *J Leukoc Biol*, 98: 791-804.

Sobue, S., K. Hagiwara, Y. Banno, K. Tamiya-Koizumi, M. Suzuki, A. Takagi, T. Kojima, H. Asano, Y. Nozawa, and T. Murate. 2005. 'Transcription factor specificity protein 1 (Sp1) is the main regulator of nerve growth factor-induced sphingosine kinase 1 gene expression of the rat pheochromocytoma cell line, PC12', *J Neurochem*, 95: 940-9.

Sofi, F., D. Valecchi, D. Bacci, R. Abbate, G. F. Gensini, A. Casini, and C. Macchi. 2011. 'Physical activity and risk of cognitive decline: a meta-analysis of prospective studies', *Journal of Internal Medicine*, 269: 107-17.

Solomon, A., M. Kivipelto, B. Wolozin, J. F. Zhou, and R. A. Whitmer. 2009. 'Midlife Serum Cholesterol and Increased Risk of Alzheimer's and Vascular Dementia Three Decades Later', *Dementia and Geriatric Cognitive Disorders*, 28: 75-80.

Sonnen, J. A., E. B. Larson, P. K. Crane, S. Haneuse, G. Li, G. D. Schellenberg, S. Craft, J. B. Leverenz, and T. J. Montine. 2007. 'Pathological correlates of dementia in a longitudinal, population-based sample of aging', *Annals of Neurology*, 62: 406-13.

Spassieva, S. D., T. D. Mullen, D. M. Townsend, and L. M. Obeid. 2009. 'Disruption of ceramide synthesis by CerS2 down-regulation leads to autophagy and the unfolded protein response', *Biochem J*, 424: 273-83.

Spiegel, S., and S. Milstien. 2002. 'Sphingosine 1-phosphate, a key cell signaling molecule', *J Biol Chem*, 277: 25851-4.

———. 2003. 'Sphingosine-1-phosphate: an enigmatic signalling lipid', *Nat Rev Mol Cell Biol*, 4: 397-407.

Stewart, R., K. Masaki, Q. L. Xue, R. Peila, H. Petrovitch, L. R. White, and L. J. Launer. 2005. 'A 32-year prospective study of change in body weight and incident dementia: the Honolulu-Asia Aging Study', *Arch Neurol*, 62: 55-60.

Sugimoto, N., N. Takuwa, H. Okamoto, S. Sakurada, and Y. Takuwa. 2003. 'Inhibitory and stimulatory regulation of Rac and cell motility by the G12/13-Rho and Gi pathways integrated downstream of a single G protein-coupled sphingosine-1-phosphate receptor isoform', *Mol Cell Biol*, 23: 1534-45.

Sugiura, M., K. Kono, H. Liu, T. Shimizugawa, H. Minekura, S. Spiegel, and T. Kohama. 2002. 'Ceramide kinase, a novel lipid kinase. Molecular cloning and functional characterization', *J Biol Chem*, 277: 23294-300.

Sunyer, Berta, Sudarshan Patil, Harald Höger, and Gert Lubec. 2007. 'Barnes maze, a useful task to assess spatial reference memory in the mice'.

Suwa, M., S. Yamaguchi, T. Komori, S. Kajimoto, and M. Kino. 2015. 'The Association between Cerebral White Matter Lesions and Plasma Omega-3 to Omega-6 Polyunsaturated Fatty Acids Ratio to Cognitive Impairment Development', *Biomed Res Int*, 2015: 153437.

Svennerholm, L., and M. T. Vanier. 1973. 'The distribution of lipids in the human nervous system. IV. Fatty acid composition of major sphingolipids of human infant brain', *Brain Res*, 55: 413-23.

Tafesse, F. G., P. Ternes, and J. C. Holthuis. 2006. 'The multigenic sphingomyelin synthase family', *J Biol Chem*, 281: 29421-5.

Takahashi, T., and T. Suzuki. 2012. 'Role of sulfatide in normal and pathological cells and tissues', *J Lipid Res*, 53: 1437-50.

Testai, F. D., J. P. Kilkus, E. Berdyshev, I. Gorshkova, V. Natarajan, and G. Dawson. 2014. 'Multiple sphingolipid abnormalities following cerebral microendothelial hypoxia', *J Neurochem*, 131: 530-40.

Thompson, C. B. 1995. 'Apoptosis in the Pathogenesis and Treatment of Disease', *Science*, 267: 1456-62.

Toman, R. E., S. G. Payne, K. R. Watterson, M. Maceyka, N. H. Lee, S. Milstien, J. W. Bigbee, and S. Spiegel. 2004. 'Differential transactivation of sphingosine-1-phosphate receptors modulates NGF-induced neurite extension', *Journal of Cell Biology*, 166: 381-92.

Tomimoto, H., M. Ihara, H. Wakita, R. Ohtani, J. X. Lin, I. Akiguchi, M. Kinoshita, and H. Shibasaki. 2003. 'Chronic cerebral hypoperfusion induces white matter lesions and loss of oligodendroglia with DNA fragmentation in the rat', *Acta Neuropathol*, 106: 527-34.

Tomlinson, B. E., G. Blessed, and M. Roth. 1970. 'Observations on the brains of demented old people', *J Neurol Sci*, 11: 205-42.

Ueno, M., T. Tomimoto, T. Akiguchi, T. Wakita, and H. Sakamoto. 2002. 'Blood-brain barrier disruption in white matter lesions in a rat model of chronic cerebral hypoperfusion', *Journal of Cerebral Blood Flow and Metabolism*, 22: 97-104.

Unal-Cevik, I., M. Kilinc, A. Can, Y. Gursoy-Ozdemir, and T. Dalkara. 2004. 'Apoptotic and necrotic death mechanisms are concomitantly activated in the same cell after cerebral ischemia', *Stroke*, 35: 2189-94.

van Harten, B., J. M. Oosterman, B. J. P. van Loon, P. Scheltens, and H. C. Weinstein. 2007. 'Brain lesions on MRI in elderly patients with type 2 diabetes mellitus', *European Neurology*, 57: 70-74.

van Meer, G., D. R. Voelker, and G. W. Feigenson. 2008. 'Membrane lipids: where they are and how they behave', *Nat Rev Mol Cell Biol*, 9: 112-24.

Vermeer, S. E., E. J. van Dijk, P. J. Koudstaal, M. Oudkerk, A. Hofman, R. Clarke, and M. M. Breteler. 2002. 'Homocysteine, silent brain infarcts, and white matter lesions: The Rotterdam Scan Study', *Annals of Neurology*, 51: 285-9.

Vessey, D. A., M. Kelley, J. Zhang, L. Li, R. Tao, and J. S. Karliner. 2007. 'Dimethylsphingosine and FTY720 inhibit the SK1 form but activate the SK2 form of sphingosine kinase from rat heart', *J Biochem Mol Toxicol*, 21: 273-9.

Vinters, H. V., W. G. Ellis, C. Zarow, B. W. Zaias, W. J. Jagust, W. J. Mack, and H. C. Chui. 2000. 'Neuropathologic substrates of ischemic vascular dementia', *J Neuropathol Exp Neurol*, 59: 931-45.

Wacker, B. K., T. S. Park, and J. M. Gidday. 2009. 'Hypoxic preconditioning-induced cerebral ischemic tolerance: role of microvascular sphingosine kinase 2', *Stroke*, 40: 3342-8.

Wacker, B. K., J. L. Perfater, and J. M. Gidday. 2012. 'Hypoxic preconditioning induces stroke tolerance in mice via a cascading HIF, sphingosine kinase, and CCL2 signaling pathway', *J Neurochem*, 123: 954-62.

Wakita, H., H. Tomimoto, I. Akiguchi, A. Matsuo, J. X. Lin, M. Ihara, and P. L. McGeer. 2002. 'Axonal damage and demyelination in the white matter after chronic cerebral hypoperfusion in the rat', *Brain Res*, 924: 63-70.

Walker, E. J., and G. A. Rosenberg. 2010. 'Divergent role for MMP-2 in myelin breakdown and oligodendrocyte death following transient global ischemia', *Journal of Neuroscience Research*, 88: 764-73.

Wang, F., J. R. Van Brocklyn, J. P. Hobson, S. Movafagh, Z. Zukowska-Grojec, S. Milstien, and S. Spiegel. 1999. 'Sphingosine 1-phosphate stimulates cell migration through a G(i)-coupled cell surface receptor - Potential involvement in angiogenesis', *Journal of Biological Chemistry*, 274: 35343-50.

Wardlaw, J. M. 2008. 'What is a lacune?', *Stroke*, 39: 2921-2.

Wardlaw, J. M., E. E. Smith, G. J. Biessels, C. Cordonnier, F. Fazekas, R. Frayne, R. I. Lindley, J. T. O'Brien, F. Barkhof, O. R. Benavente, S. E. Black, C. Brayne, M. Breteler, H. Chabriat, C. Decarli, F. E. de Leeuw, F. Doubal, M. Duering, N. C. Fox, S. Greenberg, V. Hachinski, I. Kilimann, V. Mok, Rv Oostenbrugge, L. Pantoni, O. Speck, B. C. Stephan, S. Teipel, A. Viswanathan, D. Werring, C. Chen, C. Smith, M. van Buchem, B. Norrving, P. B. Gorelick, M. Dichgans, and S. Tandards for ReportIng Vascular changes on nEuroimaging. 2013. 'Neuroimaging standards for research into small vessel disease and its contribution to ageing and neurodegeneration', *Lancet Neurol*, 12: 822-38.

Washida, K., M. Ihara, K. Nishio, Y. Fujita, T. Maki, M. Yamada, J. Takahashi, X. Wu, T. Kihara, H. Ito, H. Tomimoto, and R. Takahashi. 2010. 'Nonhypotensive dose of telmisartan attenuates cognitive impairment partially due to peroxisome proliferator-activated receptor-gamma activation in mice with chronic cerebral hypoperfusion', *Stroke*, 41: 1798-806.

Watanabe, M., Y. Toyama, and A. Nishiyama. 2002. 'Differentiation of proliferated NG2-positive glial progenitor cells in a remyelinating lesion', *Journal of Neuroscience Research*, 69: 826-36.

Watanabe, T., N. Zhang, M. Z. Liu, R. Tanaka, Y. Mizuno, and T. Urabe. 2006. 'Cilostazol protects against brain white matter damage and cognitive impairment in a rat model of chronic cerebral hypoperfusion', *Stroke*, 37: 1539-45.

Watson, D. G., F. Tonelli, M. Alossaimi, L. Williamson, E. Chan, I. Gorshkova, E. Berdyshev, R. Bittman, N. J. Pyne, and S. Pyne. 2013. 'The roles of sphingosine kinases 1 and 2 in regulating the Warburg effect in prostate cancer cells', *Cell Signal*, 25: 1011-7.

Wattenberg, B. W., S. M. Pitson, and D. M. Raben. 2006. 'The sphingosine and diacylglycerol kinase superfamily of signaling kinases: localization as a key to signaling function', *J Lipid Res*, 47: 1128-39.

Waxman , S.G. and Bangalore, L. 2004. 'Electrophysiological consequences of myelination.' in R.A. Lazzarini (ed.), *Myelin biology and disorder* (Elsevier Academic Press: San Diego, CA).

Weigert, A., S. Cremer, M. V. Schmidt, A. von Knethen, C. Angioni, G. Geisslinger, and B. Brune. 2010. 'Cleavage of sphingosine kinase 2 by caspase-1 provokes its release from apoptotic cells', *Blood*, 115: 3531-40.

Weir, J. M., G. Wong, C. K. Barlow, M. A. Greeve, A. Kowalczyk, L. Almasy, A. G. Comuzzie, M. C. Mahaney, J. B. Jowett, J. Shaw, J. E.

Curran, J. Blangero, and P. J. Meikle. 2013. 'Plasma lipid profiling in a large population-based cohort', *J Lipid Res*, 54: 2898-908.

Westerlund, B., and J. P. Slotte. 2009. 'How the molecular features of glycosphingolipids affect domain formation in fluid membranes', *Biochim Biophys Acta*, 1788: 194-201.

White, L., B. J. Small, H. Petrovitch, G. W. Ross, K. Masaki, R. D. Abbott, J. Hardman, D. Davis, J. Nelson, and W. Markesbery. 2005. 'Recent clinical-pathologic research on the causes of dementia in late life: update from the Honolulu-Asia Aging Study', *J Geriatr Psychiatry Neurol*, 18: 224-7.

WHO. 2015. 'World report on ageing and health'.

Wigley, R., N. Hamilton, A. Nishiyama, F. Kirchhoff, and A. M. Butt. 2007. 'Morphological and physiological interactions of NG2-glia with astrocytes and neurons', *J Anat*, 210: 661-70.

Wilkinson, D., R. Doody, R. Helme, K. Taubman, J. Mintzer, A. Kertesz, R. D. Pratt, and Group Donepezil 308 Study. 2003. 'Donepezil in vascular dementia: a randomized, placebo-controlled study', *Neurology*, 61: 479-86.

Wilkinson, D., G. Roman, S. Salloway, J. Hecker, K. Boundy, D. Kumar, H. Posner, and R. Schindler. 2010. 'The long-term efficacy and tolerability of donepezil in patients with vascular dementia', *Int J Geriatr Psychiatry*, 25: 305-13.

Winzeler, A. M., W. J. Mandemakers, M. Z. Sun, M. Stafford, C. T. Phillips, and B. A. Barres. 2011. 'The lipid sulfatide is a novel myelin-associated inhibitor of CNS axon outgrowth', *J Neurosci*, 31: 6481-92.

Xia, P., L. Wang, J. R. Gamble, and M. A. Vadas. 1999. 'Activation of sphingosine kinase by tumor necrosis factor-alpha inhibits apoptosis in human endothelial cells', *J Biol Chem*, 274: 34499-505.

Xia, P., L. J. Wang, P. A. B. Moretti, N. Albanese, F. G. Chai, S. M. Pitson, R. J. D'Andrea, J. R. Gamble, and M. A. Vadas. 2002. 'Sphingosine kinase interacts with TRAF2 and dissects tumor necrosis factor-alpha signaling', *Journal of Biological Chemistry*, 277: 7996-8003.

Xiong, Y. Y., and V. Mok. 2011. 'Age-related white matter changes', *J Aging Res*, 2011: 617927.

Yamada, M., M. Ihara, Y. Okamoto, T. Maki, K. Washida, A. Kitamura, Y. Hase, H. Ito, K. Takao, T. Miyakawa, R. N. Kalaria, H. Tomimoto, and R. Takahashi. 2011. 'The influence of chronic cerebral hypoperfusion on cognitive function and amyloid beta metabolism in APP overexpressing mice', *PLoS One*, 6: e16567.

Yamawaki, M., K. Wada-Isoe, M. Yamamoto, S. Nakashita, Y. Uemura, Y. Takahashi, T. Nakayama, and K. Nakashima. 2015. 'Association of cerebral white matter lesions with cognitive function and mood in Japanese elderly people: a population-based study', *Brain Behav*, 5: e00315.

Yang, Y., J. Zhang, H. Liu, J. Wang, J. Xin, and M. Deng. 2013. 'Changes in levels of hypoxia-induced mediators in rat hippocampus during chronic cerebral hypoperfusion', *Neurochem Res*, 38: 2433-9.

Yeung, T., G. E. Gilbert, J. Shi, J. Silvius, A. Kapus, and S. Grinstein. 2008. 'Membrane phosphatidylserine regulates surface charge and protein localization', *Science*, 319: 210-3.

Young, N., and J. R. Van Brocklyn. 2007. 'Roles of sphingosine-1-phosphate (S1P) receptors in malignant behavior of glioma cells. Differential effects of S1P2 on cell migration and invasiveness', *Experimental Cell Research*, 313: 1615-27.

Yu, N., K. D. Lariosa-Willingham, F. F. Lin, M. Webb, and T. S. Rao. 2004. 'Characterization of lysophosphatidic acid and sphingosine-1-phosphate-mediated signal transduction in rat cortical oligodendrocytes', *Glia*, 45: 17-27.

Yu, R. K., Y. T. Tsai, T. Ariga, and M. Yanagisawa. 2011. 'Structures, biosynthesis, and functions of gangliosides--an overview', *J Oleo Sci*, 60: 537-44.

Yuan, Y., G. Hilliard, T. Ferguson, and D. E. Millhorn. 2003. 'Cobalt inhibits the interaction between hypoxia-inducible factor-alpha and von Hippel-Lindau protein by direct binding to hypoxia-inducible factor-alpha', *J Biol Chem*, 278: 15911-6.

Yung, L. M., Y. Wei, T. Qin, Y. Wang, C. D. Smith, and C. Waeber. 2012. 'Sphingosine kinase 2 mediates cerebral preconditioning and protects the mouse brain against ischemic injury', *Stroke*, 43: 199-204.

Zekry, D., C. Duyckaerts, R. Moulias, J. Belmin, C. Geoffre, F. Herrmann, and J. J. Hauw. 2002. 'Degenerative and vascular lesions of the brain have synergistic effects in dementia of the elderly', *Acta Neuropathol*, 103: 481-7.

Zigdon, H., A. Kogot-Levin, J. W. Park, R. Goldschmidt, S. Kelly, A. H. Merrill, Jr., A. Scherz, Y. Pewzner-Jung, A. Saada, and A. H. Futerman. 2013. 'Ablation of ceramide synthase 2 causes chronic oxidative stress due to disruption of the mitochondrial respiratory chain', *J Biol Chem*, 288: 4947-56.

Zwaal, R. F., P. Comfurius, and E. M. Bevers. 2005. 'Surface exposure of phosphatidylserine in pathological cells', *Cell Mol Life Sci*, 62: 971-88.